TRIPLET STATE PROCESSES

OF

CARBAZOLE AND RELATED COMPOUNDS

IN POLYMER MATRICES

A Thesis

presented for the degree of

DOCTOR OF PHILOSOPHY

in the Faculty of Science of the

University of St. Andrews

by

Helen Williamson, B.Sc

August 1990

United College of St. Salvator

and St. Leonards College

DECLARATION

I, Helen Williamson, hereby certify that this thesis has been composed by myself, that it is a record of my own work, and that it has not been accepted in partial or complete fulfilment of any other degree or professional qualification.

I was admitted to the Faculty of Science of the University of St. Andrews under Ordinance General No. 12 in October 1987, and as a candidate for the degree of PhD. in October 1988.

Signed August 1990

CERTIFICATION

I hereby certify that the candidate has fulfilled the conditions of the Resolution and Regulations appropriate to the degree of PhD.

Signed August 1990

COPYRIGHT

ACKNOWLEDGEMENTS

I would like to thank Professor J.R. MacCallum for his supervision during the course of this work.

My thanks are also due to various members of the technical staff for building and maintaining the apparatus, especially Mr J. Rennie, Mr D. Clark, Mr R. Cathcart (Workshop); Mr J. Bews, Mr J. Ward, Mr D. Wilkie (Electronics Workshop) and Mr C. Smith (Glassblowing). Thanks also to Mr. J. Smith (Lab Technician).

I am indebted to the Science and Engineering Research Council for a grant to finance this work, and to the Chemistry Department at St. Andrews for providing the research facilities.

Thanks to David for his support over the last three years.

Finally, and most importantly, I wish to thank my parents for all the backing and encouragement they have given me throughout my entire education.

CONTENTS

CHAPTER 2

EXPERIMENTAL METHODS

CHAPTER 3

POLYMERS AS HOSTS

CHAPTER 5

MAGNETIC FIELD EFFECTS ON TRIPLET STATE PROCESSES

CHAPTER 6

POLYMER PHOTODEGRADATION

SUMMARY

The phosphorescence decay and lifetime of carbazole and N-ethyl carbazole was examined between 80 - 298K in various polymer matrices using a nitrogen laser as the excitation source. The phosphorescence lifetime, τ_p, was found to be highly dependent on both matrix and temperature. Furthermore, as the concentration of the additive was increased, an initial non-exponential decay was observed and τ_p decreased. The results were explained in terms of a thermally-assisted energy transfer mechanism from the triplet level of the additive to the triplet level of the polymer host. This energy transfer process from additive to polymer questions the suitability of using polymers as inert hosts in the study of organic photoluminescence. At high additive concentration, triplet-triplet annihilation becomes a dominant step. Since the addition of low concentrations of 3-bromocarbazole and Pr[18-crown-6].$(NO_3)_3$ quenchers had no significant effect on the phosphorescence lifetime, it was deduced that energy migration through the homopolymer matrix is an inefficient process.

Similar results were obtained in studies of various vinyl carbazole/methyl methacrylate (VC/MMA) copolymers. However, energy migration was found to be a much more efficient process in the copolymers than in the corresponding doped homopolymer. An exchange energy tranfer process was proposed, where steric or conformational effects provide better overlap of chromophores in the copolymer, thereby increasing intermolecular energy transfer.

A study of the magnetic field effect on the triplet lifetime of carbazole-doped homopolymer matrices and VC/MMA copolymer matrices yielded confusing and often conflicting results, probably due to some

spurious instrumental effects.

The addition of N-ethyl carbazole to a solution of PMMA in toluene was found to have no effect on the rate of photodegradation of the polymer. However, attaching the copolymer unit onto the backbone of the polymer chain resulted in a significant increase in the rate of photodegradation. These results were consistent with the mechanisms proposed in the VC/MMA copolymer.

TO MUM AND DAD

GENERAL INTRODUCTION

GENERAL INTRODUCTION

Polymers are convenient matrices for the study of organic photoluminescence since they can be used over a much wider temperature range than conventional frozen glasses. Ease of preparation of films and optical clarity are also extremely desirable properties often associated with these hosts. The use of **any** matrix in studies of photoluminescence assumes that the host is photophysically inert, and on first inspection, polymers such as poly(methyl methacrylate), polystyrene and poly(vinyl acetate) appear to conform to these criteria. The initial aim of the present study was to determine whether or not these polymers are capable of accepting electronic energy at the triplet level, thereby establishing their suitability as inert hosts. The phosphorescence decays and lifetimes of carbazole and N-ethyl carbazole were studied as a function of polymer environment and temperature. These additives were particularly chosen because they have triplet energy levels close to those of the polymer triplet energy levels and they have relatively long phosphorescence lifetimes, in the region of seconds.

An understanding of energy transfer processes in polymers has direct applications in the field of polymer photodegradation and photostabilisation [1,2], and the latter part of this thesis is concerned with the photophysical processes occurring when the carbazole unit forms part of a copolymer chain.

CHAPTER 1

CHAPTER 1

ORGANIC PHOTOLUMINESCENCE

INTRODUCTION

Organic photoluminescence occurs when molecules absorb high energy radiation, and the resultant uptake of energy produces excited state molecules. The physical effect of the absorption of radiation is to cause the promotion of an electron from an orbital of lower energy to one of higher energy. Excited states are relatively short-lived for they are compelled to lose their energy within a short period of time. Several processes can compete to deactivate the excited state species : these can be understood in terms of radiative transitions (where photons are emitted during energy loss) and radiationless transitions (where light is transformed into heat) (Figure 1.1) [3-7].

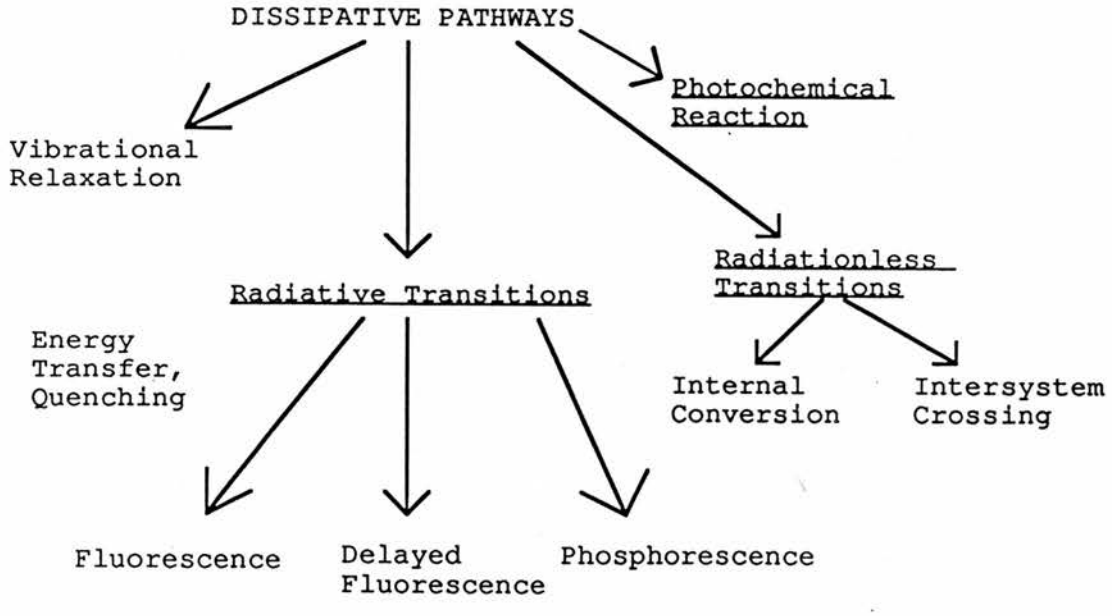

FIGURE 1.1

POSSIBLE ROUTES FOR THE DEACTIVATION OF THE TRIPLET STATE

However, before these individual processes are discussed in more detail, it is necessary to outline the terminology used when describing electronic states.

ELECTRONIC STATES [8]

The multiplicity of an electronically excited state is defined by the expression 2S+1, where S is the algebraic sum of the electrons in the system. The spin quantum numbers can be either $+\frac{1}{2}$ or $-\frac{1}{2}$. As a consequence of the Pauli Exclusion Principle, electrons in the same orbital must have their spins paired. Hence, the sum S of the spin quantum numbers must equal zero, and the multiplicity is one. The molecule is then said to be in the **singlet** state ; this state being designated by the symbol S. The ground states of the majority of organic molecules are singlet states, S_0.

If on promotion of an electron into a higher energy orbital the promoted electron retains its spin configuration, the sum of the spin quantum numbers will still be zero, but the molecule will now be in an excited singlet state. These are labelled S_1, S_2, S_3,.... in increasing order of energy. If spin inversion of the promoted electron takes place before the molecule returns to ground state, the spin of the promoted electron will not be paired with the spin of the electron in the vacated orbital. The spin quantum numbers of the unpaired electrons will be either $+\frac{1}{2}+\frac{1}{2}$ or $-\frac{1}{2}-\frac{1}{2}$ i.e. the algebraic sum equals one, and the multiplicity of the state, 2S+1, equals three. These are described as **triplet** states, and are designated T_1, T_2, T_3,.....

A triplet state has a lower energy than the corresponding singlet state due to the repulsive nature of the spin-spin interactions between electrons of the same spin (Hund's Rule). All triplets are more stable than the corresponding singlets.

FIGURE 1.2

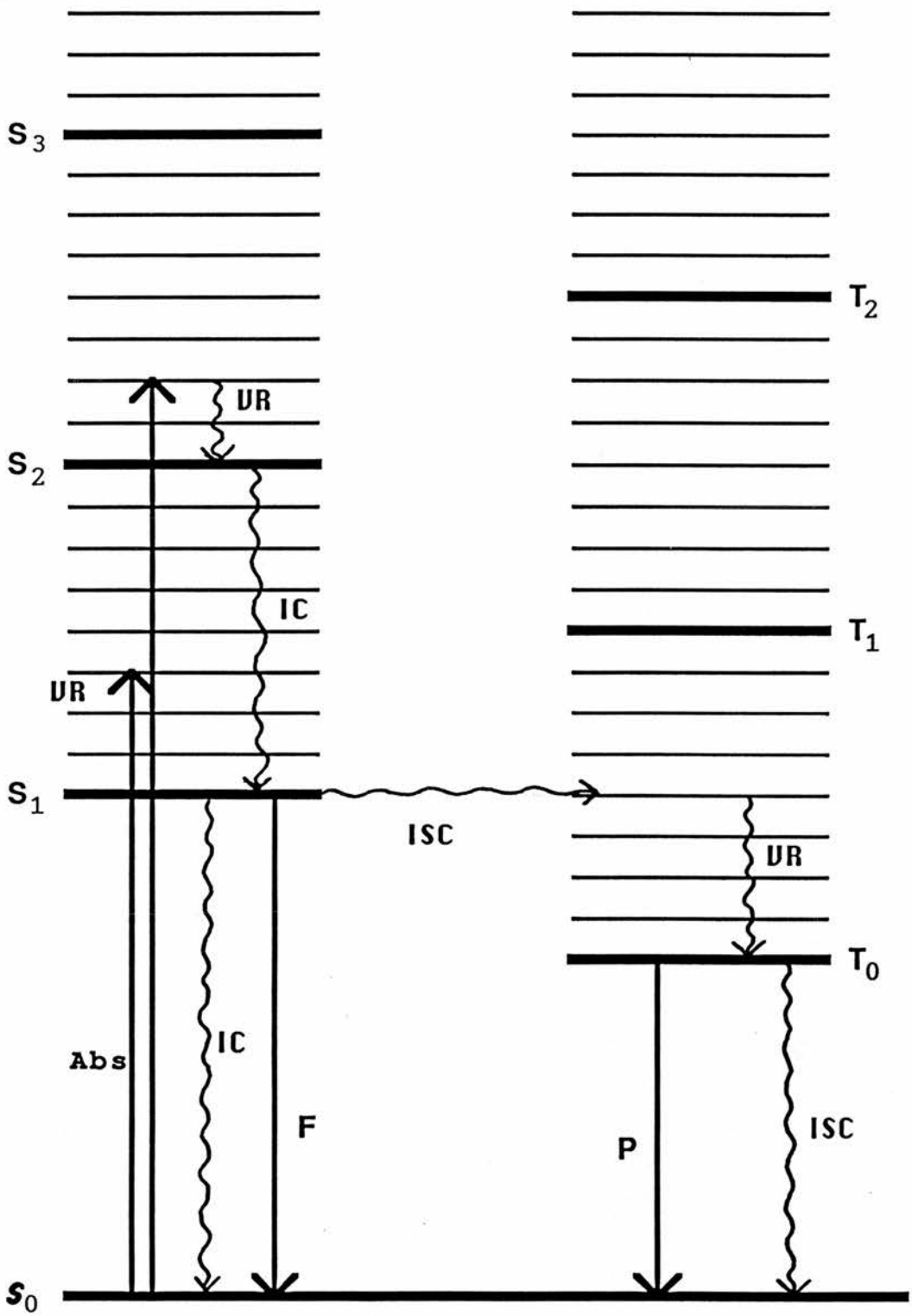

Energy diagram showing deactivation pathways for a typical organic chromaphore.

Abs = absorption IC = internal conversion
VR = vibrational relaxation F = fluorescence
P = phosphorescence ISC = intersystem crossing

THE DEACTIVATION OF EXCITED STATES [3-7]

The different deactivation routes are depicted on a Jablonski diagram (Figure 1.2). By convention, the singlet manifold is shown on the left, and the triplet manifold on the right. Each manifold comprises a series of electronic energy levels with a series of vibrational (and rotational) levels associated with each electronic state.

Absorption of light of the appropriate energy ($\Delta E=h\nu$) by the ground state, S_0, raises the molecule in energy terms into the vibrational level of a specific excited electronic state, S_n, within the singlet manifold. The value of n is determined by the wavelength of the absorbed radiation.

RADIATIVE TRANSITIONS

FLUORESCENCE

The radiation emitted when the transition is between states of the same multiplicity is termed **fluorescence**. The excited state rapidly undergoes **vibrational relaxation**, losing vibrational energy as heat to the surrounding medium, and (if in a higher electronic state initially) will undergo **internal conversion**, resulting in the molecule occupying the lowest vibrational energy level of the first excited state, S_1. Fluorescence will normally only occur from this level (Kasha's rule).

$$S_1 \text{ -----> } S_0 + h\nu_f \qquad \text{fluorescence}$$

The consequence of this relaxation is that the longest absorbed and shortest emitted wavelength maximum usually corresponds to the 0-0 transition. A mirror image relationship then usually exists between

absorption and emission spectra.

PHOSPHORESCENCE

Phosphorescence results from a radiative transition between states of different multiplicity, usually

$$T_1 \text{ -----> } S_0 + h\nu_p \qquad \text{phosphorescence}$$

The emission from T_n states (where n=2,3,4...) is very rare.

Population of the triplet manifold by direct singlet-triplet absorption is very inefficient because such transitions are forbidden, due to the change in electron spin quantum number and the relatively large energy gap between the states (typically 240 kJ mol^{-1}). Instead, the triplet manifold is usually entered indirectly, by excitation into the singlet manifold followed by **intersystem crossing** to the triplet manifold (where ΔE is typically 60 kJ mol^{-1}, allowing overlap between the vibrational levels). Just as with the singlet manifold, **vibrational relaxation** and possibly **internal conversion** follow. These processes within the triplet manifold are spin-allowed and occur at a comparable rate to the analogous processes within the singlet manifold. As a consequence, the molecule ends up in the lowest vibrational level of the T_1 state. Emission of a photon can then give rise to phosphorescence, or other non-radiative paths may compete to deactivate the triplet state.

A typical energy relationship between absorption, fluorescence and phosphorescence is shown below. Phosphorescence is at a higher wavelength than fluorescence, reflecting the lower electronic energy of the triplet state [9].

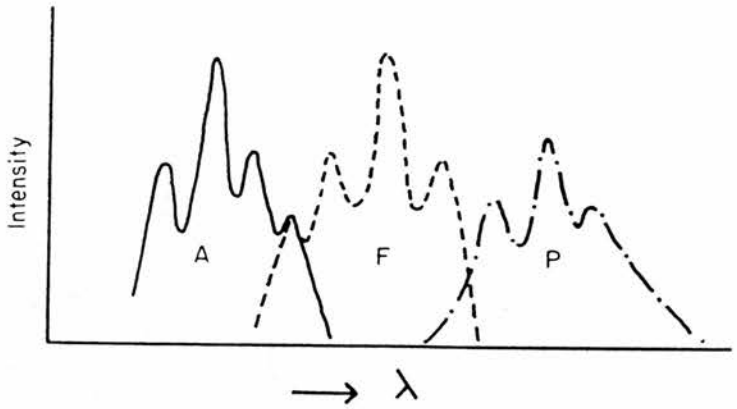

FIGURE 1.3

Energy Relationship Between Absorption, A, Fluorescence, F, and Phosphorescence, P

(Taken from D. Phillips, Polymer Photophysics, p. 4 [9])

RADIATIONLESS TRANSITIONS

Radiationless transitions occur between isoenergetic vibrational levels of different electronic states. Since there is no change in the total energy of the system, no photon is emitted. These are represented by a wavy arrow on the Jablonski diagram.

INTERNAL CONVERSION

Internal conversion is a radiationless transition between isoenergetic states of the same multiplicity. Such transitions between upper states (e.g. S_m ~~~> S_n or T_m ~~~> T_n) are extremely rapid, accounting for the negligible emission from the upper states. Internal conversion from the first excited singlet state (S_1 ~~~> S_0) is so much slower that fluorescence can compete.

INTERSYSTEM CROSSING

This is defined as a radiationless transition between states of different multiplicity. The radiationless deactivation of the lowest triplet (T_1 ~~~> S_0) is a process in competition with normal phosphorescence. The intersystem crossing (S_1 ~~~> T_1) or (S_1 ~~~> T_n) is the process by which the triplet manifolds are normally populated. S_n ~~~> T_n transitions are rare because intersystem crossing has to compete with rapid internal conversion to S_1. The transition T_1 ~~~> S_1 requires thermal activation of T_1 to a vibrational level isoenergetic with S_1 : it is the basis of one of the mechanisms leading to delayed fluorescence and will be discussed in more detail later.

A summary of all these processes and their associated rates [3] is displayed in Table 1.1.

QUANTUM YIELDS [3-7]

The fluorescence quantum yield, ϕ_F, is defined as the ratio of the number of photons emitted from the lowest singlet excited state to the number of photons absorbed. The phosphorescence quantum yield, ϕ_P, is defined as the ratio of the number of photons emitted by the lowest excited state to the number absorbed. However, because the photons do not excite the molecule into the triplet manifold initially, ϕ_P is a composite quantity : it is the product of the triplet quantum yield, ϕ_T, and the phosphorescence quantum efficiency, θ_P.

$$\phi_P = \theta_P . \phi_T$$

ϕ_T is the fraction of molecules ending up in T_1 ; θ_P is the

fraction of molecules in T_1 which emit a photon.

Some examples of ϕ_F, ϕ_T and ϕ_P are listed below [5].

Compound	ϕ_F	ϕ_T	ϕ_P
Naphthalene	0.19	0.82	0.05
Benzophenone	$4x10^{-6}$	1.00	0.74
Anthracene	0.27	0.75	0.0002

TABLE 1.1

THE PRIMARY PHOTOPHYSICAL PROCESSES.

PROCESS	DEFINITION	RATE s^{-1}
Absorption $S_0 \rightarrow S_1$	Promotion of an electron from the electronic ground state to an electronically excited level.	10^{15}
Internal Conversion $S_i \rightarrow S_1$ $i>1$	Non-radiative transition between two different electronic states of the same molecule which have the same multiplicity.	10^{11}-10^{15}
Vibrational Relaxation $S_i \rightarrow S_i$	Transitions from non-equilibrium vibrational energy distribution in a given electronic state to a thermally equilibriated vibration energy distribution relative to the zero point energy of the same state.	$>10^{12}$
Intersystem Crossing $S_1 \rightarrow T_1$	Non-radiative transition from an electronic state of a given spin multiplicity to an electronic state of different multiplicity.	10^{8}
Internal Conversion $S_1 \rightarrow S_0$	Non-radiative transition between two electronic states of the same multiplicity.	10^{5}-10^{7}
Fluorescence $S_1 \rightarrow S_0+h\nu$	Radiative transition between two states of the same multiplicity.	10^{7}-10^{9}
Phosphorescence $T_1 \rightarrow S_0+h\nu$	Radiative transition between two states of the same molecule which have different spin multiplicities.	10^{3}-10^{-1}

THE KINETICS OF PHOTOLUMINESCENCE AND DEFINITION OF LIFETIME

The photophysical scheme discussed so far in the deactivation of excited states is listed below [3-5]. All these processes are unimolecular.

Process		Rate
$S_0 + h\nu \text{ -----> } S_1^*$	Excitation	I_A
$S_1^* \text{~~~~~> } S_0$	I.C.	$k_{ic}[S_1^*]$
$S_1^* \text{-----> } S_0 + h\nu_F$	Fluorescence	$k_F[S_1^*]$
$S_1^* \text{~~~~~> } T_1^*$	I.S.C.	$k_{isc}[S_1^*]$
$T_1^* \text{~~~~~> } S_0$	I.S.C.	$k'_{isc}[T_1^*]$
$T_1^* \text{~~~~~> } S_0 + h\nu_P$	Phosphorescence	$k_P[T_1^*]$

where * denotes an excited state.

Using the steady state hypothesis, which applies to conditions of constant illumination, the rate of formation of the intermediates will equal their rate of removal. Thus,

(a) Rate of formation of S_1 = rate of removal of S_1

$$I_A = (k_{ic} + k_F + k_{isc})$$

(b) Rate of formation of T_1 = rate of removal of T_1

$$k_{isc}[S_1] = (k'_{isc} + k_P)[T_1]$$

The phosphorescence quantum yields for this scheme can now be given as

$$\phi_F = \frac{k_F}{k_{isc} + k_F + k_{ic}}$$

$$\phi_T = \frac{k_{isc}}{k_{isc} + k_F + k_{ic}}$$

$$\theta_P = \frac{k_P}{k_P + k'_{isc}}$$

The observed lifetime, τ, of an excited state is defined as the inverse sum of all the rate processes which deactivate the excited state.

i.e. $\tau = 1/k_x$ where $k_x = \Sigma(k_i)$

Simple expressions for fluorescence and phosphorescence lifetimes can easily be derived from this equation:

$$\tau_P = \frac{1}{k'_{isc} + k_P}$$

$$\tau_F = \frac{1}{k_F + k_{isc} + k_{ic}}$$

Measurements of the lifetimes τ_P and τ_F will give information on the physical processes undergone by excited state molecules. In this present study, phosphorescence lifetimes are obtained by monitoring the decay of the emitted radiation with time. The decay of phosphorescence is very often first order, and in such instances the rate of decay can be written as

$$\frac{-d[A]}{dt} = k_x[A^*]$$

Integration yields

$$[A^*]_t = [A^*]_0 \exp(-k_x t)$$

which can be rewritten as

$$\ln[A^*]_t = \ln[A^*]_0 - k_x t$$

where $[A^*]_0$ and $[A^*]_t$ are the concentrations of triplet species at times t=0 and t=t respectively.

Hence the value of k_x can be obtained from a plot of ln(phos. intensity) versus time. The resulting slope is linear and the decay is termed exponential. The lifetime obtained is the observed lifetime : it must be noted that the intrinsic lifetime, τ_0, which is sometimes referred to, is defined as the lifetime when no non-radiative processes are occurring.

i.e. $\tau_0 = 1/k_P$ for phosphorescence

However, not all phosphorescence decays are exponential. There may be other routes, some bimolecular, which can compete to deactivate the triplet state.

DELAYED FLUORESCENCE [3-7]

A further deactivation process associated with the triplet state is that of delayed fluorescence. Delayed fluorescence can occur in two separate ways, by thermal depopulation of T_1 to S_1 or by triplet-triplet annihilation. The former process is known as E-type delayed fluorescence and the latter as P-type delayed fluorescence.

E-TYPE DELAYED FLUORESCENCE

E-type delayed fluorescence, which was first observed in eosin, is simply the reverse of the T_1 --> S_1 intersystem crossing process and it occurs when the T_1 - S_1 energy gap is small.

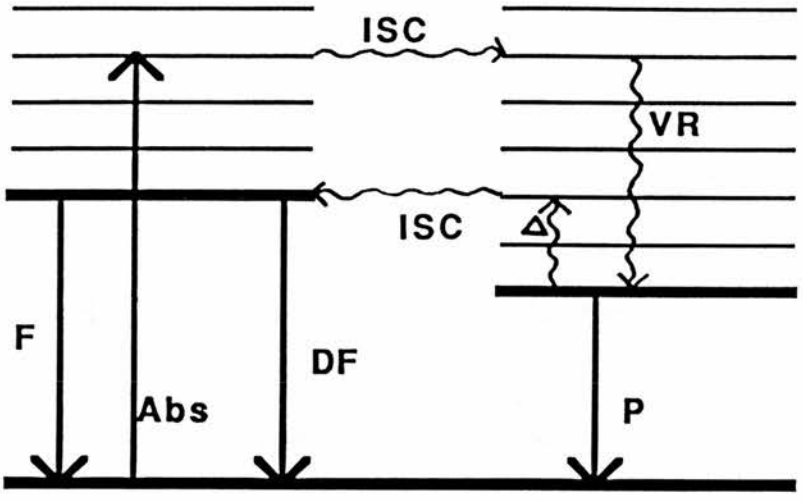

FIGURE 1.4: E-TYPE DELAYED FLUORESCENCE

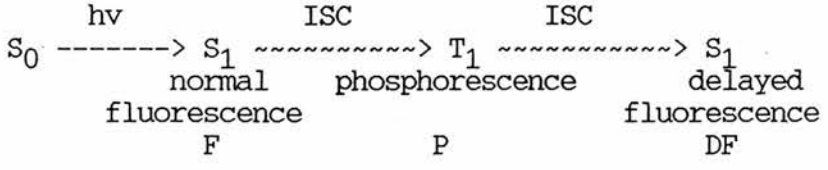

The fluorescence of this newly-populated singlet state has the same spectral distribution as normal fluorescence, but its lifetime is

the same as the phosphorescence lifetime. This is the usual diagnostic test for E-type fluorescence. Since the singlet states responsible for this delayed emission are thermally populated, the intensity of E-type fluorescence should increase with temperature, with an activation energy corresponding to the energy gap between S_1 and T_1. However, when the energy gap exceeds about 40 kJ mol^{-1}, E-type emission is insignificant at normal temperatures. E-type fluorescence is observed mainly in dye molecules and does not normally occur in aromatic molecules because the singlet-triplet energy gap is relatively large.

P-TYPE DELAYED FLUORESCENCE

P-type delayed fluorescence, first observed in pyrene, occurs for many aromatic hydrocarbons in fluid solution, concentrated rigid solution and in the crystal phase. This process arises when the triplet lifetimes are sufficiently long that an encounter occurs between them. The net result of this bimolecular interaction between pairs of triplet-excited molecules which have total energy greater than S_1 is the formation of two singlet states, one of which may be excited.

$$T_1 + T_1 \text{ -----> } S_1 + S_0$$

Then,

$$S_1 \text{ -----> } S_0 + h\nu$$

and/or

$$T_1 + T_1 \text{ -----> } 2S_0$$

Obviously, this triplet-triplet annihilation process is most likely to occur when a high concentration of triplets is present. In fluid solution it is believed that the triplet-excited molecules

interact by a diffusion-controlled process, whereas in rigid media and in crystals, triplet energy migration occurs.

The lifetime of the P-type delayed fluorescence is approximately half the triplet lifetime and the intensity of the delayed fluorescence is dependent of the square of the incident light. This, however, is not always the case in polymer systems.

ENERGY TRANSFER [3-7]

Energy transfer is another process whereby the energy of electronically excited molecules can be dissipated. This is an intermolecular process, where an excited state donor D^* collapses to its ground state with the simultaneous transfer of its energy to an acceptor molecule A which is promoted to an excited state.

$$D^* + A \text{ -----> } D + A^*$$

It should be noted that the acceptor can itself be an excited state, as in the case of triplet-triplet annihilation.

$$^3M^* + {}^3M^* \text{ -----> } {}^1M^* + {}^1M$$

The quenching of the emission associated with D^* and its replacement by the emission of A^* is observed. Hence, although photons are absorbed by D^*, it is A that becomes excited. The processes resulting from A^* generated in this manner are said to be sensitised. When the donor and acceptor are identical, the term energy migration is used.

Energy transfer can be divided up into the following mechanistic steps:

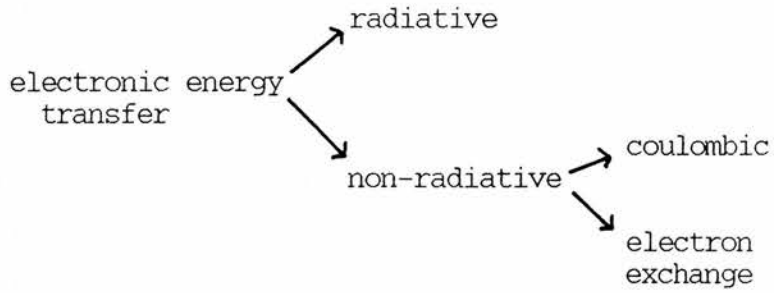

RADIATIVE ENERGY TRANSFER

This depends on the capture by the acceptor of photons emitted by the donor.

$$D^* \text{ -----> } D + h\nu$$

$$A + h\nu \text{ -----> } A^*$$

This is a long-range process and is dependent on

(i) The quantum efficiency of emission by the donor

(ii) The number of acceptor molecules in the path of the photon

(iii) The light absorbing power of the acceptor

(iv) The extent of overlap between the emission spectrum of the donor and the absorption spectrum of the acceptor.

The efficiency of this 'trivial' process is also dependent on the shape and size of the vessel used, since photons emitted near the walls have less chance of capture by the acceptor than those emitted in the

centre of the cell. By dispersing the sample in thin polymer films, this process is considerably reduced.

COULOMBIC INTERACTION

Energy transfer of this type is a long-range process, effective over 5-10nm. As the donor relaxes to the electronic ground state, the transition dipole moment, instead of leading to the emission of a photon, interacts by simple electrostatic (Coulombic) repulsion with the transition dipole involved in electronic excitation of the acceptor.

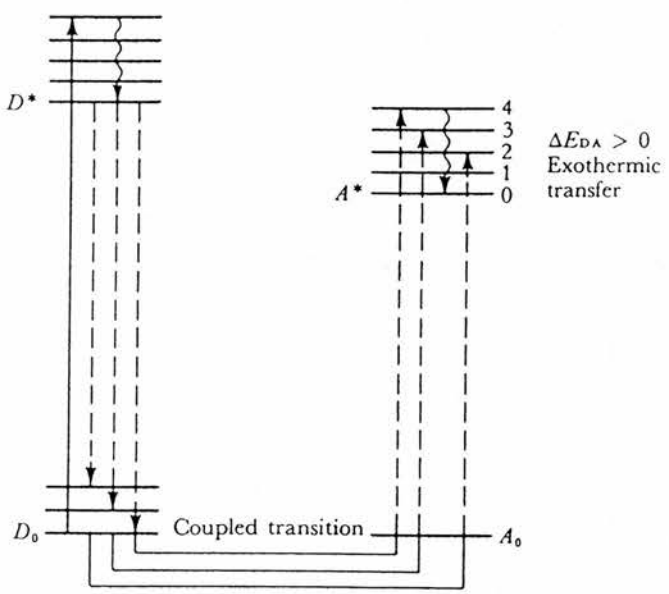

Coupled Energy Transfer Between Excited Donor, D^*, and Acceptor, A.

(Taken from N.J. Turro, Molecular Photochemistry, p97[4])

Förster [10] developed a detailed theory of energy transfer by this mechanism. He showed that the rate constant (s^{-1}) for this dipole-dipole energy transfer between a donor D and acceptor A is

$$k_{ET} = 1.25 \times 10^{17} \frac{\phi_E}{n^4 \tau_D r^6} \int F_D(v) \epsilon_A(v) \frac{dv}{v^4}$$

where ϕ_E is the quantum yield for donor emission, τ_D is the lifetime of emission, n is the solvent refractive index and r is the distance in nm between D^* and A. $F_D(v)$ is the emission spectrum of the donor, expressed in wavenumbers, scaled such that the area under the spectrum is equal to 1

$$\text{i.e.} \quad \int_0^\infty F_D(v)\, dv = 1$$

and $\epsilon_A(v)$ is the molar absorption coefficient of the acceptor at wavenumber v.

For most purposes, it is not the absolute rate of energy transfer that is important, it is the rate relevant to other possible processes. It is useful to define a distance, R_0, at which the probability of emission and energy transfer are equal. The value of R_0, the critical transfer distance in nm, is given by

$$R_0^6 = 1.25 \times 10^{17} \frac{\phi_E}{n^4} \int F_D(v) \epsilon_A \frac{dv}{v^4}$$

Typical values for R_0 lie between 4-7nm.

The requirements for rapid and efficient energy transfer by dipole-dipole, i.e. R_0 large, are listed below:

(i) Good spectral overlap between emission of the donor and the absorption of the acceptor.

$$\text{i.e.} \quad \int_0^{\infty} F_D(\nu)\, \epsilon_A(\nu)\, \frac{d\nu}{\nu^4} \quad \text{is large}$$

(ii) The transition corresponding to the emission of the donor should be allowed (necessary for ϕ_E large).

(iii) The relevant absorption band(s) of the acceptor should have high absorption coefficients (ϵ_A large).

(iv) There should be a favourable orientation of the transition dipoles.

The only allowed Coulombic energy transfer processes are those in which there is no change in spin in either component. Thus

$$D^*(S_1) + A(S_0) \text{ -----> } D(S_0) + A^*(S_0)$$

$$D^*(S_1) + A(T_1) \text{ -----> } D(S_0) + A^*(T_n)$$

are fully allowed Coulombic processes.

The process

$$D^*(T_1) + A(S_0) \text{ -----> } D(S_0) + A^*(S_1)$$

is spin forbidden, but is observed. This is because the slower rate for the spin-forbidden process is compensated for by the relatively long lifetime of the T_1 state, and long-range energy transfer can compete effectively with phosphorescence and $T_1 \sim\sim\sim\sim\sim>$ intersystem crossing as a means of deactivating the triplet state of organic molecules.

EXCHANGE ENERGY TRANSFER

Exchange energy transfer from a donor D^* to an acceptor A will occur when the donor and acceptor molecules are very close together, so that the electron clouds tend to overlap in space. The transfer process

can be written as

$$D^* + A \text{ -----> } (D\cdots A)^* \text{ -----> } D + A^*$$

During the existence of the transient bimolecular intermediate, electrons can be exchanged between the donor and acceptor molecules, and energy transfer thus takes place. Because of the intervention of this intermediate, the energy transfer is subject to conservation of electron spin. Under Wigner's spin rules, the following processes are allowed.

$$D^*(S_1) + A(S_0) \text{ -----> } D(S_0) + A^*(S_1) \quad \text{singlet-singlet}$$

and

$$D^*(T_1) + A(S^0) \text{ -----> } D(S_0) + A^*(T_1) \quad \text{triplet-triplet}$$

The efficiencies of such processes depends on the relative energies involved in the transfer steps. If the energy of D^* is greater than A^*, then transfer is relatively efficient, but when the reverse is the case, the transfer is relatively inefficient.

A mathematical equation for the exchange mechanism has been derived by Dexter [11]

$$k_{ET} \quad \alpha \quad e^{-2R/L} \int_0^\infty F_D(v)\ \epsilon_A(v)\ dv$$

where R is the distance between D^* and A, and L is a constant. $F_D(v)$ and $\epsilon_A(v)$ have both been normalised to unity.

The negative exponential term shows that energy transfer by this mechanism is a short range phenomenon, effective over, typically, 0.6 - 1.5nm.

QUENCHING [3-7]

A substance which accelerates the decay of an excited state to the ground state or to a lower electronically excited state is described as a quencher and is said to quench that state. It is a reversible effect, in which removal of the quenching agent restores the original luminescence intensity, and requires collisional or close interactions between the two molecules involved.

The process can be represented as

$$M^* \xrightarrow{Q} M'$$

where M' is the ground state or another excited state of M and Q is the quencher.

Oxygen is a very efficient and ubiquitous quencher of the excited state and is the most probable cause of confusion in the measurement and interpretation of the excited state. Consequently, in studies of the triplet state, it is essential to reduce the concentration of dissolved oxygen to the smallest possible value, and to use carefully purified solvents and solutes.

Other effective quenchers of the triplet state are

(a) Nitrous oxide and aromatic triplets ($k_Q \approx 10^9 - 10^{10}$ mol s^{-1})

(b) Metal ions of the first transition series and the rare earth lanthanides ($k_Q \approx 10^7 - 10^9$ mol s^{-1})

(c) Paramagnetic molecules if energy transfer is energetically possible

(d) In some cases, a chemical quenching may occur, as for example with the carbonyl compounds which abstract hydrogen atoms.

$$^3(C_6H_5)_2CO + RH \longrightarrow (C_6H_5)_2COH + R\cdot$$

$$2(C_6H_5)_2COH \text{ -----> benzpinacal} \quad k_Q \approx 10^5 \text{ mol } s^{-1}$$

(e) Concentration quenching is also a commonly observed process. As the concentration of the solute increases, there is a decrease in the quantum yield.

e.g. in pyrene, the violet fluorescence in dilute solution is gradually replaced by a blue fluorescence with increasing pyrene concentration.

$$M + h\nu \xleftrightarrow{} {}^1M^* \xleftrightarrow[\text{fluorescence}]{} {}^1(MM^*) \xleftrightarrow{} \underset{\text{fluorescence}}{M + M + h\nu}$$
monomer excimer excimer

PHOTOCHEMICAL REACTION [3]

Another route to deactivation of the excited state is via photochemical reaction. The vast majority of photochemical reactions occur when a molecule is raised to either S_1^* or T_1^*. The likelihood of a photochemical reaction occurring is dependent on the rates of the other energy dissipation processes, i.e. an excited state may lose its excess energy and return to the stable ground state before a photochemical reaction can occur.

CHAPTER 2

CHAPTER 2

EXPERIMENTAL METHODS

A MATERIALS

1 Solvent Purification [12]

Most solvents were dried and redistilled prior to use.

2 Solute Purification [12]

Carbazole (BDH), N-ethylcarbazole (Aldrich) and naphthalene (M&B) were purified by recrystallisation from freshly distilled ethanol three times. Carbazole and N-ethylcarbazole were dried in an oven at 100^0C, and naphthalene at 60^0C.

3 Purification of Monomers [12]

Styrene (Aldrich) and methyl methacrylate (Aldrich) monomers were washed several times with 5% w/v NaOH to remove inhibitors, and then twice with water. Styrene was dried for several hours over $MgSO_4$ and redistilled under reduced pressure. Methyl methacrylate was dried over Na_2CO_3, then with CaH_2 and was redistilled from CaH_2 under reduced pressure. Both were stored in a cool, dark environment over Linde type 4A molecular sieve.

4 Purification of Polymers [12]

Poly(methyl methacrylate) (BDH) and polystyrene (BDH) were purified by dissolving the polymer in CH_2Cl_2, then reprecipitating from a large volume of methanol. Best results were obtained if the polymer

solution was added dropwise to the methanol, and the precipitation process was agitated with a rapidly vibrating stirrer.

A similar technique was used for poly(vinyl acetate) purification, except the precipitating solvent was petroleum ether (40 - 60^0C), and there was no agitation since this resulted in the polymer drops aggregating together.

After repeating this process three times, the polymer was dried in a vacuum oven for one week.

5 Preparation of Copolymers

A range of methyl methacrylate / vinyl carbazole copolymers were prepared by a free radical polymerisation at 60^0C under high vacuum. The reaction vessel containing the starting monomers, 10^{-3}M *AIBN initiator and benzene solvent was thoroughly degassed by several freeze/pump/thaw cycles and sealed under vacuum. The sample tube was then heated in an oven at 60^0C for approximately 18 hours. The resulting copolymer was dissolved in dichloromethane, filtered and reprecipitated from methanol. This purification procedure was repeated at least four times to ensure complete removal of the unreacted monomer. The copolymers were then dried in a vacuum oven for one week at room temperature.

^{1}H nmr spectra run on each copolymer sample showed that the vinyl carbazole had been incorporated into the polymer; however it was not possible to determine the copolymer composition from such spectra since the vinyl carbazole: methyl methacrylate integral ratio was too small.

The composition of each copolymer was obtained by C-H-N analysis. Further characterisations of the copolymers included Tg, obtained by differential scanning calorimetry (Perkin-Elmer DSC 7), and molecular

weight distribution, using Gel Permeation Chromatography supplied by RAPRA Technology Ltd.

* 2,2-azobis-2-methylpropionitrile (Aldrich)

6 Preparation of Deuterated Polystyrene (d-Psty)

Since only 2g of styrene-d^8 monomer was available, no attempt was made to remove the 0.5% hydroquinone inhibitor since this would involve loss of monomer. As with the copolymer samples, the monomer/AIBN/benzene solution was degassed by several freeze/thaw cycles and the ampoule sealed. The solution was heated at 60^0C for 5 days to ensure a relatively high molecular weight sample which could easily be precipitated from methanol. A small quantity of CH_2Cl_2 was added to the resulting viscous solution, and the polymer reprecipitated twice from methanol.

Yield: 1.42g (71%)

7 Preparation of $Pr(NO_3)_3$.[18-crown-6] [13,14]

18.5g (0.007 moles) of 18-crown-6 in 30 ml of acetonitrile was added to 2.93g (0.007 moles) of $Pr(NO_3)_3.5H_2O$ in 10 ml of the corresponding solvent. The reaction was carried out at room temperature. A light green precipitate formed after a few minutes. The mixture was stirred vigorously for an hour. After standing for a further hour at room temperature, the crystalline complex was filtered, washed with two 10 ml portions of acetonitrile and dried for 5 days in a vacuum dessicator over P_2O_5.

Analysis:	% C	% H	% N
calc.	24.38	4.09	7.11
actual	24.54	4.17	7.24

The IR spectrum (nujol mull) is the same as reported spectra [13,14].

8 Preparation of 3-Bromocarbazole [15]

6.68g carbazole in 20 ml pyridine was left standing at room temperature for 2 hours with 6.4g bromine in 10 ml pyridine. The reaction mixture was then poured into 6N HCl, the resulting precipitate washed with water and dried in a vacuum dessicator over P_2O_5.

The dried product was reprecipitated three times from toluene and dried in a vacuum dessicator.

Analysis:	% C	% H	% N
calc.	58.57	3.28	5.69
actual	60.64	3.01	5.77

The ^1H nmr spectrum was the same as reported spectra [15].

9 Film Preparation

Preparation of the thin molecularly doped polymer films proceeded in the following manner:

0.5g of the polymer was weighed out. Since the concentration of the dopant was too small to be weighed out easily, a stock solution in CH_2Cl_2 (Aldrich spectroscopic grade) was prepared, from which films were cast. The variation in dopant concentration was made by dilution of the stock solution, and the concentration in each film calculated from the volume of solution added to the polymer, knowing the density of each polymer. Films were cast by placing 5 ml of the dopant/polymer mixture onto a carefully cleaned 6cm diameter Petri dish. The dish was covered

by a large beaker and the solvent slowly allowed to evaporate, thus ensuring the formation of optically clear films. This film casting procedure was always carried out in a dark environment.

After several hours, the film was loosened from the Petri dish by cooling with liquid nitrogen and secured onto a cardboard sheet to prevent buckling. It was then pumped out for one week in a vacuum oven at room temperature to ensure complete removal of traces of dichloromethane solvent.

10 Preparation of deuterated Psty Films

It was not possible to cast a film of d^8-Psty, since on evaporating off the solvent, the matrix crystallised. A film containing 87.5% d^8-Psty / 12.5% Psty was an improvement on the pure Psty, but could still not be used. A 50% Psty / 50% d^8-Psty matrix containing 0.0029M carbazole was the only film successfully cast from CH_2CH_2.

STRUCTURAL FORMULAE OF THE MATERIALS USED IN THIS STUDY

POLYMERS

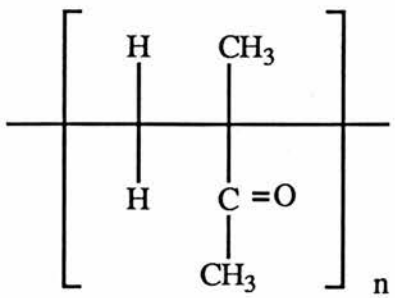

Poly(methyl methacrylate)

(PMMA)

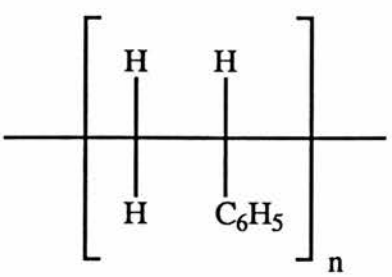

Polystyrene

(Psty)

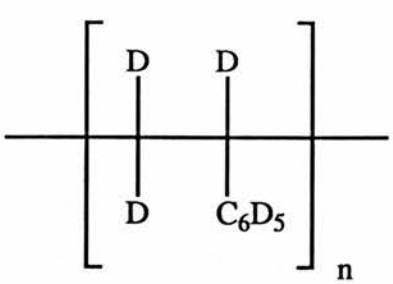

d^8-Polystyrene

(d^8Psty)

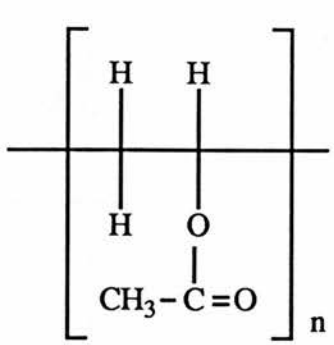

Poly(vinyl acetate)

(PVA)

ADDITIVES

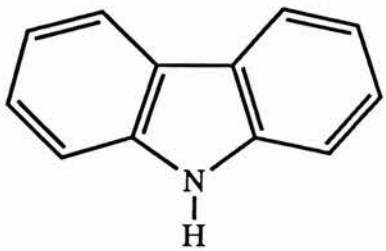

Carbazole

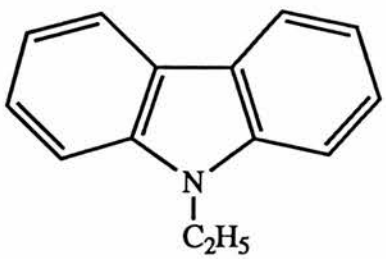

N-ethyl carbazole

(NEC)

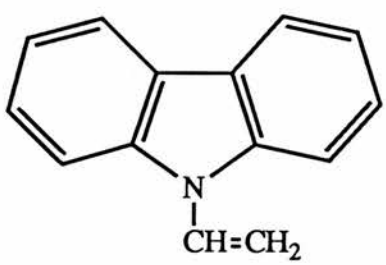

Vinyl carbazole

QUENCHERS

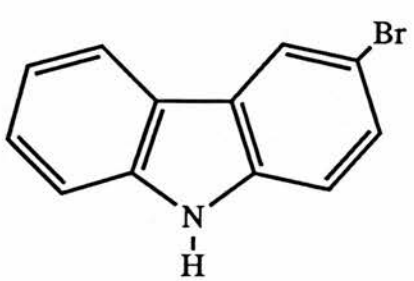

3-Bromocarbazole

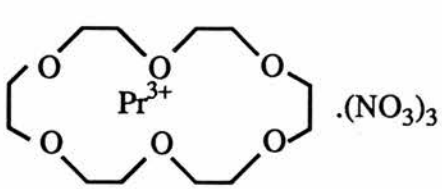

Pr(18-crown-6) $(NO_3)_3$

B APPARATUS

1 Phosphorescence Lifetime Apparatus

A schematic diagram of the layout of the components of this apparatus is shown in Figure 2.1. The overall layout and operation of this equipment will now be discussed, and individual components described later.

(a) Layout and operation

The excitation source was a Lambda Physik pulsed nitrogen laser, emitting very intense monochromatic radiation at 337.1 nm. The excellent reproducibility of each pulse minimises noise levels.

The laser was linked to the sample compartment by a cylindrical light tunnel, fitted with a variable iris/shutter system. Thus, if necessary, the dimensions of the excitation beam could be varied, or it could be cut off from the sample completely. A 337.1 nm filter, or various neutral density filters could easily be slotted in front of the beam if required.

The sample compartment was essentially a large metallic box, sprayed matt black on the inside to minimise internal light reflections. The wooden lid, which was in two sections, had a circular opening which had been cut to accommodate the cryostat. When the laser was in operation, the excitation beam passing through the iris would strike the sample, held in the cryostat under vacuum at the desired temperature. The sample holder was positioned at approximately 45^0 to the incident beam. The resulting emission, viewed at 90^0 to the direction of excitation, was focussed by a quartz lens onto the input slit of a high quality grating monochromator. The input and exit slits of the monochromator were set at 5nm and 20nm respectively. Phosphorescence

selected by the monochromator was detected at the exit slit by a photomultiplier.

The pulsed N_2 laser, running at 100 Hz, is essentially being used as a continuous source. The lifetimes of the molecules studied were typically 2-10 seconds, so therefore only minimal decay has taken place before the next pulse arrives to excite the molecule.

After establishing a steady state concentration of triplet species, the laser was switched off. The missing pulse detector, adapted to trigger when pulses reduce to less than 20Hz, sends a single trigger pulse to the Datarecorder Signal Averager, thus starting collection of the phosphorescence decay. The Datarecorder stores 2000 points over a scan. The scan time is selected on the Datarecorder. To improve the signal to noise ratio, nine or sixteen scans were averaged. If noise is random, then it is expected that it will eventually average to zero while the signal tends to its true value. It can be shown that the signal to noise ratio improves as the square root of the number of scans. The decay curve is viewed on an X-Y oscilloscope.

The resulting 2000 data points were transferred to the University VAX mainframe computer via a BBC microcomputer. The were processed by a smoothing algorithm, written in Fortran, which gave equal weight to each original point to reduce the number of data points. This reduced data was then plotted out and analysed using the Minitab statistical package available on the VAX.

All decays discussed here, unless stated otherwise, were studied at 410nm.

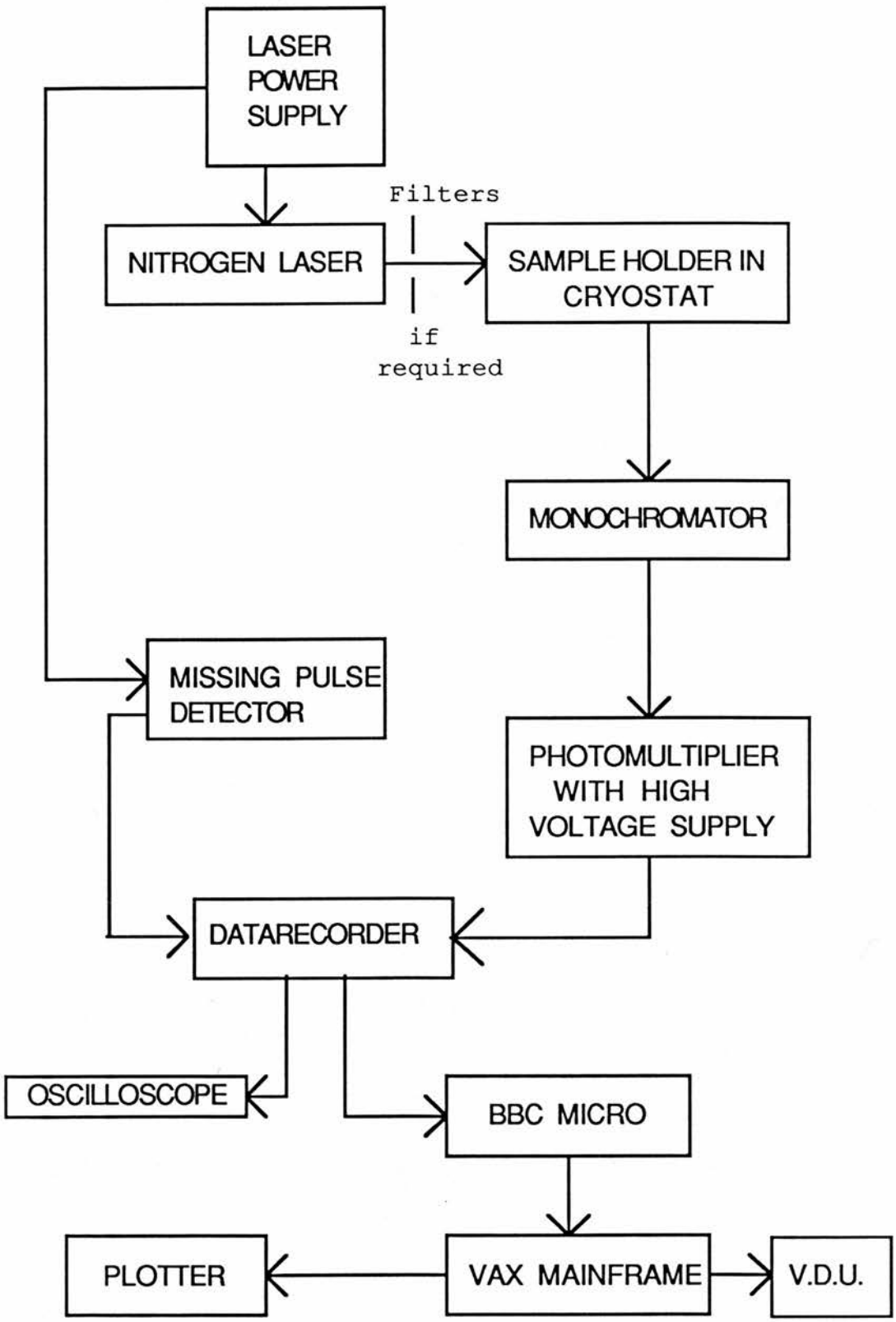

PHOSPHORESCENCE LIFETIME APPARATUS

FIGURE 2.1

FIGURE 2.2

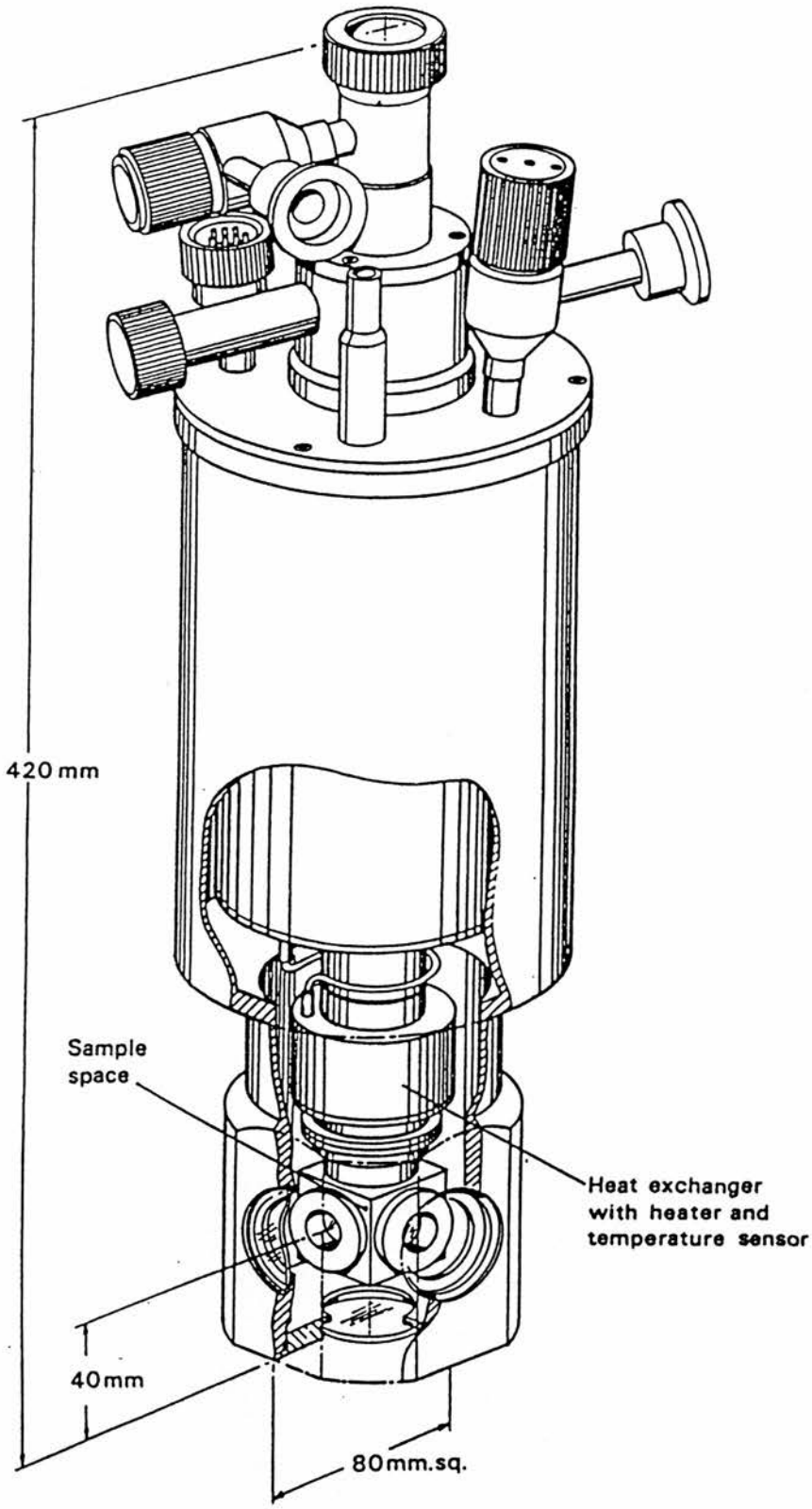

THE CRYOSTAT

FIGURE 2.3

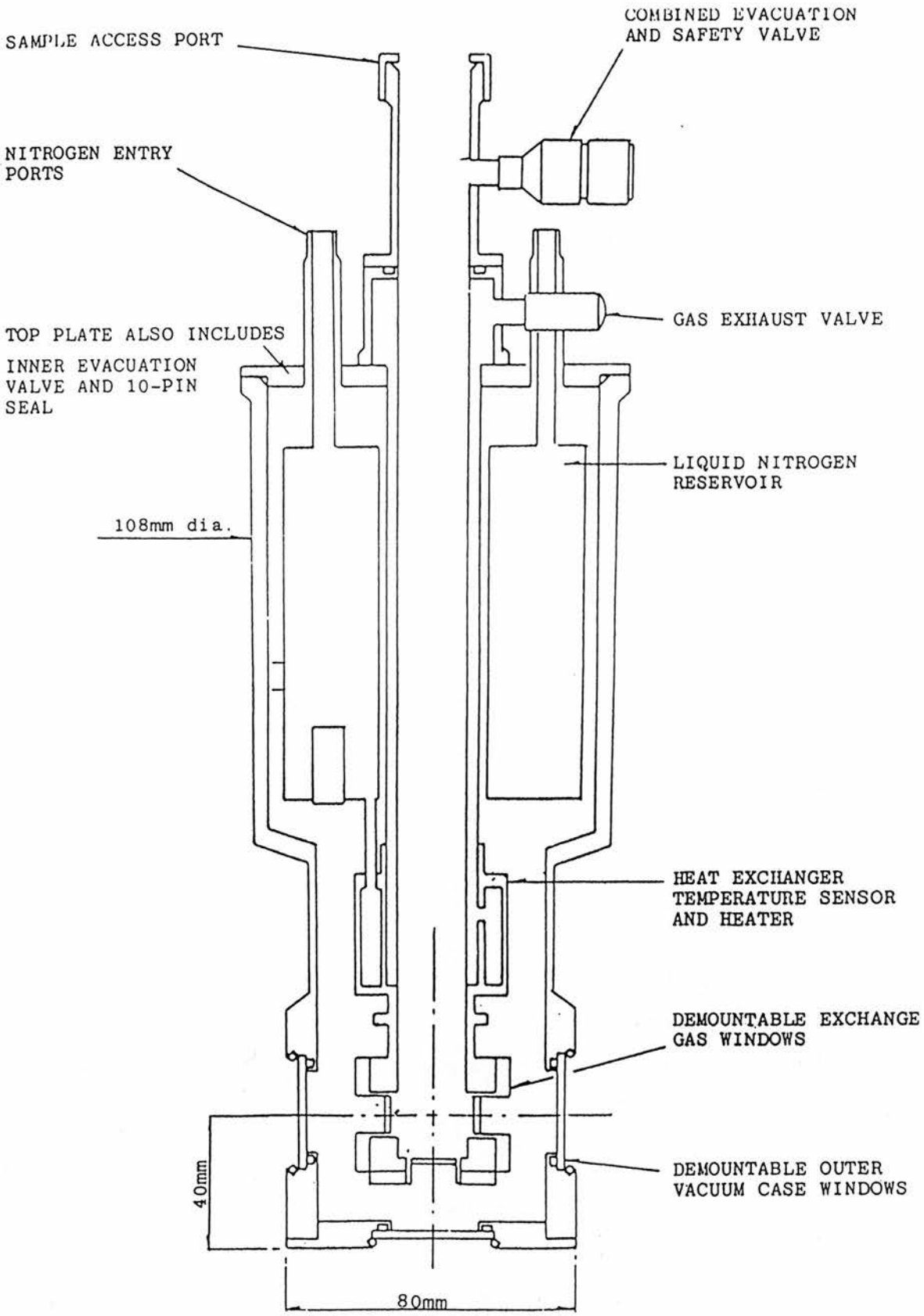

THE CRYOSTAT

(b) The Cryostat and Temperature Controller

Throughout this work, temperature variation and control of the polymer sample was achieved using an Oxford Instruments cryostat, shown schematically in Figure 2.2 and Figure 2.3 (type A2597 cryostat with DCT2-digital temperature controller). The sample temperature could be varied between 77K and 300K with an accuracy of better than ± 0.2K.

The cryostat operates on the principle of the controlled continuous transfer of liquid nitrogen from a reservoir to a heat exchanger which surrounds the sample. The coolant flows from the 650 cc nitrogen reservoir down the feed capillary and into the copper heat exchanger. It leaves the heat exchanger by a stainless steel tube and passes through a capillary before exhausting through a valve at the top plate.

A platinum temperature sensor and a non-inductively wound heater are fixed to the heat exchanger. The temperature controller is fitted to these via a 10-pin feed on the top plate of the cryostat.

The windows on the cryostat are made of synthetic sapphire which has good light transmission properties.

Before use, the cryostat was evacuated overnight using the standard combination of rotary oil and oil diffusion pump. A liquid nitrogen trap was placed immediately in front of the outlet on the vacuum line leading to the cryostat so that any moisture which may have accumulated in the cryostat could be removed. This process normally needed to be repeated every 3-4 weeks due to loss of the vacuum through time.

Since phosphorescence has been shown to be sensitive to triplet quenchers, particularly oxygen, the polymer film held in the sample holder within the cryostat was pumped out overnight prior to use and held under vacuum for the duration of the experiment. The sample holder

was sealed by an 'O' ring.

(c) Analysis of Data

The data was plotted out on a Hewlett Packard 7470A plotter. Plots of phosphorescence intensity versus time and Ln(phosphorescence intensity) versus time were normally obtained.

The rate constant, k_τ, was obtained from the Ln(phos. intensity) plot, using the Minitab statistical package regression analysis commands. The gradient is $-k_\tau$. From this the lifetime was easily calculated.

$$\tau = 1/k_\tau$$

Minitab also calculates a value for R-sq, which gives an indication of the linearity of the slope.

Values of lifetime quoted for decays which showed initial non-exponential behaviour were estimated assuming the terminal decay to be exponential, unless otherwise stated. This assumption is not completely valid, and in some cases the lifetimes depended on the interval over which the decay was measured; these values should therefore be regarded as approximate. Lifetimes were generally reproducible to ± 0.2 seconds with different samples and for measurements made at intervals over several months.

Some use was made of a three variable iterative fitting routine to produce best fits for triplet - triplet annihilation and emission from two species to explain non-exponentiality in some samples. The T-T fitting routine (TRIP) gave a value for k_1 and a value proportional to

k_2, and the double exponential fitting routine (DEX) gave values for the activation energy A, k_1 and k_2 [16] (see Appendix).

2 MAGNETIC FIELD APPARATUS

The effect of a magnetic field on the phosphorescence lifetime was studied, and a schematic diagram of the apparatus is shown in Figure 2.4. The equipment works on the same principal as the phosphorescence lifetime apparatus, but with a few necessary alterations.

The sample, held in an evacuated quartz sample holder, and the electromagnet were accommodated in a wooden box which was sprayed matt black on the inside to minimise light reflections. A special quartz window glass dewar was made to fit between the poles of the electromagnet which were only 1½" apart. The dewar was filled with liquid nitrogen and the sample holder placed in the centre of the poles facing the laser beam. After excitation, the sample emission was viewed straight on, with the monochromator only allowing 410nm light to reach the photomultiplier tube. The operation of the apparatus is the same as described previously for the phosphorescence lifetime equipment. The magnetic field was varied between 0 - 1.25kG.

3 VISCOMETRY

A suspended level viscometer (BS188, type BS/IP/SL, IP71) immersed in a glass window 25^0C thermostat bath was used to determine the limiting viscosity number and average molecular weight of various polymer samples before and after UV degradation. The polymers were dissolved in toluene. The flow times in the viscometer for pure toluene and for the polymer solutions were measured using an electronic timer. The method of calibration of the viscometer and calculations will be discussed in more detail in Chapter 6.

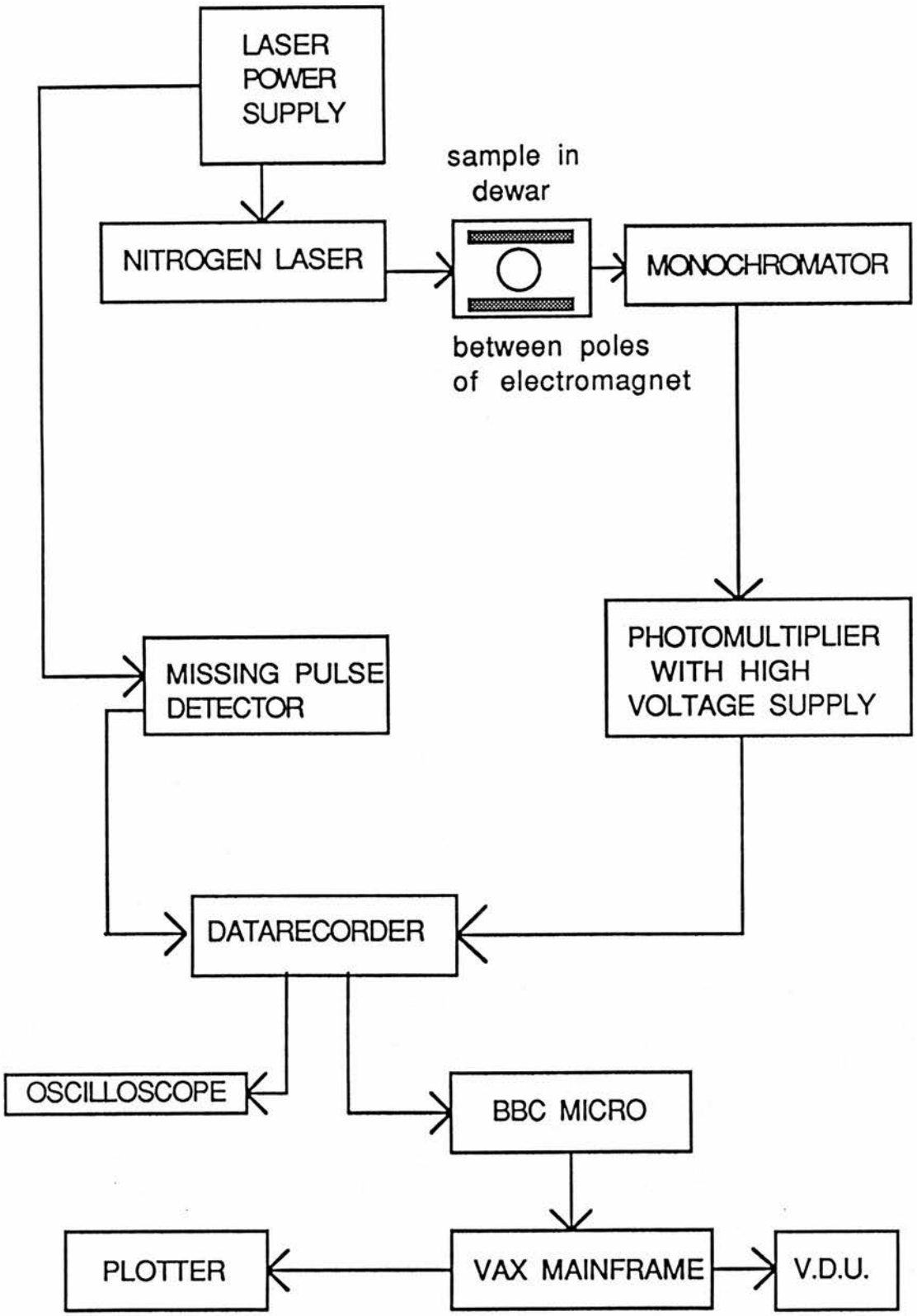

MAGNETIC FIELD APPARATUS

FIGURE 2.4

CHAPTER 3

CHAPTER 3

POLYMERS AS HOSTS

INTRODUCTION

Polymer glasses are convenient matrices for the study of the excited states of organic guest molecules since they can be used over a much wider temperature range than conventional frozen solutions. Before discussing the further advantages of polymer matrices, it is necessary to mention the other commonly used hosts, and their uses and major disadvantages: [17]

(a) Ether-isopentane-alcohol (EPA) glasses are suitable matrices for studying hydrocarbon phosphorescence at 77K, but are limited to this temperature region.

(b) Glycerol, used to observe the phosphorescence of dyes, is only suitable from $-30^{0}C$ to $-130^{0}C$, below which it shatters.

(c) Boric acid glass is a suitable matrix for the observation of phosphorescence at room temperature, but its formation requires the use of high temperatures, which usually causes some decomposition of the solute being studied. The glass is very sensitive to moisture, is difficult to prepare in a reproducible manner and crystallises. It is very difficult to obtain free from impurities.

(d) Glucose is another common matrix for studying the phosphorescence of dyes, but is very sensitive to moisture and often displays strong near-UV absorption.

Poly(methyl methacrylate) and polystyrene are the most commonly

used polymer support matrices since they remain glasses up to fairly high temperatures (Tg_{PMMA} = 114^{0}C ; Tg_{Psty} = 100^{0}C), and can therefore be used over a wide temperature range. Poly(vinyl acetate) can also be used, although because of its lower Tg (30^{0}C), the range of temperatures is slightly more limited. Diffusion of molecules in the solid polymer is very slow, and at temperatures below Tg, thermal motion is considerably reduced. Other advantages of polymer matrices over the alternatives already outlined include the ease of preparation of polymer films containing organic solutes at room temperature, where solute decomposition is negligible, insensitivity to moisture, and optical clarity. Although optical clarity of the polymer film is not essential, it greatly facilitates experimental work since excitation scattering is minimised and more of the bulk is excited, thereby enhancing the emission intensity.

A necessary feature of a polymer matrix is that the absorption spectrum of the polymer should not prohibit the the selective excitation of the guest i.e. the host polymer must absorb shorter wavelength light than the species that is the object of the spectroscopic study. PMMA, Psty and PVA matrices all satisfy this condition since they do not absorb above 290nm. Furthermore, for a matrix to be considered inert, it must not be directly capable of accepting electronic energy or contain a heavy atom since this could interfere with the decay process being studied. Examples of unsuitable polymers include poly(vinyl carbazole) which has a very wide absorption spectrum, poly(vinyl naphthalene) which has a low accessible triplet level, and poly(vinyl chloride) which contains a heavy atom.

It has been suggested that the triplet state of PMMA may be capable of accepting electronic energy from the guest [33,36], therefore questioning the assumption that the polymer matrix is inert. Another

theory is that at the temperatures between T_β (the onset of ester side-group rotation of the matrix) and Tg (the glass transition temperature), a diffusion-controlled quenching reaction of the solute triplet state by side chain ester groups in the polymer is occurring [40,44]. Secondary relaxation processes have also been proposed to affect the triplet state lifetime [27-29,46,47]. These two individual processes will be discussed in more detail later : the important point is that the suitability of polymer matrices as inert hosts is in question.

In this study, the effect of temperature on the phosphorescence lifetime of carbazole and related compounds is investigated in various polymer hosts in an attempt to determine whether or not the matrix is involved in the deactivation of the triplet state. Heavy atom quenchers have also been added to polymer films which contained low concentrations of guest carbazole, to see if there is any effect on the carbazole lifetime, and in particular, energy transfer from guest to polymer triplet level.

POLYMER CHARACTERISATION

Polymers are characterised best by a molar mass distribution and the associated molar mass averages, rather than by a single molar mass. The typical distributions, shown in Figure 3.1, can be described by a number of averages [18]:

$$M_N = \frac{\Sigma N_i M_i}{\Sigma N_i} \qquad \text{number average molar mass}$$

$$M_W = \frac{\Sigma N_i M_i^2}{\Sigma N_i M_i} \qquad \text{weight average molar mass}$$

$$M_Z = \frac{\Sigma N_i M_i^3}{\Sigma N_i M_i^2}$$ z-average molar mass

A guide to the breadth of the distribution can be found from the heterogenity index (M_W/M_N).

These average molar mass values for the polymer matrices used in this study (Table 3.1) were provided by the Polymer Supply and Characterisation Centre (RAPRA Technology Ltd), using gel permeation chromatography (GPC). Gel permeation chromatography separates the polymer samples into fractions according to their sizes by means of a sieving action. This is achieved using a non-ionic stationary phase of packed spheres (often cross-linked polystyrene beads) whose pore size distribution can be controlled.

The glass transition temperature, Tg, for each polymer matrix was obtained using differential scanning calorimetry (Perkin-Elmer 7 DSC). The DSC curve for PMMA is shown in Figure 3.2.

TRIPLET STATE ENERGY LEVELS

The lowest triplet state energy levels (E_τ) of the polymer matrices and additives used in this study are shown in Table 3.2.

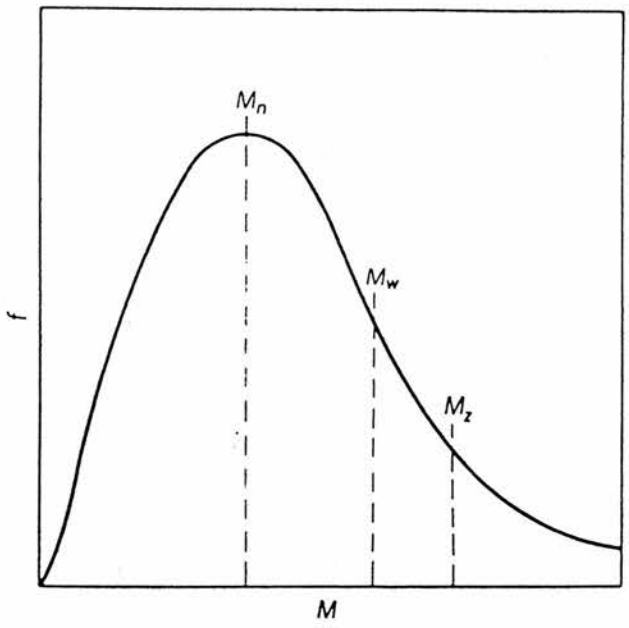

FIGURE 3.1 : Typical distribution of molar masses for a synthetic polymer sample, where f is the fraction of polymer in each interval of M considered

TABLE 3.1

CHARACTERISATION OF HOMOPOLYMERS

POLYMER	Tg	Mn	Mw	Mn	Mw/Mz
PMMA	114^0C	$6.87x10^4$	$1.30x10^5$	$1.20x10^5$	1.90
Psty	95^0C	$6.99x10^4$	$3.16x10^5$	$8.27x10^5$	4.52
PVA	105^0C	$6.29x10^4$	$1.17x10^5$	$1.89x10^5$	1.86
d^8-Psty	95^0C	$1.16x10^4$	$2.32x10^4$	$4.32x10^4$	2.00

TABLE 3.2

TRIPLET STATE ENERGY LEVEL

POLYMER/SOLUTE	E/kJ mol^{-1}	Ref
PMMA	297-301	19
PVA	292	19
Psty	285	19
Carbazole	294	36
N-Ethyl Carbazole	295	36

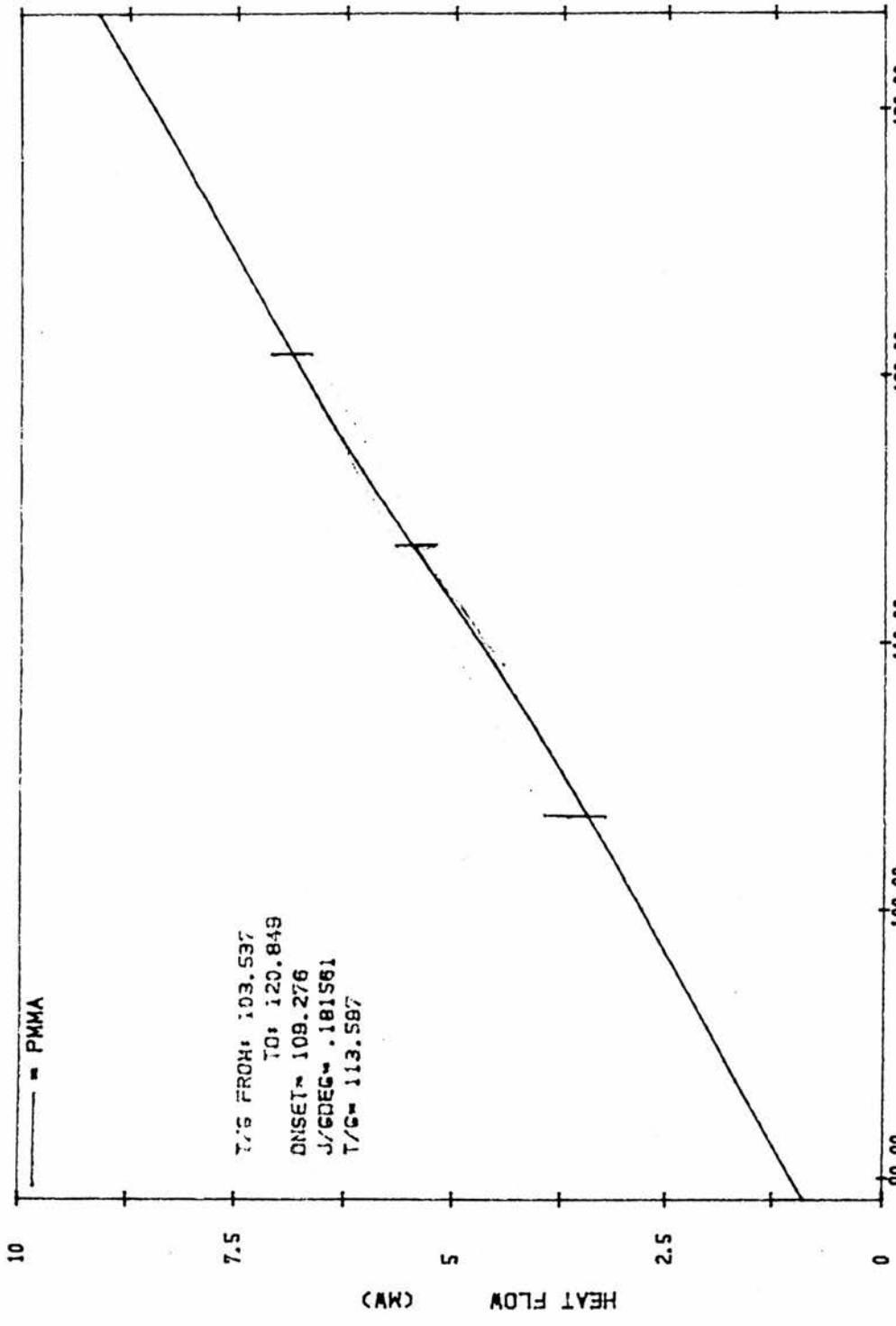

FIGURE 3.2 : DSC curve for PMMA

FACTORS AFFECTING EXCITED STATE LIFETIMES

Various compounds, their excited state transitions and lifetimes are listed below [20].

MOLECULE	TRANSITION	τ_F (ns)	τ_P (s)	MATRIX (77K)
Benzene	(π,π^*)	29	6.3	EPA
Naphthalene	(π,π^*)	96	2.3	EPA
Phenanthrene	(π,π^*)	57.5	3.9	EPA
Carbazole	(n,π^*)	16.1		EPA
Anthrone	(n,π^*)		1.7	EPA
Acetophenone	(n,π^*)		2.8	EPA

In the carbonyl compounds, an electron is promoted from n --> π^* (n,π^* transition), whereas in the aromatic hydrocarbons a (π,π^*) transition takes place. Generally, (π,π^*) singlet states have shorter intrinsic lifetimes than (n,π^*) states, whereas in the triplet state τ_0 is smaller for (n,π^*) states (10^{-4} - 10^{-2} s) than for (π,π^*) states (1-10^2 s).

Triplet state lifetimes are longer than fluorescence lifetimes, the former in the region of 10^{-4} - 10^2 s, and the latter 10^{-9} - 10^{-6} s.

PERDEUTERATION

On deuteration, the phosphorescence lifetime of aromatic compounds is dramatically increased. This is shown below [21].

Compound	C_6H_6	C_6H_5D	C_6D_6	$C_{10}H_8$	$C_{10}D_8$
τ_P (s)	5.75	8.90	12.0	2.3	19.0

This arises because deuteration markedly reduces k_{ISC}(T1 ~~~~> S_0) and τ_P is increased accordingly.

THE HEAVY ATOM EFFECT

This increases the rate of all singlet <-> triplet processes, both radiative and non-radiative. τ_P, τ_F and θ_F will all decrease [22].

Compound	τ_P (s)
naphthalene	2.4
1-fluoronaphthalene	1.4
1-chloronaphthalene	0.23
1-bromonaphthalene	0.014
1-iodonaphthalene	0.002

EXPERIMENTAL RESULTS

1 PHOSPHORESCENCE DECAY OF CARBAZOLE IN HOMOPOLYMER MATRICES

The concentration of carbazole in polystyrene film was varied between 0.0029M and 0.182M, and in poly(methyl methacrylate) between 0.0029M and 0.2467M. Typical phosphorescence decays, studied over several lifetimes, are shown in Figure 3.3 and Figure 3.4.

In both polymer matrices, the phosphorescence lifetime was found to be dependent on the additive concentration (Table 3.3 and Table 3.4). As the concentration of the carbazole increased, the phosphorescence lifetime decreased. An indication of the exponentiality of the decays is given by the R-sq values (%). These show that, generally, the decay is more exponential

(a) for lower concentrations of additive

(b) at lower temperatures

The phosphorescence lifetime also appeared to be matrix dependent, since in films containing identical carbazole concentrations, the lifetime is considerably larger in PMMA than in Psty. In both PMMA and Psty matrices, there is a significant drop in phosphorescence intensity and lifetime between 225-250K (Figure 3.5).

Delayed fluorescence was also observed at 380nm, but at considerably lower intensity than the phosphorescence obtained at 410nm. It was noted that in all cases, the delayed fluorescence was more easily observed in the higher concentration samples; in 0.0029M, even at very high photomultiplier sensitivity, delayed fluorescence could not be detected.

TABLE 3.3

LIFETIME RESULTS:

VARIOUS CONCENTRATIONS OF CARBAZOLE IN Psty FILM.

CONC	0.182M		0.0716M		0.0146M		0.0029M	
TEMP	τ/s	R-sq	τ/s	R-sq	τ/s	R-sq	τ/s	R-sq
80K	4.3	99.7%	4.8	99.8%	6.1	100%	6.5	99.9%
100K	4.7	99.7%	5.4	99.9%	6.1	100%	6.3	99.9%
125K	4.8	99.8%	5.5	99.9%	6.0	100%	6.3	99.9%
150K	4.8	99.8%	5.5	99.9%	6.0	100%	6.3	99.9%
175K	4.7	99.8%	5.4	99.9%	6.0	100%	6.3	99.9%
200K	4.6	99.8%	5.2	99.9%	5.9	100%	6.2	99.9%
225K	4.3	99.7%	4.9	99.9%	5.7	99.9%	6.0	99.9%
250K	4.0	99.6%	4.5	99.9%	5.2	99.9%	5.6	99.9%
275K	3.3	99.6%	3.5	99.2%	4.1	99.8%	4.3	99.9%
298K	2.0	99.1%	2.5	98.4%	1.6	99.6%	1.8	99.6%

TABLE 3.4

LIFETIME RESULTS:

VARIOUS CONCENTRATIONS OF CARBAZOLE IN PMMA FILM.

CONC	0.2467M		0.0735M		0.0147M		0.0029M	
TEMP	τ/s	R-sq	τ/s	R-sq	τ/s	R-sq	τ/s	R-sq
80K	5.2	99.8%	5.8	99.8%	6.6	99.8%	8.3	99.9%
100K	5.2	99.7%	5.8	99.8%	6.6	99.6%	8.1	99.9%
125K	5.1	99.6%	5.8	99.7%	6.6	99.7%	8.0	99.9%
150K	4.9	99.6%	5.8	99.7%	6.5	99.8%	7.9	99.9%
175K	4.9	99.4%	5.8	99.7%	6.5	99.8%	7.9	99.9%
200K	4.8	99.4%	5.8	99.7%	6.5	99.8%	7.8	99.9%
225K	4.6	99.3%	5.6	99.8%	6.4	99.8%	7.7	99.9%
250K	4.3	99.3%	5.4	99.8%	6.1	99.8%	7.4	99.9%
275K	2.9	99.6%	3.9	99.0%	4.6	99.7%	6.2	99.9%
298K	/	/	/	/	/	/	4.4	99.5%

Ln(PHOS. INTENSITY) Vs TIME PLOT FOR 0.0029M IN PMMA FILM

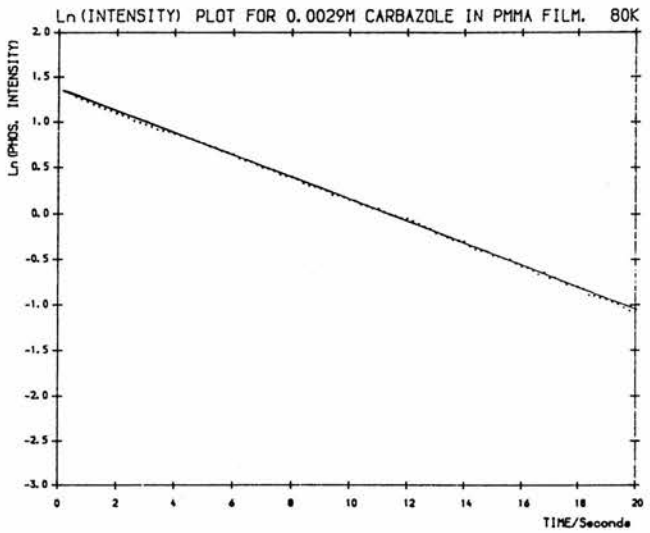

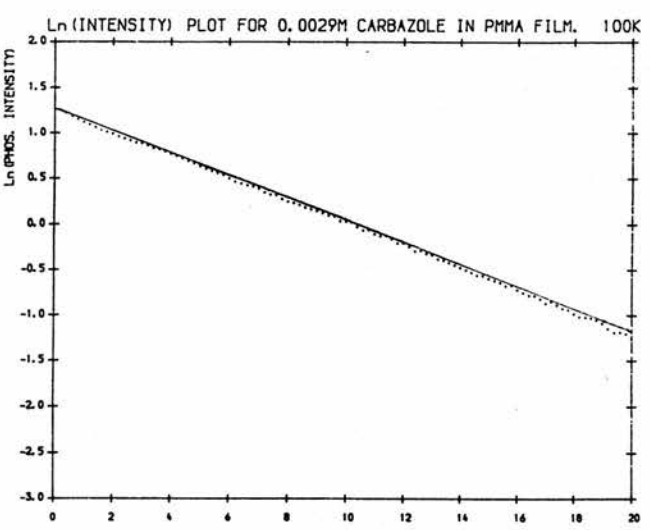

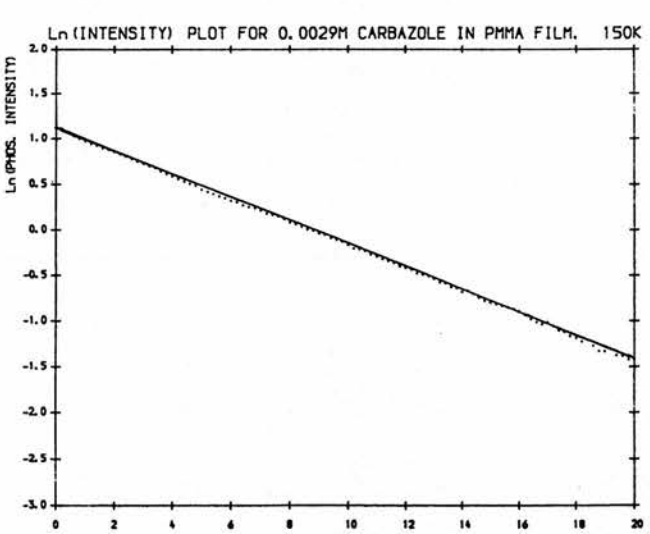

FIGURE 3.3 (b)

Ln(PHOS. INTENSITY) Vs TIME PLOTS FOR 0.0029M IN PMMA FILM

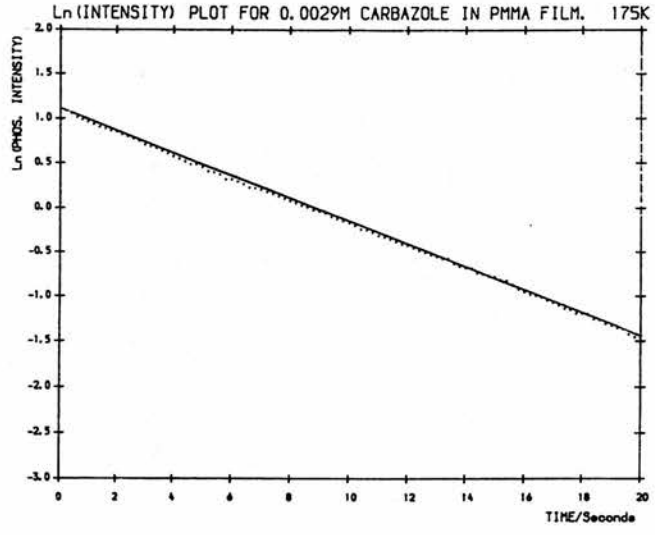

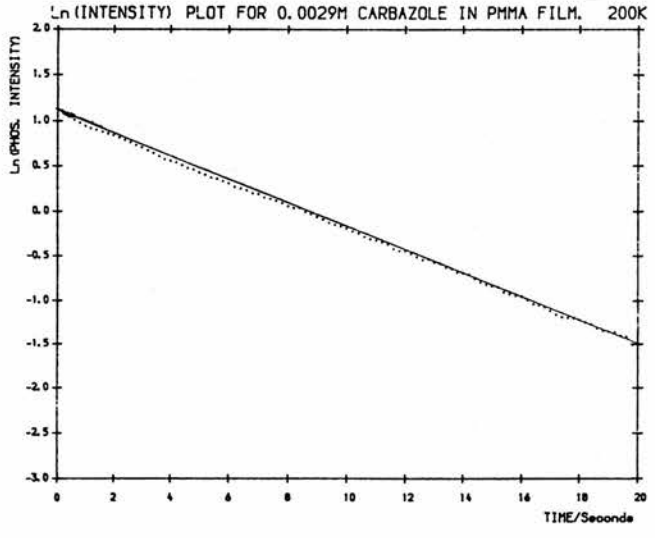

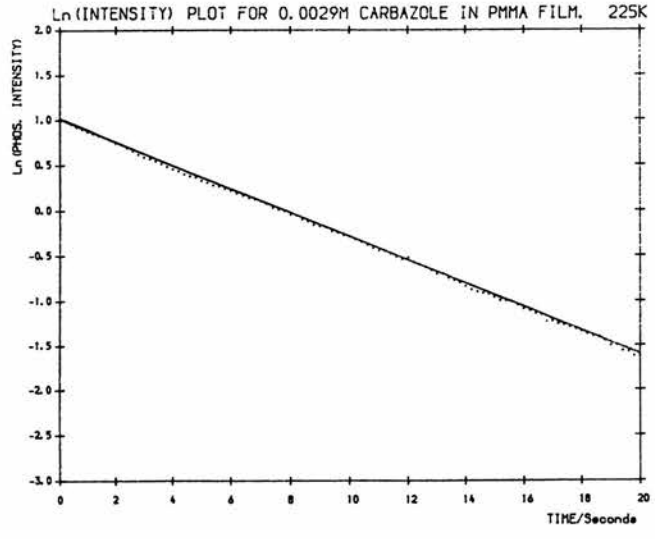

FIGURE 3.3 (c)

Ln(PHOS. INTENSITY) Vs TIME PLOTS FOR 0.0029M IN PMMA FILM

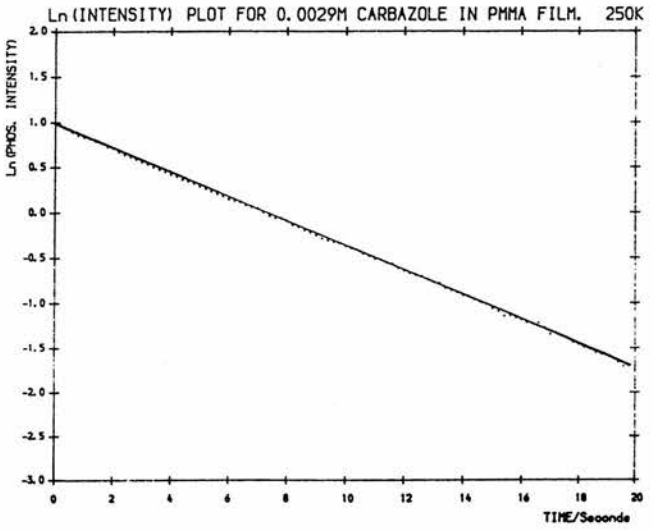

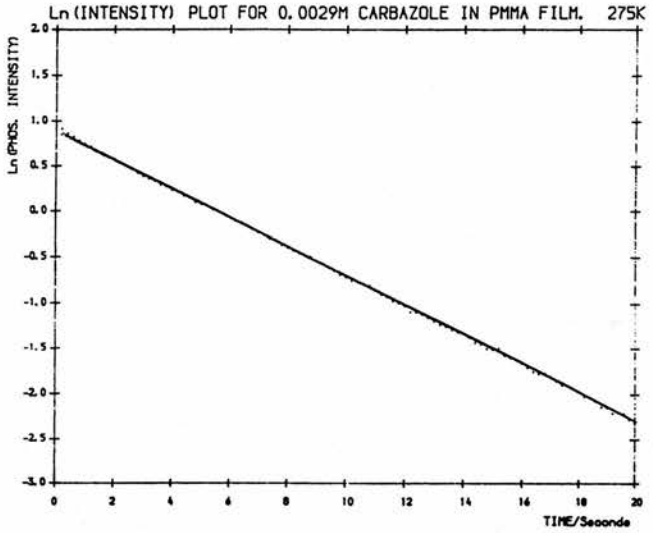

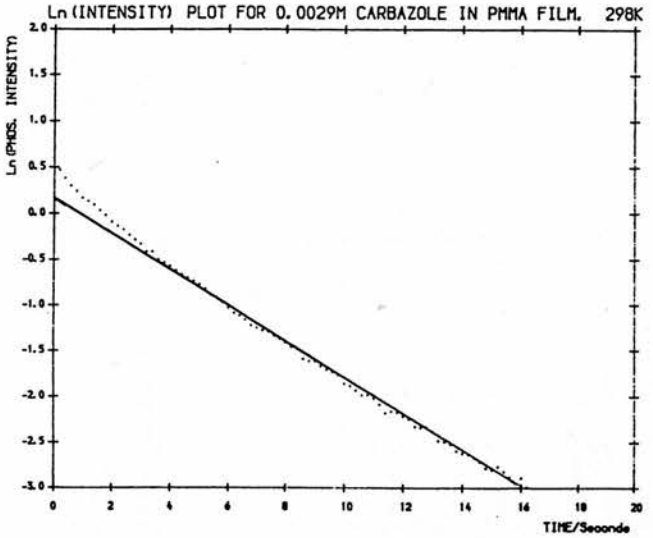

FIGURE 3.4 (a)

Ln(PHOS. INTENSITY) Vs TIME PLOTS FOR 0.0147M IN PMMA FILM

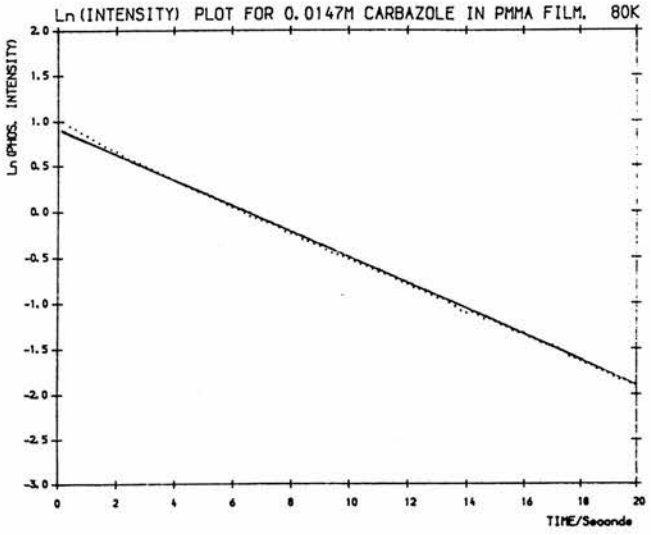

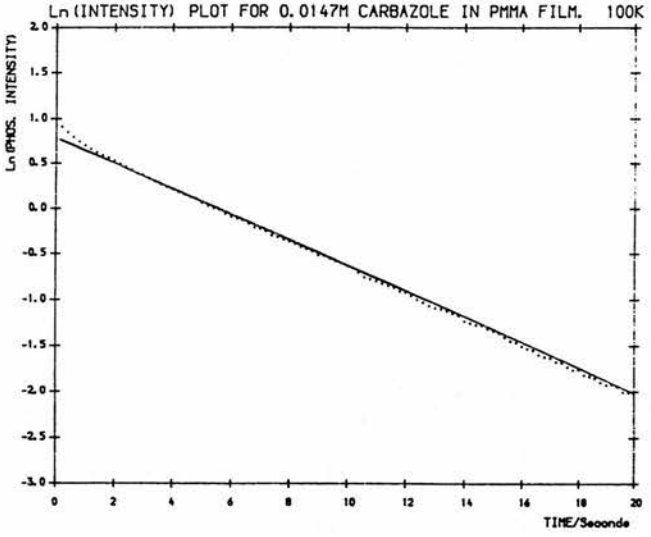

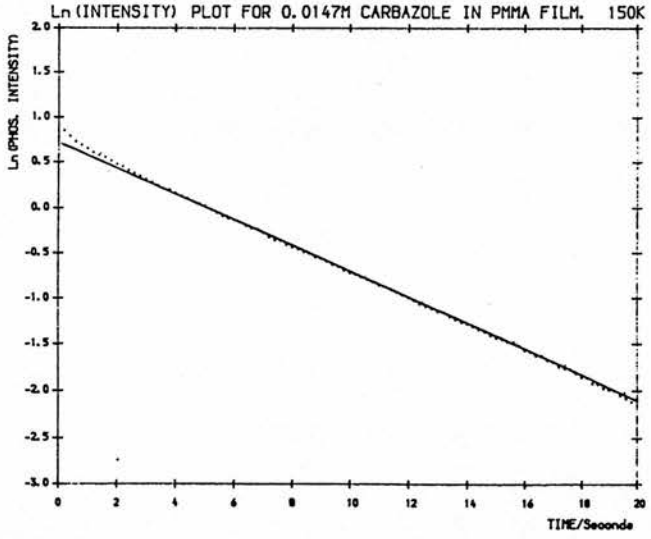

FIGURE 3.4 (b)

Ln(PHOS. INTENSITY) Vs TIME PLOTS FOR 0.0147M IN PMMA FILM

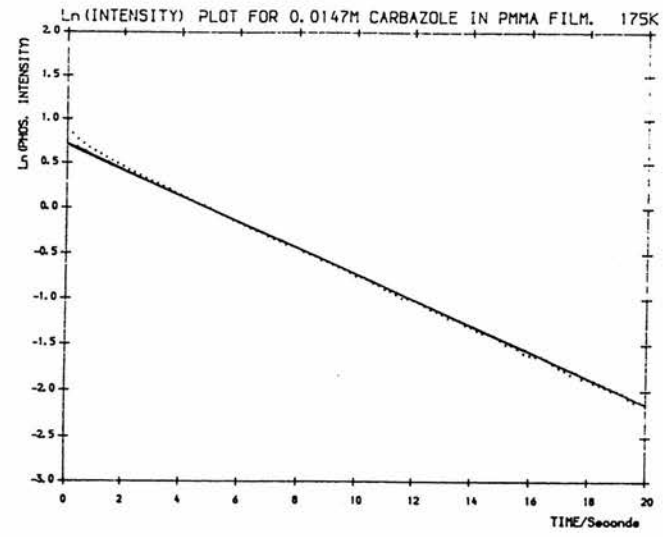

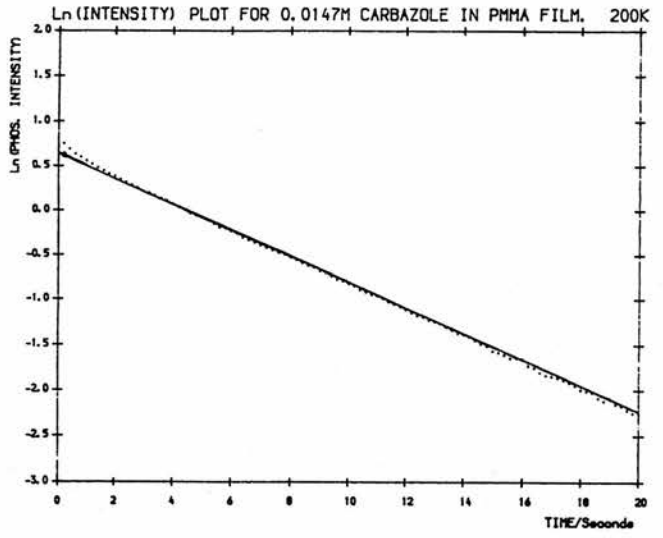

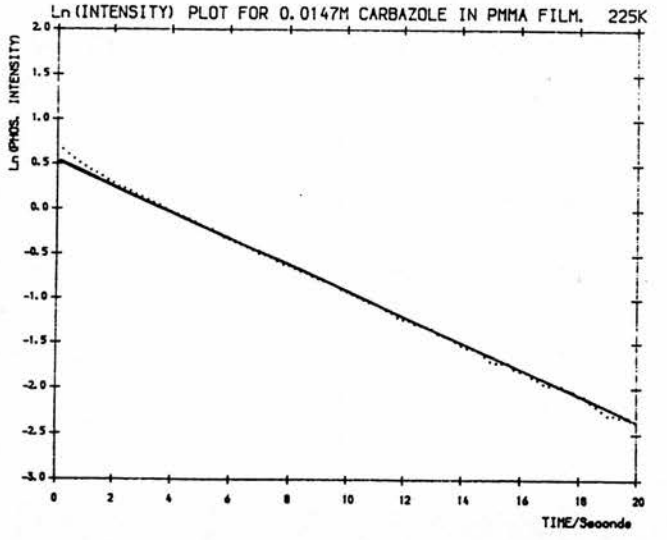

FIGURE 3.4 (c)

Ln(PHOS. INTENSITY) Vs TIME PLOTS FOR 0.0147M IN PMMA FILM

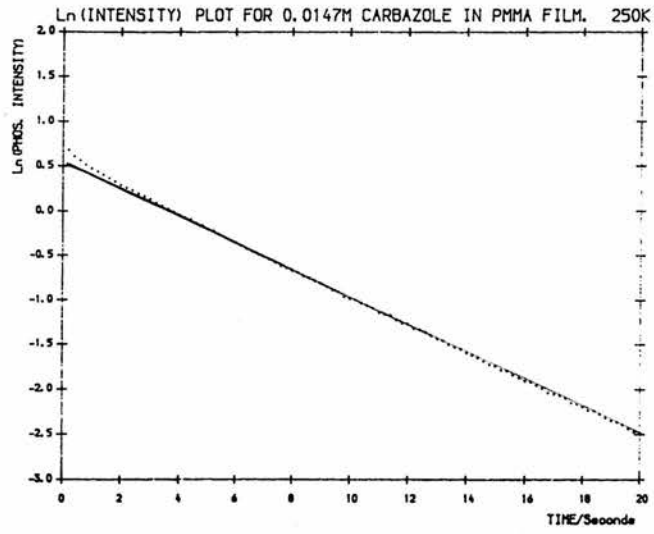

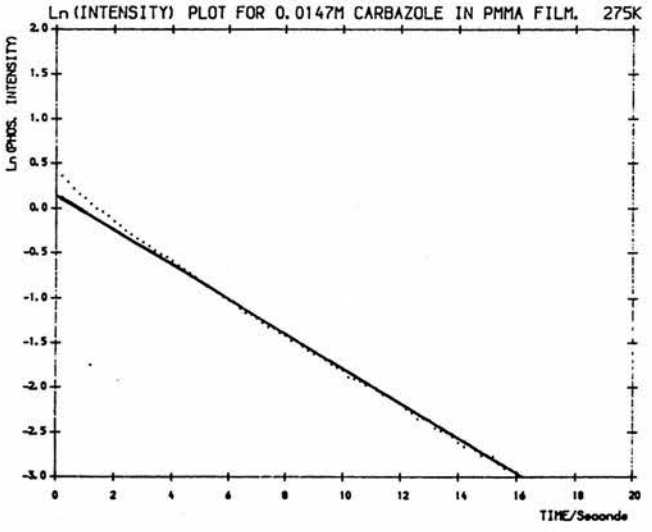

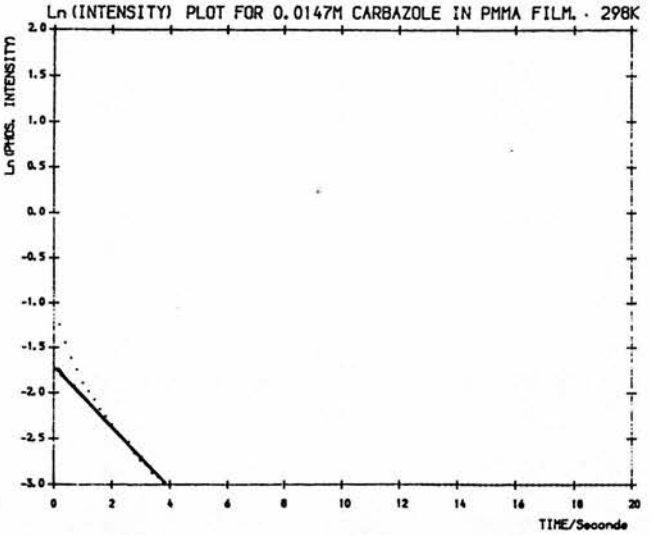

FIGURE 3.5

EFFECT OF TEMPERATURE ON THE DECAY OF 0.0029M AND 0.0147M CARBAZOLE IN PMMA

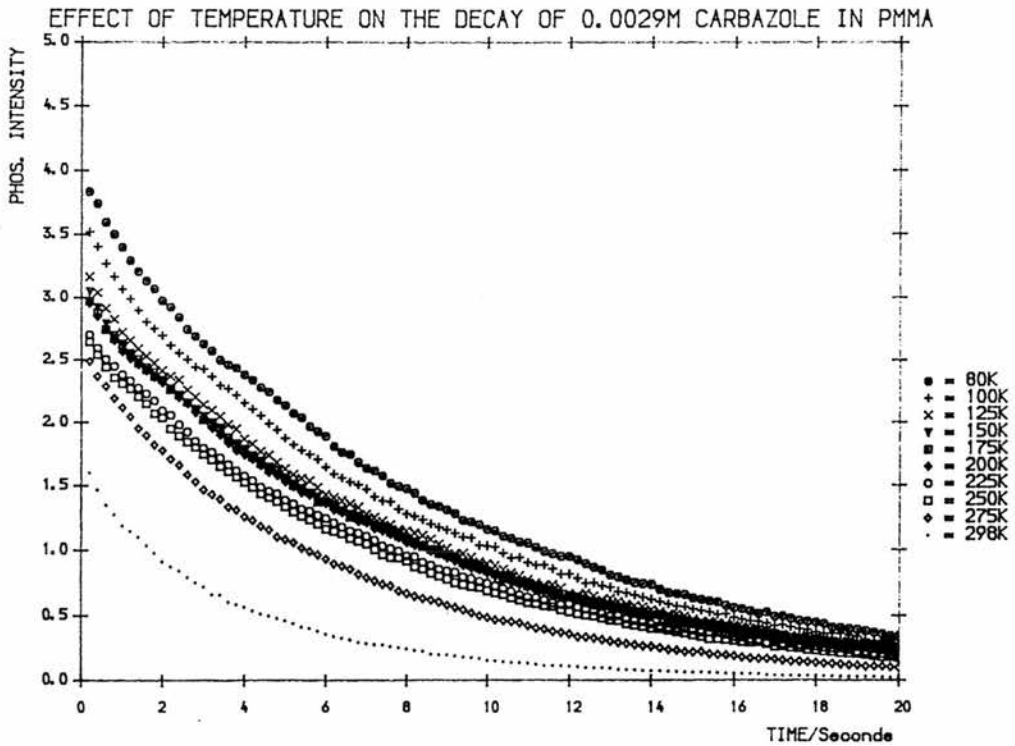

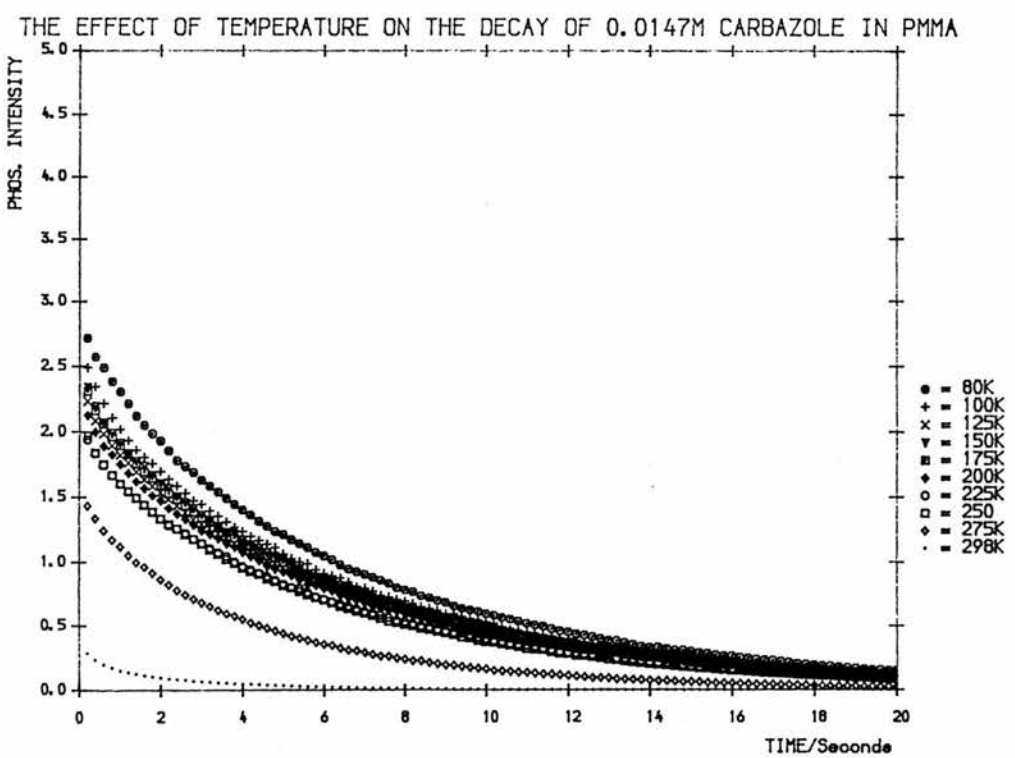

2 PHOSPHORESCENCE DECAY OF N-ETHYLCARBAZOLE IN HOMOPOLYMER MATRICES

The phosphorescence decay of 0.022M and 0.279M N-ethylcarbazole (NEC) in PMMA, Psty and PVA was measured. Very similar results to the carbazole in homopolymer films were observed. Some typical plots are shown (Figure 3.6), and the lifetimes for each film are listed in Table 3.5.

Delayed fluorescence was observed at 380nm on a relatively low photomultiplier tube sensitivity for 0.279M NEC in PMMA and Psty. The photomultiplier voltages were 1.36kV and 1.35kV respectively. It was necessary to use much higher voltages to observe delayed fluorescence intensity in the 0.022M NEC films (2.2kV for Psty (Figure 3.7) and higher in PMMA). Unfortunately, it was not possible to compare directly the phosphorescence intensity between films, since this is highly dependent on the sample position in the laser beam : however these results do show that delayed fluorescence is more readily produced by the higher concentration samples.

Figure 3.8 shows the dependence of the initial non-exponentiality at 410nm on the excitation intensity. By using a small 337.1nm filter, the degree of non-exponentiality was reduced.

TABLE 3.5

LIFETIME RESULTS:

VARIOUS CONCENTRATIONS OF N-ETHYLCARBAZOLE IN POLYMER FILMS.

POLYMER	Psty FILM				PMMA FILM			
CONC	0.279M		0.0223M		0.279M		0.0223M	
TEMP	τ/s	R-sq	τ/s	R-sq	τ/s	R-sq	τ/s	R-sq
80K	4.8	*99.4%*	5.9	*99.9%*	5.9	*99.7%*	8.7	*99.7%*
100K	5.1	*99.6%*	6.2	*99.9%*	5.9	*99.7%*	8.6	*99.8%*
125K	5.1	*99.6%*	6.1	*99.9%*	5.8	*99.7%*	8.7	*99.7%*
150K	4.9	*99.4%*	6.2	*99.9%*	5.8	*99.7%*	8.5	*99.8%*
175K	4.8	*99.5%*	6.1	*99.9%*	5.4	*99.6%*	8.6	*99.7%*
200K	4.7	*99.4%*	6.0	*99.9%*	4.7	*99.6%*	8.5	*99.8%*
225K	4.1	*99.3%*	5.6	*99.9%*	4.5	*99.2%*	8.1	*99.7%*
250K	2.6	*99.2%*	5.1	*99.7%*	4.3	*99.2%*	7.0	*99.9%*
275K	2.0	*99.0%*	4.7	*99.5%*	/	/	4.4	*99.8%*
298K	0.8	*99.6%*	3.7	*99.4%*	/	/	2.7	*99.6%*

TABLE 3.5 (cont)

POLYMER	PVA FILM			
CONC	0.279M		0.0223M	
TEMP	τ/s	R-sq	τ/s	R-sq
80K	5.3	*99.6%*	6.8	*99.9%*
100K	5.3	*99.6%*	6.8	*99.9%*
125K	5.3	*99.5%*	6.8	*99.9%*
150K	5.9	*99.6%*	6.8	*99.9%*
175K	5.2	*99.5%*	6.8	*99.9%*
200K	5.0	*99.5%*	6.7	*99.9%*
225K	4.8	*99.6%*	6.7	*99.9%*
250K	4.2	*99.3%*	6.1	*99.9%*
275K	3.9	*98.5%*	5.0	*99.5%*
298K	2.9	*97.3%*	4.4	*98.8%*

FIGURE 3.6(a)

Ln(PHOS. INTENSITY) Vs TIME PLOTS FOR 0.279M NEC IN Psty FILM

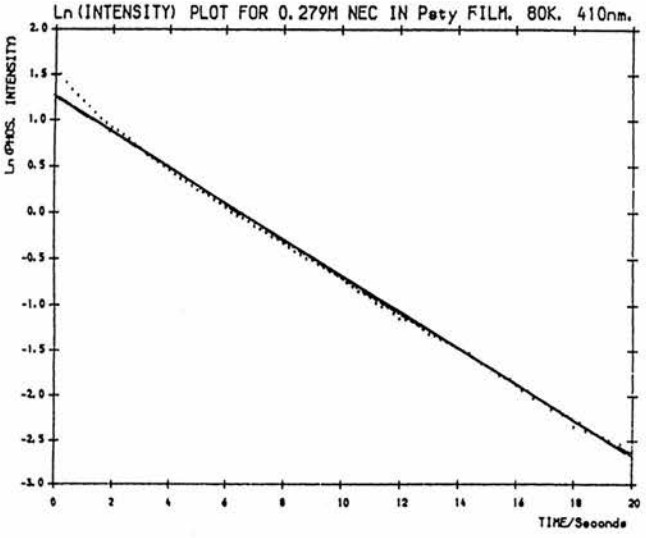

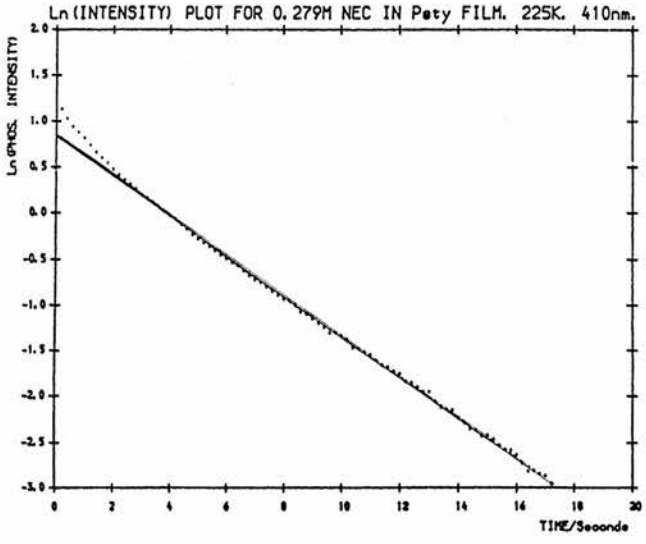

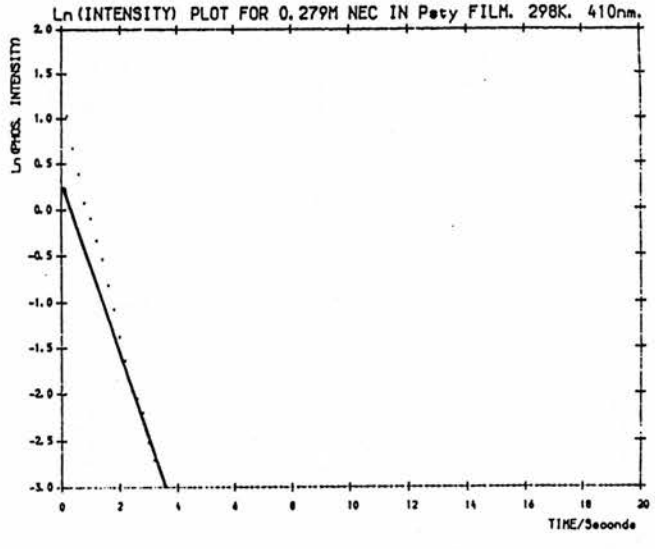

FIGURE 3.6(b)

Ln(PHOS. INTENSITY) Vs TIME PLOTS FOR 0.022M NEC IN Psty FILM

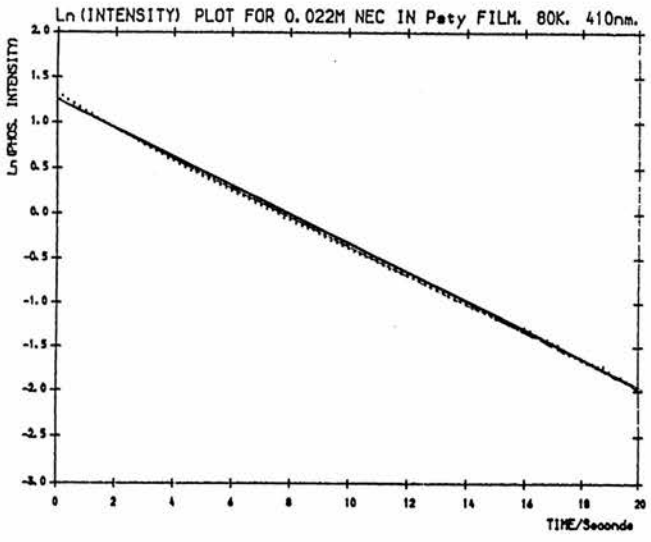

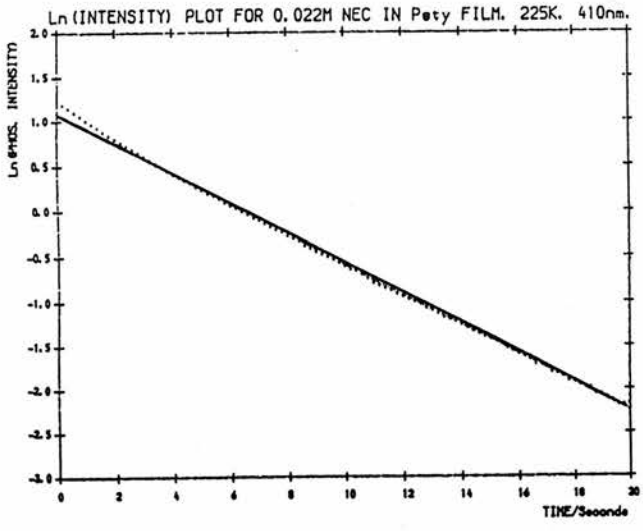

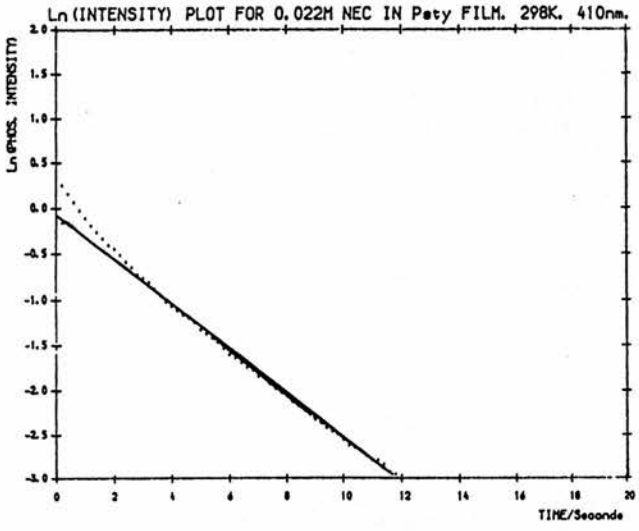

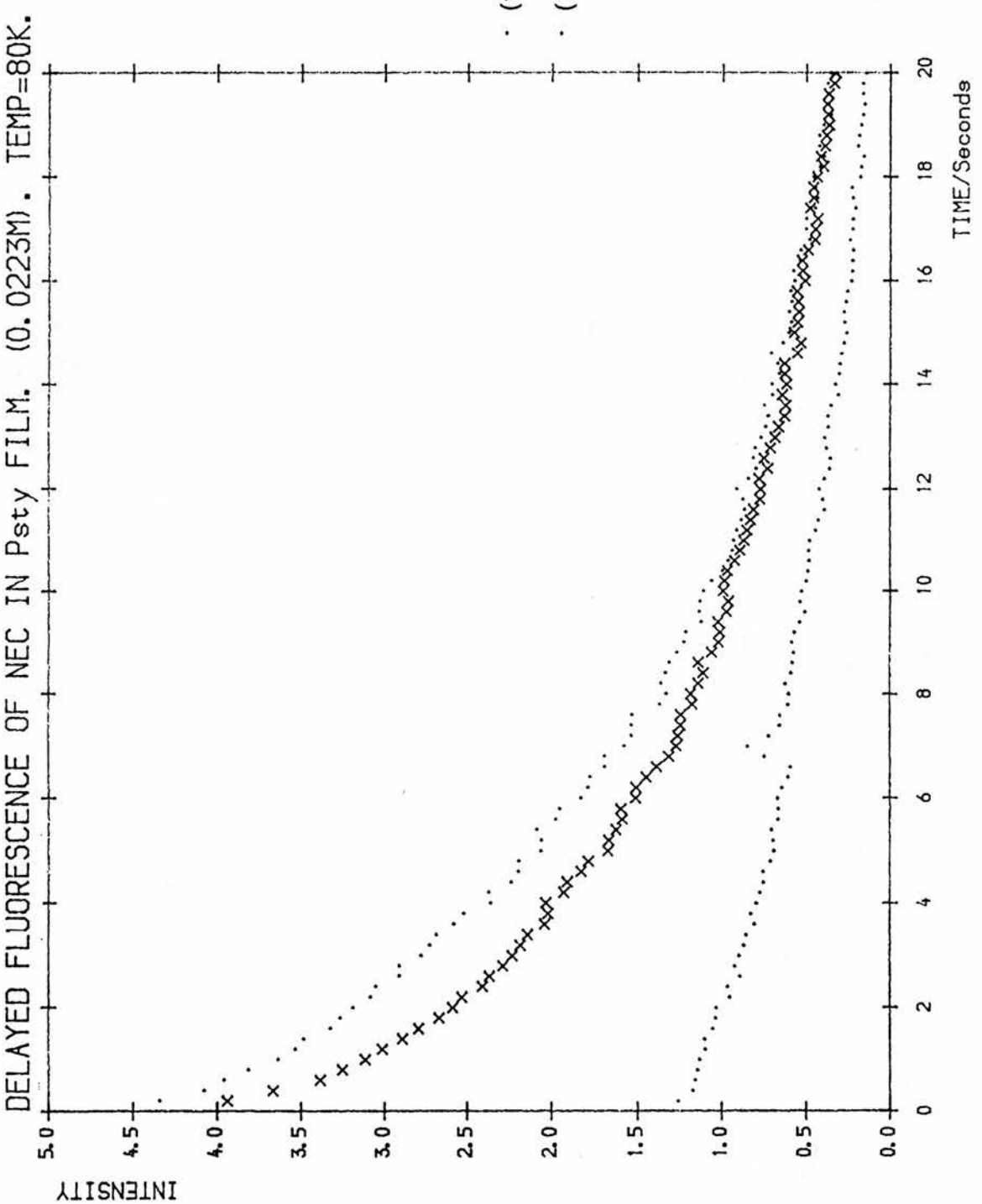
DELAYED FLUORESCENCE OF NEC IN Psty FILM. (0.0223M). TEMP=80K.
· (upper plot) = 380nm
x = 360nm
· (lower plot) = 370nm
INTENSITY
TIME/Seconds
0.0
0.5
1.0
1.5
2.0
2.5
3.0
3.5
4.0
4.5
5.0
0
2
4
6
8
10
12
14
16
18
20

FIGURE 3.7

FIGURE 3.8

Effect of Reducing Laser Intensity on Phosphorescence Decay

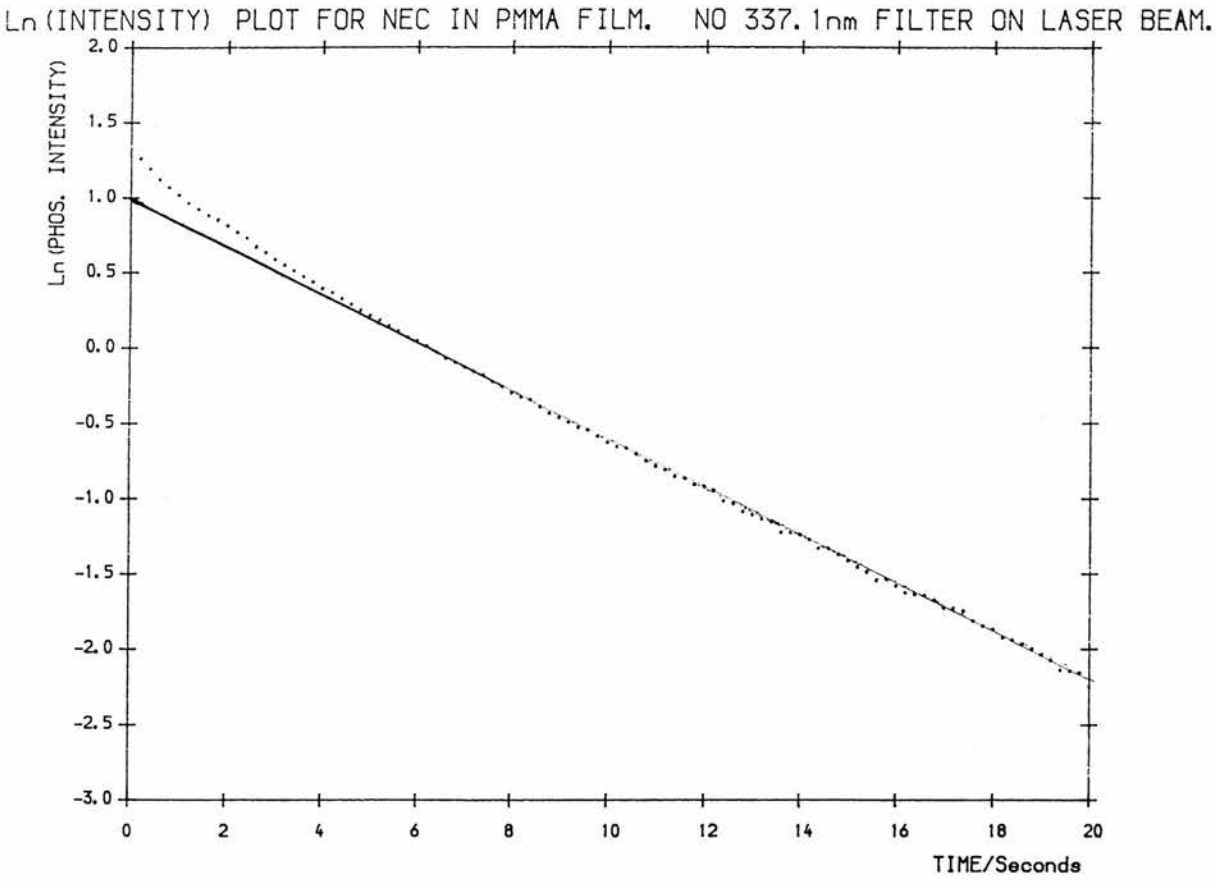

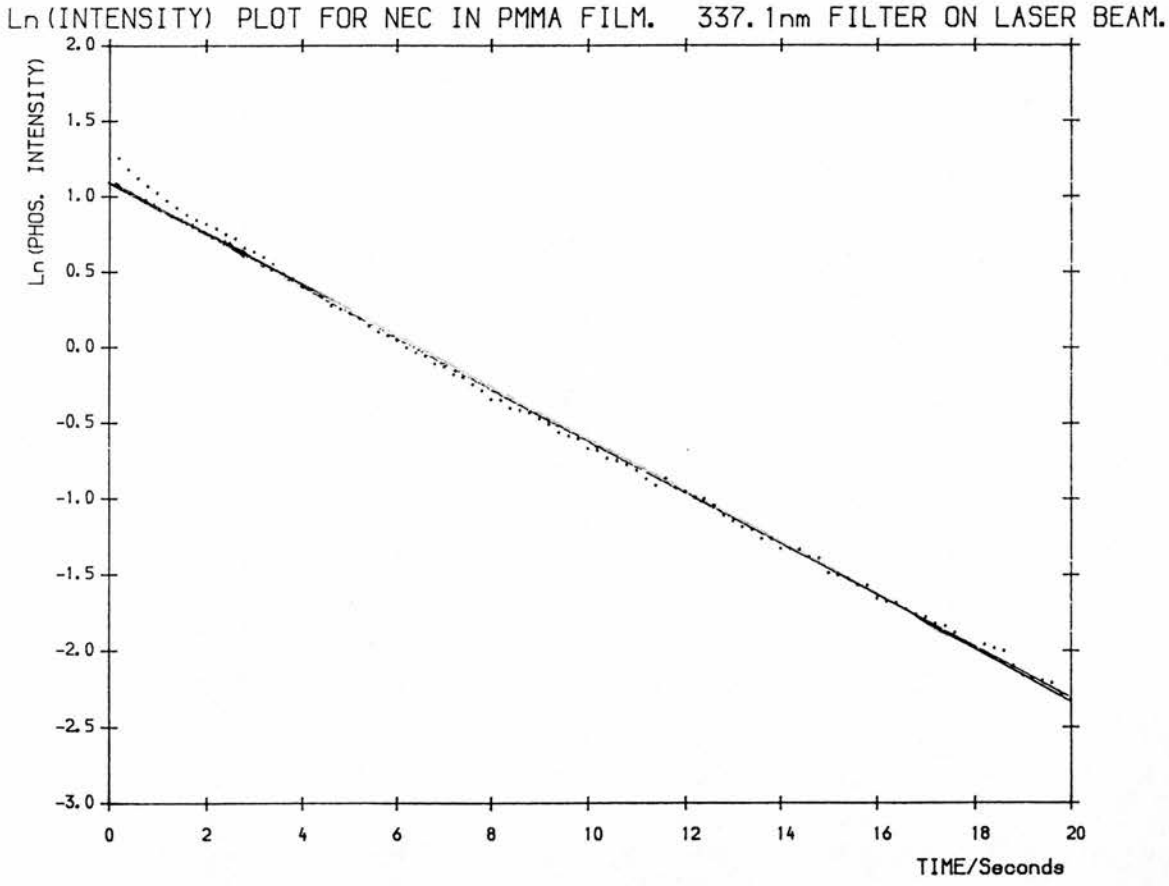

3 PHOSPHORESCENCE DECAY OF CARBAZOLE IN A PARTIALLY DEUTERATED POLYSTYRENE MATRIX

As already described in Chapter 2, it was not possible to incorporate carbazole into a fully deuterated matrix due to cracking of the polymer on evaporation of the casting solvent. Only one partially deuterated film was successfully made, that of 0.0029M carbazole in an 87.5% Psty / 12.5% d^8-Psty blend.

Partial deuteration of the host matrix resulted in a reduction of the carbazole phosphorescence lifetime, when compared with the same concentration of carbazole in a fully protonated host. The lifetime results are shown in Table 3.6

Several Ln(intensity) vs Time plots for the carbazole decay at various temperatures are shown in Figure 3.9.

TABLE 3.6

LIFETIME RESULTS

0.0029M CARBAZOLE IN Psty AND A PARTIALLY DEUTERATED Psty MATRIX

	MATRIX	
TEMP	Psty	87.5% Psty/12.5% d^8-Psty
80K	6.5	5.9
100K	6.3	5.8
125K	6.3	5.7
150K	6.3	5.6
175K	6.3	5.6
200K	6.2	5.6
225K	6.0	5.2
250K	5.6	4.3
275K	4.3	0.7
298K	1.8	/

FIGURE 3.9(a)

Ln(PHOS. INTENSITY) Vs TIME PLOTS FOR 0.00029M CARBAZOLE IN A PARTIALLY DEUTERATED MATRIX

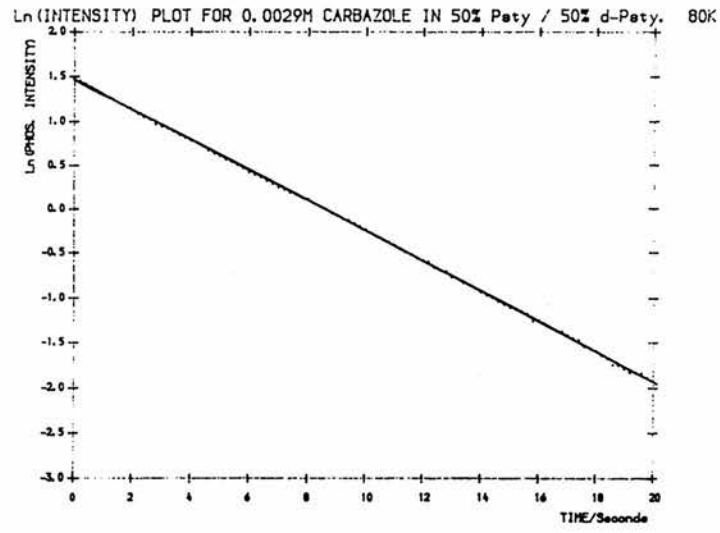

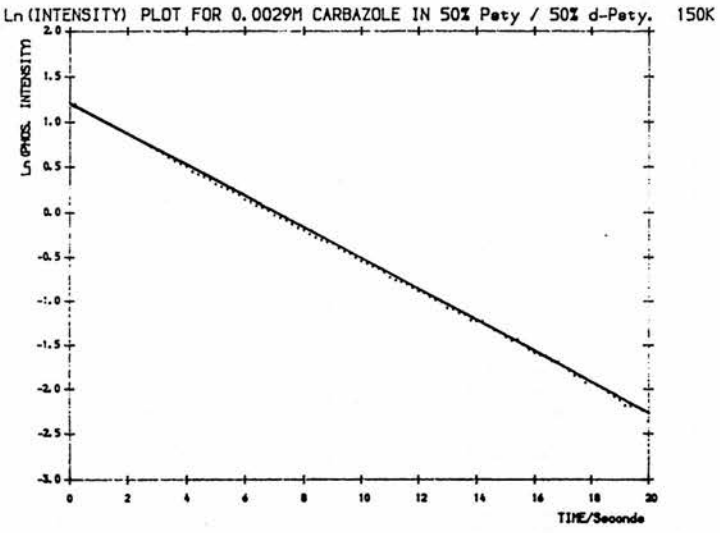

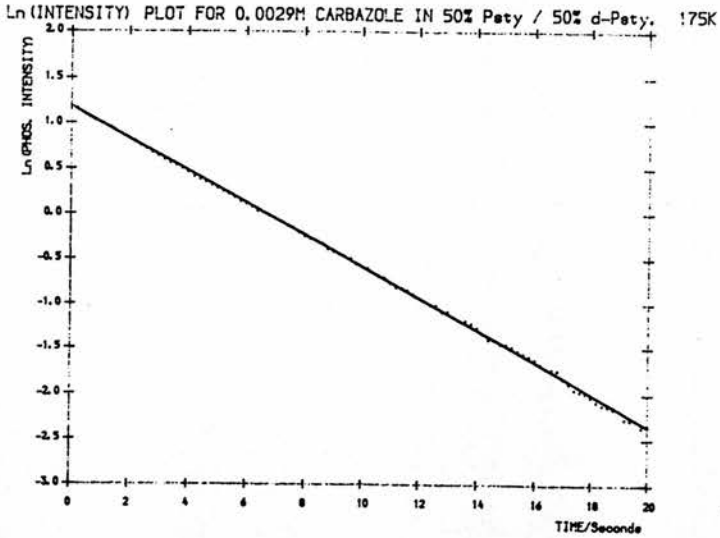

FIGURE 3.9(b)

Ln(PHOS. INTENSITY) Vs TIME PLOTS FOR 0.00029M CARBAZOLE IN A PARTIALLY DEUTERATED MATRIX

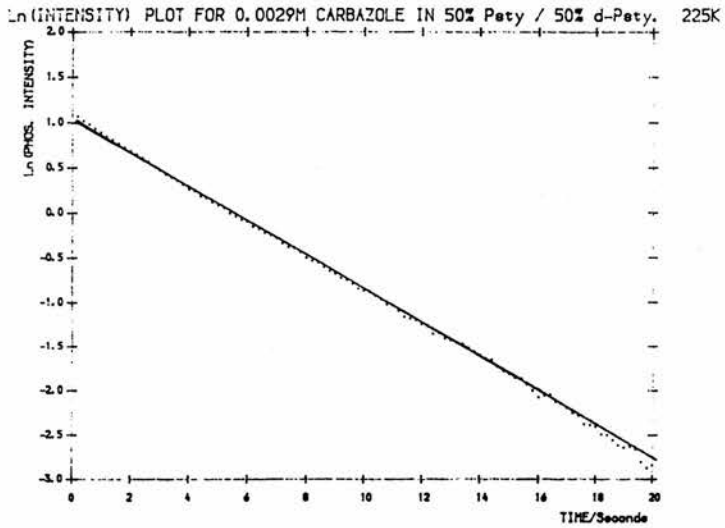

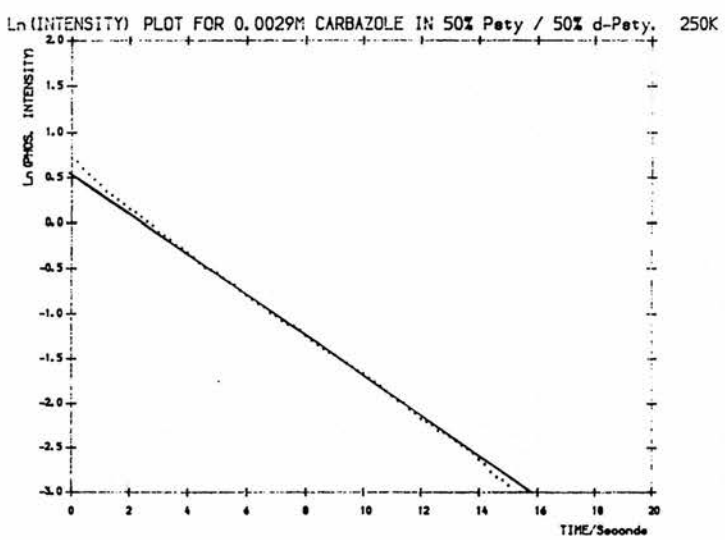

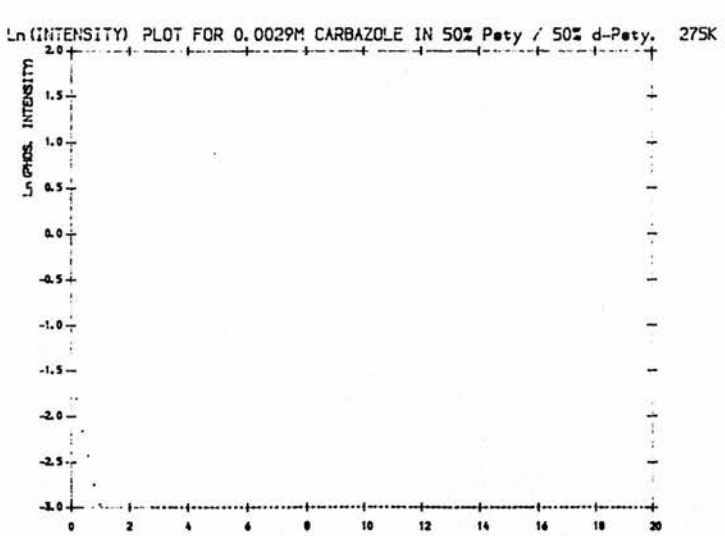

CAUSES OF NON-EXPONENTIAL DECAY AND TEMPERATURE DEPENDENCE OF PHOSPHORESCENCE IN POLYMER HOSTS

Non-exponential decay was observed at room temperature for both carbazole and N-ethyl carbazole in all polymer matrices studied. There was also a significant decrease in both the phosphorescence intensity and the lifetime as the temperature increased. Similar results have been reported in the literature for the phosphorescence of aromatic hydrocarbons and many explanations as to why this non-exponentiality and temperature dependence occurs have been offered. These are summarised below:

(a) Direct quenching of the triplet state by impurities.

In this present work, the possibility of impurities in the matrix or sample itself acting as quenchers [23,24] has been dismissed. Careful recrystallisation of the solutes and repurification of polymers were repeated several times, thereby eliminating impurities. Furthermore, since each polymer host, carbazole and N-ethyl carbazole would presumably all contain different impurities, then it is expected that if quenching by these impurities was occurring, different trends would be observed according to the host matrix and/or solute used. This was not found. The lifetime and phosphorescence intensity dropped dramatically between 225-250K, and this showed essentially identical behaviour independent of additive or medium.

(b) Quenching by molecular oxygen [25].

Great care was taken to exclude oxygen from the system by pumping out the sample holder on a vacuum line overnight. The vacuum was in the region of $< 10^{-5}$ atm. Hence, the partial pressure of $O_2 < 2x10^{-6}$ atm.

Clough et al [26] have shown that the diffusion coefficient of O_2 is dependent on matrix rigidity and temperature. Over the temperature

range studied, both PMMA and Psty matrices are rigid glasses, whereas PVA is much softer : Tg(PMMA) > Tg(Psty) >> Tg(PVA). The diffusion of oxygen through the polymer is therefore expected to be a much more efficient process in PVA than in Psty and PMMA, and this should be reflected in the lifetime of the additive. However, $\tau_{PMMA} > \tau_{PVA} > \tau_{Psty}$ was obtained for NEC in these three polymers. The possibility of some oxygen quenching occurring cannot be totally dismissed, since oxygen is a very effective and ubiquitous quencher of the triplet state even at very low concentrations; however, these results show that it cannot be the dominant process.

(c) Free radicals in the PMMA matrix.

Jones and Siegel [27] observed quenching at room temperature in studies of several aromatic hydrocarbons in PMMA when they irradiated the sample with intense broad-band radiation. This non-exponential decay did not occur at 77K or when low intensity monochromatic radiation was used. They suggested that a free-radical quenching species was produced by the broad-band radiation, which was able to diffuse at 300K but not 77K.

In this study, a monochromatic 337nm laser was used as the excitation source. This would minimise the photolytic production of quenching radicals since the wavelength used is appreciably longer than the absorption region of the polymer. It is assumed that any radicals present are at such low concentrations that the effect on quenching the phosphorescence decay is negligible.

(d) Pseudo first-order quenching processes occurring in regions of relatively low viscosity in the polymer.

West et al [28] attributed non-exponential decay at room temperature to diffusion-controlled quenching reactions occurring in low

viscosity regions of the polymer. The low viscosity regions in the matrix are the result of unpolymerised or partially polymerised monomer.

However, El-Sayed et al [29] have reported that non-exponential decay may occur in PMMA irrespective of whether the plastic matrix is prepared by thermal, chemical or photochemical initiation methods or by reconstitution of high molecular weight PMMA which is monomer-free. This clearly suggests that the proposal by West is unlikely.

(e) Interactions between solute and polymer matrices.

No evidence of photochemical addition of carbazole to PMMA was obtained. The polymer sample was irradiated for several hours, dissolved in CH_2Cl_2 and the PMMA reprecipitated twice from methanol. No carbazole emission was observed in the polymer.

(f) Non-exponential decays at all temperatures have been reported for some organic molecules with lifetimes in the millisecond range, but these have been explained as the result of fundamental properties of the molecule [30,31]. This is not relevant in this particular study since exponentiality has been shown to be a function of both additive concentration and temperature.

(g) Diffusion-controlled T-T annihilation.

El-Sayed et al [29] suggested a diffusion-controlled T-T annihilation process to explain the non-exponential phosphorescence decay at room temperature. This coincided with their findings that the degree of non-exponentiality was dependent on excitation intensity. Delayed fluorescence was also observed, and a T-T annihilation fitting routine gave a good fit to the data. Their argument was based on available information about diffusion constants in PMMA.

(h) Triplet energy transfer to the polymer matrix.

Several authors are in favour of energy transfer to the polymer matrix.

Kropp and Dawson [32], investigating the lifetimes of delayed fluorescence and phosphorescence as a function of temperature for coronene in PMMA, found that the activation energy obtained was not in agreement with the known spectroscopic value of the T_1 - S_1 gap in coronene. They proposed that the temperature-dependent deactivation of coronene may be due to the thermal activation from the T_1 of coronene at 19 700 cm^{-1} to the lowest triplet state of the plastic. They estimated the triplet level of the PMMA triplet to be approximately 25 000 cm^{-1}.

Graves, Hofeldt and McGlynn [33] studied the phosphorescence of naphthalene, chrysene and phenanthrene in PMMA. They suggested the important energy transfer step as

$$^0P + {}^3A \longrightarrow {}^3P + {}^0A$$

The lowest triplet energy state, ^3P, was estimated at 25 100 cm^{-1}, very close to the value proposed by Kropp and Dawson [32].

Jassim et al [34] studied various aromatic additives in PMMA, Psty and a series of Psty/MMA copolymers. They suggested that the matrix quenches the triplet state of the additive, the styrene unit being more efficient than the methacrylate. They agreed with Mcglynn's proposal of energy transfer to the polymer host.

A later paper by Jassim [35] suggested the additional step of triplet energy migration through the polymer matrix. Fraser, MacCallum and Moran [36] took this further in their study of benzophenone in PMMA, proposing energy transfer from benzophenone to the polymer, followed by a triplet-triplet annihilation process in which the polymer matrix is involved to explain non-exponentiality.

(i) Secondary relaxation processes in polymer matrices.

Many authors propose that the dependence of τ reflects the secondary relaxation processes of the polymer host. Following the original observations of Charlesby and Partridge [37] and of Bousted

[38], Somersall et al [39] observed that the discontinuities in the Arrhenius plots were coincident with temperatures corresponding to the onset of sub-group motion in polymers. Since the phosphorescence in this case was being quenched by oxygen, it was suggested that the movement of oxygen and other small molecules through polymer matrices is facilitated by the small scale rotations and vibrations of groups pendant to the main polymer chain.

Horie and Mita reported that in the temperature range between T_β and Tg, the decay of benzophenone is non-exponential, while at temperatures both above Tg and below T_β the decay is exponential [40]. The non-exponential decay is attributed to the intermolecular quenching of benzophenone triplet by the carbonyl group in PMMA. Again, the discontinuities of τ with temperature was reported to reflect the molecular motion of the polymer matrix. In subsequent papers [41-44], Horie and co-workers present the kinetic scheme for a diffusion-controlled quenching reaction with a time-dependent rate coefficient for the quenching of the benzophenone triplet by side chain ester groups of the polymer. They later dismissed all proposals of T-T annihilation since they found no dependence of exponentiality on laser intensity [42].

MATHEMATICAL TREATMENT OF LIFETIME RESULTS

The following photophysical reaction scheme is considered:

$S_0 + h\nu \text{ -----> } S_1^*$	I_A
$S_1^* \text{ ~~~~~> } S_0$	$k_{nr}^S [S_1^*]$
$S_1^* \text{ -----> } S_0 + h\nu_F$	$k_F [S_1^*]$
$S_1^* \text{ ~~~~~> } T_1^*$	$k_{ISC} [S_1^*]$
$T_1^* \text{ ~~~~~> } S_0$	$k_{nr} [T_1^*]$

$$T_1^* \text{ -----> } S_0 + h\nu_P \qquad k_P\,[T_1^*]$$

The rate constants k_{nr}^S and k_{nr} refer to all radiationless deactivation steps of the excited singlet and triplet states respectively (e.g. internal conversion, intersystem crossing), and can be expanded to accomodate bimolecular quenching.

The lifetime of phosphorescence is given by

$$\tau_P = \frac{1}{k_{nr} + k_P}$$

The rate constant for phosphorescence emission, k_P, is generally regarded as being independent of temperature over the temperature range of this experiment i.e. $k_P = k_P^0$, while the rate constant k_{nr} for the non-radiative deactivation can be separated into two terms, a temperature-independent part (k_{nr}^0) and a temperature-dependent component (A exp(-E/RT).

Thus, equation can be written as

$$\frac{1}{\tau} = k_P^0 + k_{nr}^0 + A\exp(-E/RT)$$

$$\text{As } T \text{ -> } 0, \quad \frac{1}{\tau} \text{ -> } k_P^0 + k_{nr}^0 = \frac{1}{\tau_0}$$

Hence

$$\frac{1}{\tau} - \frac{1}{\tau_0} = A\exp(-\Delta E/RT)$$

and rearrangement gives

$$\ln(1/\tau - 1/\tau_0) = A\exp(-\Delta E/RT)$$

Thus, an Arrhenius plot of the form $\ln(1/\tau - 1/\tau_0)$ vs $1/T$ will give an activation energy for the temperature-dependent process.

Typical Arrhenius plots are shown in Figure 3.10. These curves can generally be fitted to two temperature-dependent processes. The first, $k_1(T)$, is predominant at low temperatures and has a small activation energy, ΔE_1, and the second process, $k_2(T)$, occurs at higher temperatures with a much larger activation energy ΔE_2.

The values of $k_1(T)$ are indicated by dotted lines on the Arrhenius plot. The gradient of this line, calculated from least-squares regression analysis, corresponds to $-\Delta E/R$.

ΔE_1 was determined first. The contribution from this lower energy process was then subtracted from the Arrhenius plot, and the resulting values of $k_2(T)$ plotted logarithmically against $1/T$. From the slope of this plot, ΔE_2 was calculated.

The calculated activation energies ΔE_1 and ΔE_2 for each of the films studied are listed in Table 3.7.

FIGURE 3.10

ARRHENIUS PLOTS

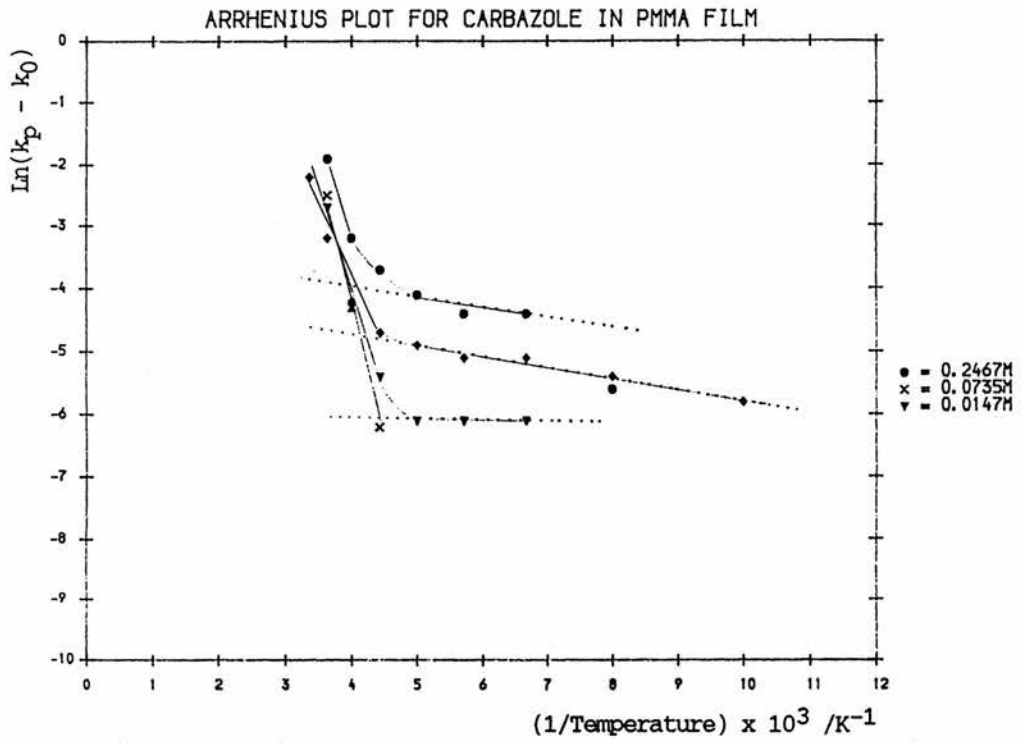

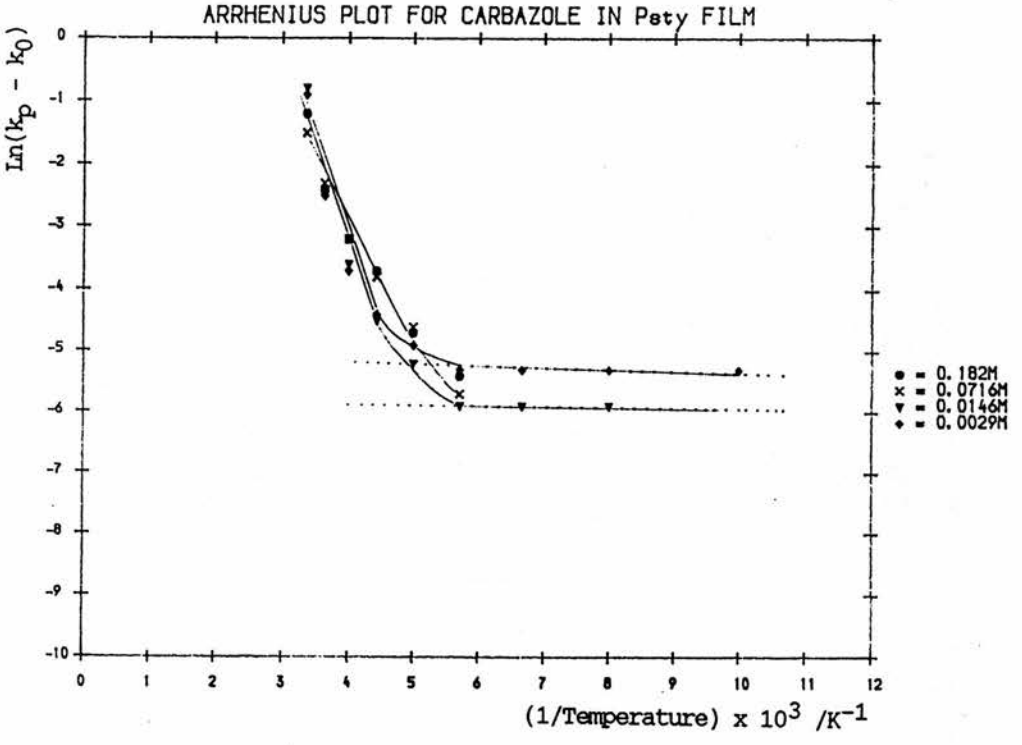

TABLE 3.7

Δ E VALUES FROM EXPERIMENTAL RESULTS

MATRIX - PMMA
DOPANT - CARBAZOLE

[DOPANT]	0.0029M	0.0147M	0.2467M
E_2/kJ/mol	36.7	34.2	28.8
E_1/kJ/mol	1.5	1.5	1.4

MATRIX - Psty
DOPANT - CARBAZOLE

[DOPANT]	0.0029M	0.0146M
E_2/kJ/mol	24.7	24.4
E_1/kJ/mol	0	0

MATRIX - PMMA
DOPANT - NEC

[DOPANT]	0.279M	0.0223M
E_2/kJ/mol	35.8	/
E_1/kJ/mol	3.4	2.2

MATRIX - Psty
DOPANT - NEC

[DOPANT]	0.279M	0.0223M
E_2/kJ/mol	12.5	18.6
E_1/kJ/mol	0	0

No values were calculated for NEC in PVA due to the large scattering of points.

SUMMARY OF LIFETIME RESULTS FOR CARBAZOLE AND N-ETHYL CARBAZOLE IN POLYMER MATRICES

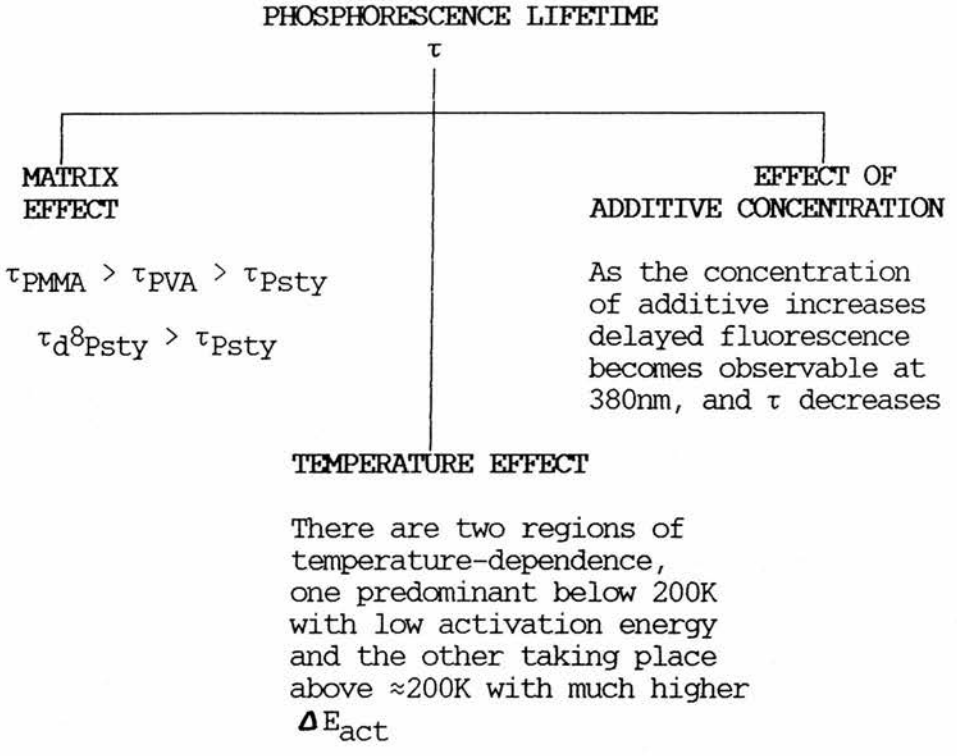

Any proposed mechanism for the deactivation of the triplet state of the additive must satisfactorily account for each of these effects on the phosphorescence lifetime.

As previously mentioned, many authors have reported that the temperature and matrix dependence of τ are related to the secondary relaxation processes of the polymer host [37-44]. These relaxation processes in polymers will now be briefly outlined.

RELAXATION EFFECTS IN POLYMERS [45]

The types of relaxational processes which take place in polymers can be divided into three classes:

(a) Primary main chain motions involving segments containing up to 20-40 monomer units. This is the main glass-rubber transition at Tg and is termed the α-process.

(b) Secondary main-chain motions involving the cooperative but restricted motions of a few contigious monomer units. This is the ß-process, and occurs at temperatures below Tg.

(c) Side-chain motions involving rotations of small groups such as alkyl or aryl groups. These processes are designated γ , δ,ϵ... with decreasing temperature.

These molecular movements in polymers are commonly studied over a wide range of frequencies and temperatures by various kinds of dynamic mechanical techniques, by dielectric methods or by nuclear magnetic resonance. However, there are appreciable difficulties in relating relaxation temperature regions located with one type of measurement at one frequency range to measurements made with a different technique in a different area of the frequency-temperature spectrum. The region in which a transition will occur is very dependent on the frequency used to detect it.

Table 3.8 summarises the secondary relaxation temperatures obtained from mechanical studies on PMMA and Psty and the suggested modes of molecular motion.

The detection of transitions in bulk polymers by the study of the temperature dependence of phosphorescence intensity [38-40,46,47], lifetime [46,47] and polarisation [46,47] has been reported. When the

data are plotted in Arrhenius form, typical plots show two or more straight line portions which intersect at temperatures claimed to correspond to the onset of relaxation. If phosphorescence is to be quenched by some process related to matrix relaxation, then the relaxation time of the process must be comparable with the triplet lifetime. It is therefore expected that there will be a correlation with other local relaxation detection methods using frequencies similar to the probe molecule. For example, ketones have a triplet lifetime in the millisecond range and should therefore be in agreement with other results in the frequency range of 10^2 - 10^4 Hz. Similarly, naphthalene, having a triplet lifetime of seconds should have correlation with other results in the region of 1Hz.

Somersall et al [39], studying a wide range of polymer films containing ketone and/or naphthalene groups reported two transition temperatures for PMMA. Generally, these were found to coincide with reported relaxation values obtained from mechanical measurements. Rutherford and Soutar also reported two transitions in PMMA [47], while Ghiggino et al [48] found three transition temperatures in the same temperature region (Table 3.9). The latter authors, using two types of indole-based probe, identified two separate transitions in poly(vinyl alcohol), but only one was common to each probe. They could also only locate one transition in polystyrene over a range in which both ß and γ transitions have been detected.

Although there would appear to be a correlation between the dissociations in the Arrhenius plot and the temperatures associated with polymer relaxations, the reported results are often conflicting. Furthermore, polymer relaxations cannot explain many of the effects obtained in this present study, namely the decrease in lifetime and observation of an emission at 380nm as the dopant concentration

increases, and the initial non-exponential decay at high additive concentrations, even at very low temperatures. Horie, Mita et al, in a series of papers, reported that above Tg and below T_β the decays are exponential, and attribute the non-exponentiality at $T_\beta > T < Tg$ to intermolecular quenching by the matrix [41-44]. However, their studies were carried out on films containing additive concentrations of ca 10^{-3}M and are therefore consistent with the results obtained in this present study for low additive concentration. At higher concentrations of dopant, this work has shown that non-exponential decay would be expected at all temperatures, and hence Horie's mechanism of diffusion-controlled intermolecular quenching can be questioned.

TABLE 3.8

RELAXATION TEMPERATURES, ACTIVATION ENERGIES AND MODES OF MOLECULAR MOTION FOR PMMA AND Psty

From Mechanical Measurements [45]

PMMA

Relaxation	Relaxation Temperature	Activation energy kJ/mol^{-1}	Molecular motion
T_{α}'	301K	177	local mode relaxation
T_{β}	273K	78	ester group rotation
T_{γ}	100K	13	ester methyl group rot^{n}

Psty

Relaxation	Relaxation Temperature	Activation energy kJ/mol^{-1}	Molecular motion
Tg	377K	335	main chain relaxation
T_{β}	300K	126	local mode relaxation
T_{γ}	138-153K	33.5	restricted phenyl rot^{n}

TABLE 3.9

From Arrhenius intensity plots (Temperature range does not include Tg)

POLYMER/PROBE	T_1	ΔE	T_2	ΔE	T_3	ΔE	REF
PMMA-MVK (Copolymerised)			248	31.8	148	17.5	39
PMMA-NMA (Copolymerised)			245	38.5	148	23.4	39
PMMA-NMA-MVK (80:10:10)			236	25.1	173	12.5	39
PMMA/Naphthalene			250	14	155	7	47
PMMA/Acenaph			253	20	173	9	47
PMMA/1VN (Copolymerised)			259	20	160	5	47
PMMA/2-VN (Copolymerised)			263	19	159	5	47
PMMA-NMA			257	13	163	5	47
PMMA/ 1	270	267	240	14.5	157	8	48
PMMA/2			252	16.4	181	9.1	48

MVK = methyl vinyl ketone

NMA = 1-naphthyl methacrylate

1-VN = 1-vinyl naphthalene

2-VN = 2-vinyl naphthalene

Acenaph = acenaphthalene

1 ß-carboline (9H-pyrido [3,4] indole)

2 Indole-3-acetic acid

COMMENT

The experimental results are more consistent with a mechanism in which triplet-triplet annihilation occurs with energy transfer from the solute to the lowest triplet energy level of the polymer as the first step. This intramolecular energy transfer process from the triplet state of the additive to the host matrix is well established in mixed crystal systems and is dependent on the energy levels of both guest and host, T_G and T_H respectively. Energy transfer is favourable if $T_G > T_H$; however if the energy gap between T_G and T_H is small (when $T_H > T_G$), thermally assisted energy transfer from T_G to T_H has been shown to occur in both mixed crystal [49-51] and polymer host-guest systems.

Before discussing the proposed mechanism in more detail, several experiments were carried out in order to determine how triplet-triplet annihilation can occur. El-Sayed et al [29] have suggested that it is a diffusion-controlled reaction, but this does not seem appropriate in the case of the films with high additive concentration. Non-exponentiality was observed at 80K, where diffusion through the very rigid matrix is unlikely. Also, if diffusion was the likely mechanism, then it would be expected that self-quenching would be more prominent in the softer PVA, since at higher temperatures this matrix is just below its Tg. This was not observed. Another possible mechanism for T-T annihilation to occur is via energy migration through the host. Energy migration was first proposed by Naqvi [52] for small molecules in rigid solutions. Slow diffusive transport and/or rotation of $^3T^*$ was suggested by Parker [53], but this was shown to be an inadequate explanation in some cases, since polarisation studies by El-Sayed [54] showed that emitting molecules retain their initial orientation throughout the period of absorption and emission. Naqvi [52] proposed a triplet energy migration mechanism, occurring by electron exchange interaction over distances up to 1.5nm,

to sites at which two triplets can interact by another electron exchange interaction process

i.e. $^3M^* + {}^1M_0 \longrightarrow {}^1M_0 + {}^3M^*$ energy migration

$^3M^* + {}^3M^* \longrightarrow {}^1M^* + {}^1M_0$ T-T annihilation

In polymers, this mechanism has been shown to be intramolecular, and will be discussed in more detail in Chapter 4.

The efficiency of this energy migration process is studied by adding small quantities of quencher to the matrix and examining the effect on the triplet state lifetime.

EXPERIMENTAL RESULTS (cont)

4 THE PHOSPHORESCENCE DECAY OF CARBAZOLE IN THE PRESENCE OF Br-CARBAZOLE QUENCHER IN POLYMER FILMS

3-Bromocarbazole is expected to act as a good phosphorescence quencher because it contains a heavy atom. The aim of the work in this section was to study the effect of altering the concentration of Br-carbazole on the lifetime of phosphorescence. Since very small quantities of Br-carbazole were required, stock solutions of carbazole and bromocarbazole in CH_2Cl_2 were made up. Lifetime has already been shown to be dependent on solute concentration so the total number of carbazole units (i.e. non-brominated plus brominated) were kept constant. This assumed that carbazole and bromocarbazole have identical absorbance at 337nm : in fact, carbazole was found by UV spectroscopy to have a higher absorbance (Σ=256) at 337nm than bromocarbazole (Σ=174). However, since the concentrations of carbazole ranged from 0.05M - 0.04M, and bromocarbazole from 0M - 0.01M, this change in total absorbance is , at worst, only 7%, and should not therefore give a significant change to the phosphorescence lifetime.

Surprisingly, there was no significant decrease in the lifetime of the film as a result of increasing the bromocarbazole concentration, even at a carbazole:bromocarbazole ratio of 4:1 (Table 3.10 and Table 3.11). No quenching appears to have taken place.

One very interesting discovery was the very fast decay over the initial part of the curve. This was not observed for the 0% and 1% bromocarbazole films, but became much more prominent as the Br-carbazole concentration increased (Figure 3.11). This initial decay was not affected by reducing the intensity of the laser by filters.

The three variable fitting routines for double exponential decays

The three variable fitting routines for double exponential decays (DEX) and T-T annihilation (TRIP) (see Appendix) were used to analyse the experimental data. In all cases, the double exponentials gave an excellent fit, whereas T-T annihilation gave a poor fit to the data (Figure 3.12). It appears as though bromocarbazole is <u>not</u> acting as a quencher in the system, but is absorbing the 337nm excitation and producing a very fast decay at 410nm. The decays obtained are made up of two separate emissions : for example, at 80K, a very fast bromocarbazole decay (k_1 calculated using DEX $\approx$ 12 s^{-1}) and a slower carbazole decay ($k_1 \approx 0.16\ s^{-1}$) was observed.

As with all the other carbazole-related compounds studied, the bromocarbazole lifetimes decreased with temperature, to the extent that above 200K, the decay was too fast for the apparatus to detect. Also, the intensity of the decays decreased with temperature (Figure 3.13).

TABLE 3.10

LIFETIME RESULTS:

VARIOUS CONCENTRATIONS OF CARBAZOLE / BROMOCARBAZOLE IN Psty FILM

Total concentration of carbazole units = 0.05M.

%Cz	100%		98%		96%		92%	
(%BrCz)	(0%)		(2%)		(4%)		(8%)	
TEMP	τ/s	R-sq	τ/s	R-sq	τ/s	R-sq	τ/s	R-sq
80K	5.4	*100%*	5.6	*99.9%*	5.2	*99.9%*	6.0	*99.9%*
100K	5.2	*99.9%*	5.3	*99.9%*	5.0	*99.9%*	5.7	*99.9%*
125K	5.1	*100%*	5.2	*99.9%*	5.0	*99.9%*	5.7	*99.9%*
150K	5.0	*99.9%*	5.2	*99.9%*	4.9	*99.9%*	5.5	*99.9%*
175K	4.9	*99.9%*	4.9	*99.8%*	4.9	*100%*	5.3	*99.9%*
200K	4.8	*99.9%*	4.7	*99.9%*	4.7	*99.9%*	4.6	*99.9%*
225K	3.2	*99.8%*	3.9	*99.8%*	4.1	*99.9%*	3.9	*99.8%*
250K	3.0	*99.7%*	2.6	*99.6%*	3.0	*99.7%*	3.2	*99.7%*
275K	/	/	/	/	1.6	*99.5%*	0.9	*99.3%*

TABLE 3.10 (cont)

%Cz	84%		80%		70%		60%	
(%BrCz)	(16%)		(20%)		(30%)		(40%)	
TEMP	τ/s	R-sq	τ/s	R-sq	τ/s	R-sq	τ/s	R-sq
80K	5.6	*99.9%*	5.1	*99.7%*	5.3	*99.7%*	5.3	*99.2%*
100K	5.6	*99.8%*	5.3	*99.8%*	5.2	*99.6%*	5.0	*99.2%*
125K	5.4	*99.9%*	5.3	*99.8%*	5.0	*99.8%*	4.9	*99.2%*
150K	5.2	*99.9%*	5.0	*99.9%*	5.0	*99.8%*	4.9	*99.2%*
175K	5.1	*99.9%*	4.9	*99.9%*	4.8	*99.9%*	4.8	*99.9%*
200K	4.8	*99.9%*	4.2	*99.9%*	4.5	*99.9%*	4.5	*99.9%*
225K	3.8	*99.7%*	3.8	*99.7%*	3.5	*99.8%*	3.7	*99.9%*
250K	2.6	*99.6%*	2.8	*99.4%*	2.3	*99.4%*	2.5	*99.5%*
275K	0.6	*99.1%*	0.5	*99.7%*	0.8	*99.1%*	0.8	*99.4%*

TABLE 3.11

LIFETIME RESULTS:

VARIOUS CONCENTRATIONS OF CARBAZOLE / BROMOCARBAZOLE IN PMMA FILM

Total concentration of carbazole units = 0.05M.

%Cz	100%		98%		96%		92%	
(%BrCz)	(0%)		(2%)		(4%)		(8%)	
TEMP	τ/s	R-sq	τ/s	R-sq	τ/s	R-sq	τ/s	R-sq
80K	6.2	*99.9%*	6.2	*99.9%*	6.4	*99.9%*	6.5	*99.8%*
100K	6.2	*99.9%*	6.1	*99.9%*	6.2	*99.9%*	6.1	*99.9%*
125K	6.1	*99.9%*	6.0	*99.9%*	6.2	*99.9%*	6.2	*99.8%*
150K	6.0	*99.9%*	5.9	*99.9%*	6.0	*99.9%*	6.0	*99.9%*
175K	6.0	*99.9%*	5.7	*99.9%*	5.9	*99.9%*	5.9	*99.9%*
200K	5.9	*99.9%*	5.7	*99.9%*	5.8	*99.9%*	5.6	*99.9%*
225K	5.5	*99.9%*	4.8	*99.9%*	5.6	*99.9%*	5.3	*99.9%*
250K	4.4	*99.9%*	4.0	*99.8%*	5.0	*99.9%*	3.9	*99.8%*
275K	2.3	*99.0%*	2.7	*99.6%*	3.5	*99.7%*	2.5	*99.2%*

TABLE 3.11 (cont)

%Cz	84%		80%	
(%BrCz)	(16%)		(20%)	
TEMP	τ/s	R-sq	τ/s	R-sq
80K	6.7	*99.8%*	6.4	*99.7%*
100K	6.3	*99.8%*	6.5	*99.8%*
125K	6.3	*99.8%*	6.4	*99.7%*
150K	6.2	*99.9%*	6.5	*99.9%*
175K	6.2	*99.9%*	6.4	*99.9%*
200K	6.3	*100%*	6.4	*99.9%*
225K	5.9	*100%*	6.0	*99.9%*
250K	4.2	*99.9%*	4.9	*99.9%*
275K	2.1	*99.5%*	3.2	*99.7%*

FIGURE 3.11

EFFECT OF 3-BROMOCARBAZOLE CONCENTRATION ON THE INITIAL NON-EXPONENTIAL DECAY OF CARBAZOLE

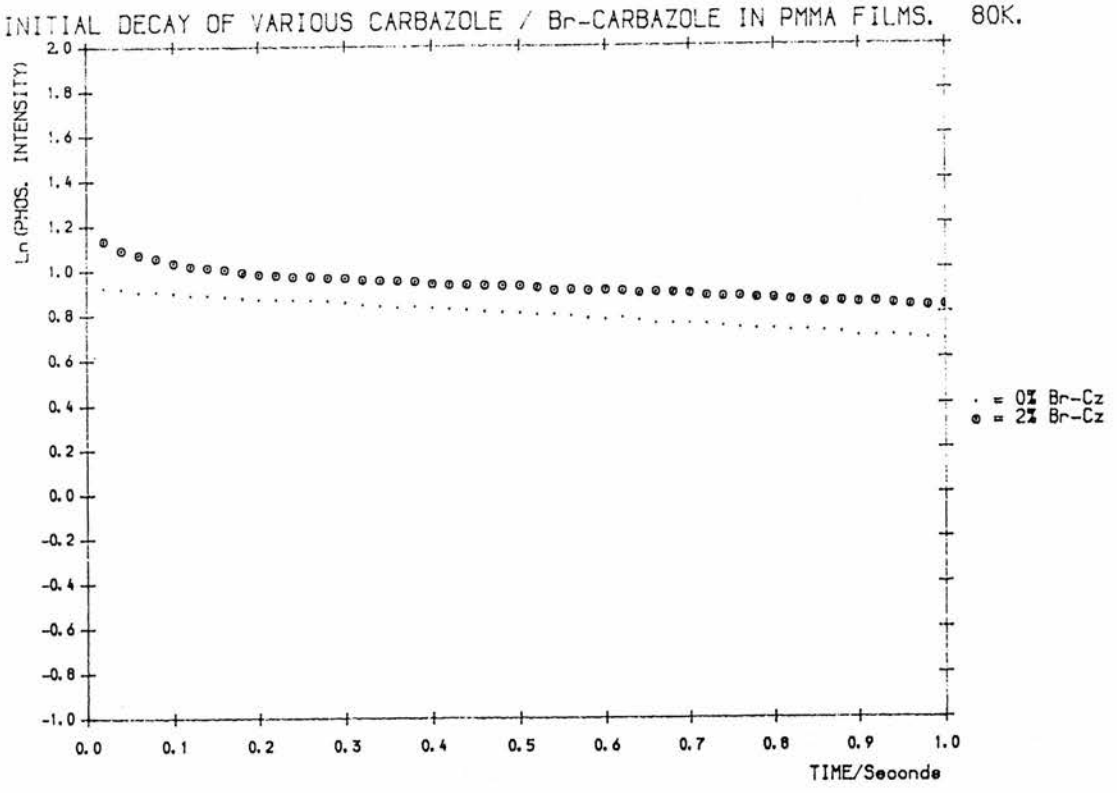

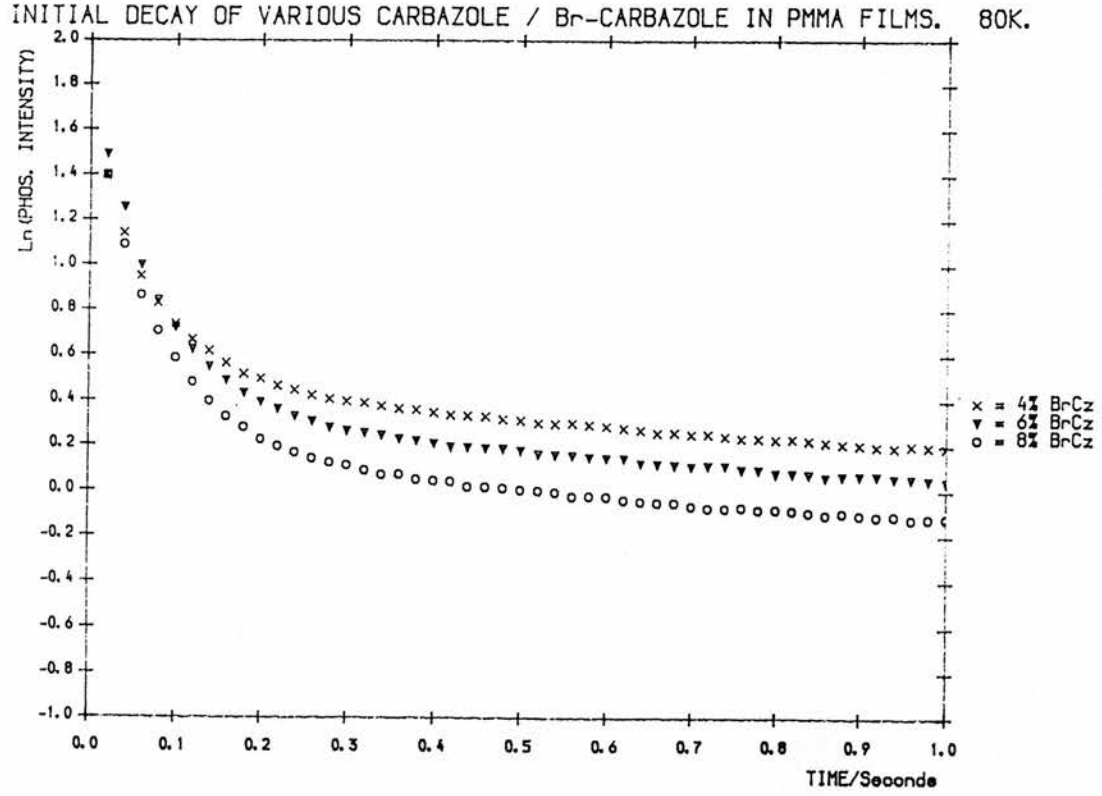

FIGURE 3.12

USE OF FITTING ROUTINES TRIP AND DEX

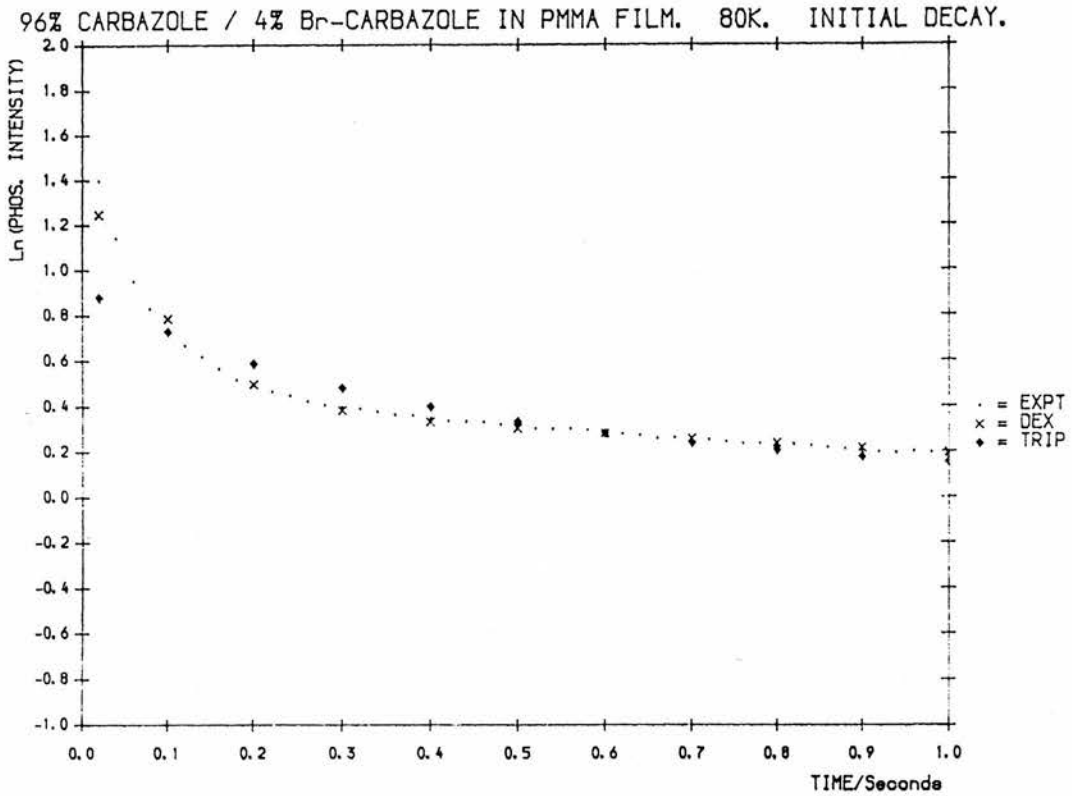

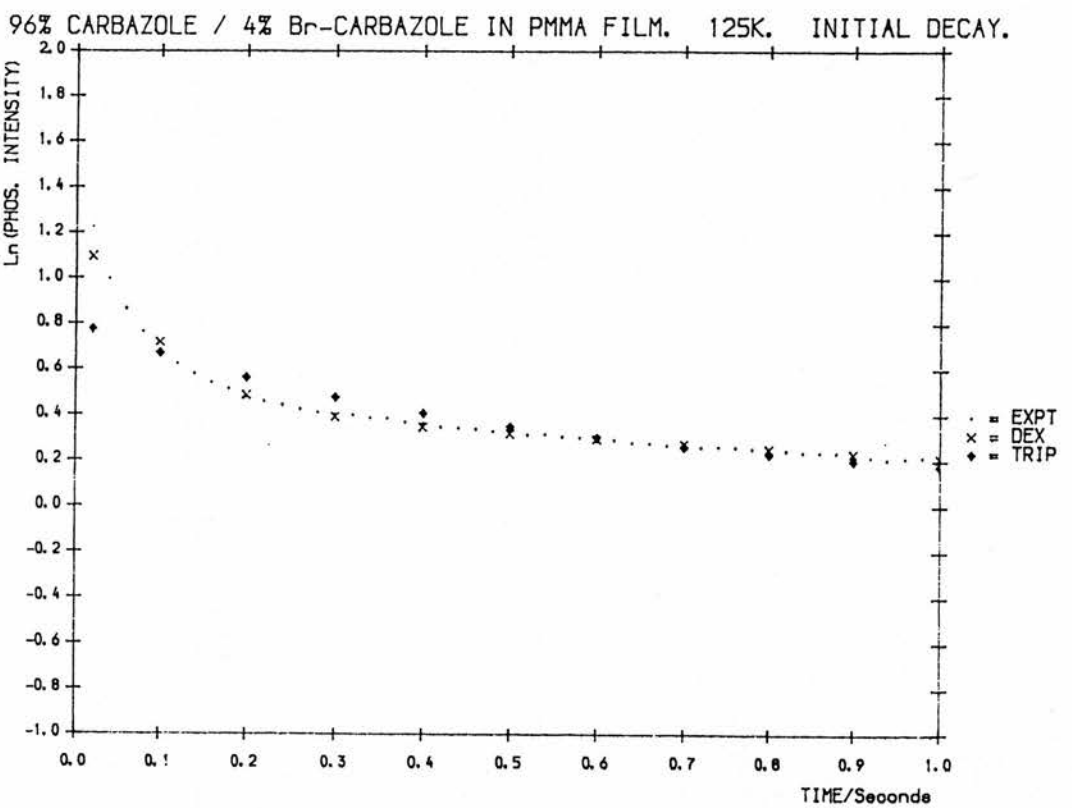

FIGURE 3.13

EFFECT OF TEMPERATURE ON THE INITIAL DECAY OF 3-BROMOCARBAZOLE

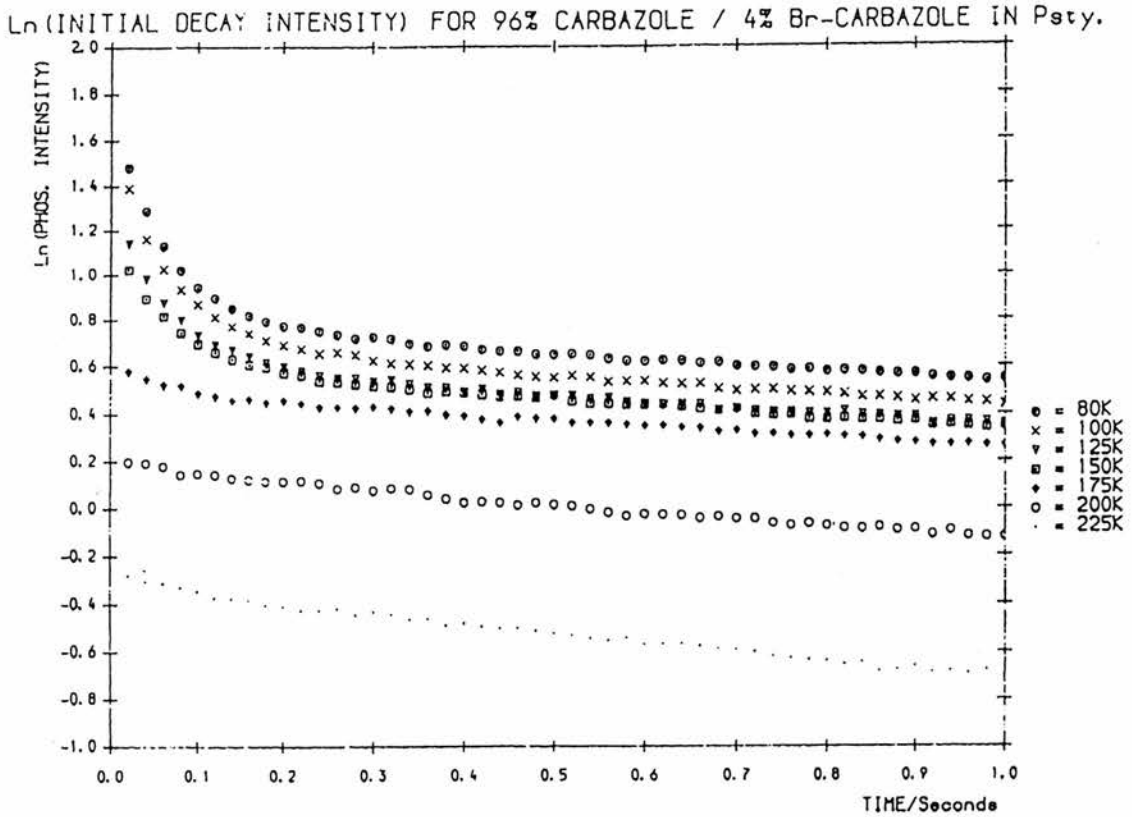

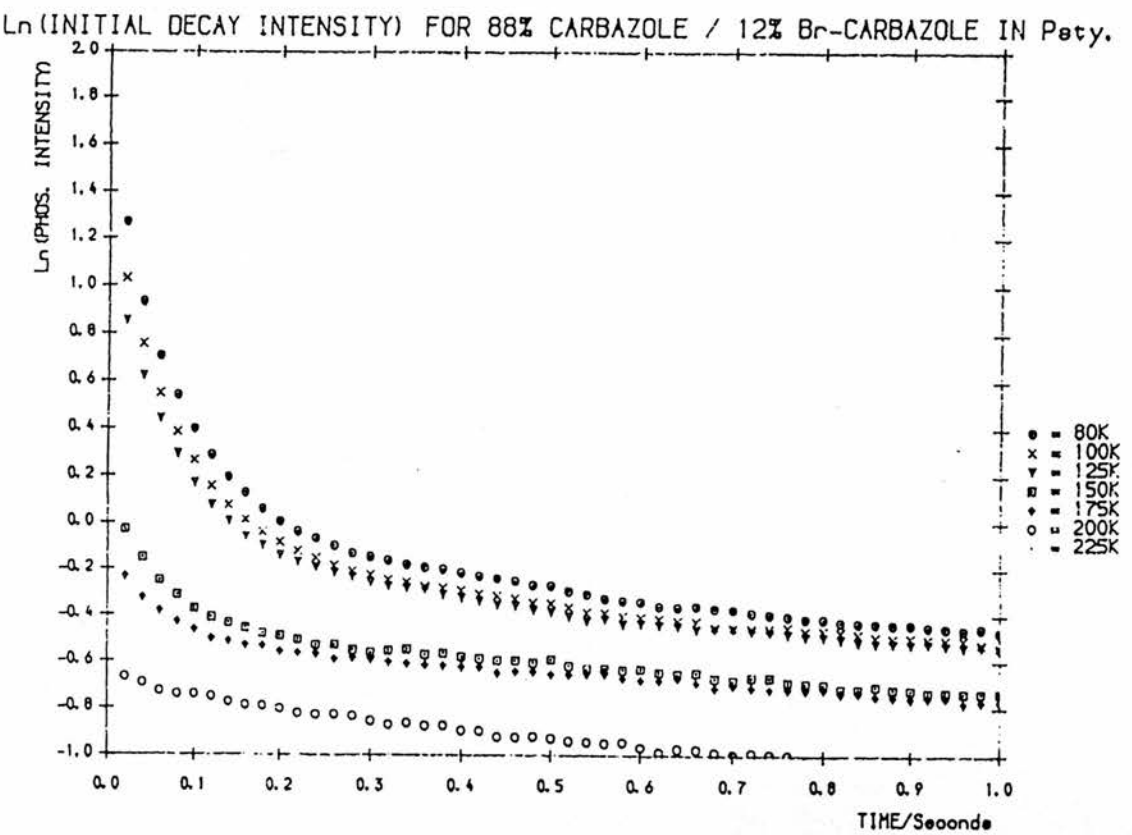

5 PHOSPHORESCENCE LIFETIME OF NEC / Pr[18-CROWN-6].$(NO_3)_3$ IN POLYSTYRENE FILM

Metals of the first transition series and the rare earth lanthanides are found to be very effective triplet quenchers of the triplet state ($k_Q \approx 10^7 - 10^9$ mol^{-1} sec). However, they tend to be very insoluble - one possible method of dissolving them in CH_2Cl_2 is by complexing them with a crown ether. They can then be incorporated into a polymer film and their effect on quenching the decay of N-ethylcarbazole can be looked at.

The results show that Pr[18-crown-6].$(NO_3)_3$ does not quench the NEC lifetime (Table 3.12)

TABLE 3.12

LIFETIME RESULTS:

THE EFFECT OF ADDING VARIOUS CONCENTRATIONS OF

$Pr[18\text{-CROWN-6}].(NO_3)_3$ TO A POLYSTYRENE THIN FILM CONTAINING 0.12M N-ETHYLCARBAZOLE

TEMP	CONCENTRATION OF CROWN ETHER COMPLEX					
	0M	7.4×10^{-4}M	1.5×10^{-3}M	4.5×10^{-3}M	1.0×10^{-2}M	1.9×10^{-2}M
80K	6.3	6.0	6.2	6.0	6.2	6.4
100K	6.8	6.5	6.2	6.1	6.3	6.9
125K	6.9	6.3	6.1	6.1	6.2	7.0
150K	6.9	6.5	6.1	6.0	6.2	7.0
175K	6.9	6.3	6.1	6.0	6.1	7.0
200K	5.5	6.0	5.9	5.9	6.0	6.8
225K	5.3	5.4	/	5.6	5.7	6.1
250K	4.3	4.8	4.1	4.4	4.7	4.9
275K	3.4	3.9	2.9	3.8	3.1	3.9
298K	2.5	2.5	1.1	2.2	1.5	2.7

DISCUSSION AND PROPOSED MECHANISM

The following mechanism for the decay of triplet species once excitation has ceased is proposed:

$T_1^* \text{ -----> } S_0 + h\nu_P$ phosphorescence..... (1)

$T_1^* \text{ -----> } S_0$ non-radiative.....(2)

$T_1^* + P_0 \text{ -----> } P_T^* + S_0$ energy transfer to matrix.(3)

$P_T^* \text{ -----> } P_0$ radiative/non-radiative deactivation of P_T^*.....(4)

$P_T^* + P_0 \text{ -----> } P_0 + P_T^*$ energy migration of P_T^*...(5)

$P_T^* + T_1^* \text{ -----> } P_0 + S_0$

$\text{-----> } P_0 + S_1^*$ T-T annihilation producing delayed fluorescence.....(6)

$S_1^* \text{ -----> } S_0 + h\nu_D$

$T_1^* + S_0 \text{ -----> } S_0 + T_1^*$ energy migration of T_1^*...(7)

$T_1^* + T_1^* \text{ -----> } 2S_0$

$\text{-----> } S_1^* + S_0$ T-T annihilation involving T_1^*.....(8)

$S_1^* \text{ -----> } S_0 + h\nu_{DF}$

Steps (1)-(3) are identical to those proposed by McGlynn et al [33] to explain the drop in lifetime with increasing temperature. The Arrhenius plots showed a low activation process ΔE_1 at low temperatures, related to the temperature dependent radiationless transfer from T_1^* --> S_0 of the additive, and a higher activation energy process, ΔE_2, at higher temperatures associated with energy transfer to the matrix (step 3). This triplet energy transfer step accounts for the dependence of phosphorescence lifetime on polymer matrix. The energy levels of the triplets are listed in Table 3.2. Energy transfer to PVA and Psty is slightly exothermic and is presumably more favourable than transfer to

PMMA which is slightly endothermic. Thus, quenching by PMMA is less than PVA and Psty, and this is reflected in the lifetimes obtained. Since long-range transfer in this system is unlikely because the overlap between donor emission and acceptor concentration is negligible, energy transfer must occur by the exchange mechanism.

Steps 7 & 8 account for the self-quenching of carbazole and N-ethylcarbazole in homopolymer films at high concentration. Delayed fluorescence was much more easily observed at high [carbazole], and by reducing the intensity of the excitation source, this T-T annihilation process is limited.

After P_T^* has been formed, it can either return quickly to the ground state polymer, P_0 (step 4), or undergo energy transfer through the polymer matrix (step 5) and/or T-T annihilation between P_T^* and T_1^* takes place. In PMMA, Psty and PVA matrices, the fast return to the ground state is the preferred route, deduced from the fact that the introduction of quenchers to the system had no effect on the phosphorescence lifetime. Triplet polymer P_T^* is a very short-lived species in these matrices. By using a partially deuterated polystyrene matrix, the lifetime of the polymer triplet is extended, thus favouring steps 5 and/or 6, and quenching of the emission by poly(d^8-styrene) P_T^* is more efficient than by the undeuterated polymer P_T^*.

In conclusion, the suitability of polymers as inert host matrices in studies of phosphoresence of additives is in question, since there is energy transfer from the guest to the host.

CHAPTER 4

CHAPTER 4

ENERGY TRANSFER IN COPOLYMERS

Similar studies to those described in Chapter 3 were carried out on various vinyl carbazole/methyl methacrylate copolymers to find if the kinetic scheme proposed for carbazole and related compounds in homopolymer matrices can be extended to the copolymer analogs.

The vinyl carbazole/methyl methacrylate (VC/MMA) copolymer compositions ranged from 0.6 - 4.9 mole % vinyl carbazole (0.06 - 0.45M). These are characterised in Table 4.1.

TABLE 4.1

CHARACTERISATION OF MMA/VC COPOLYMERS

NO	[Cz] units	%VC (mole %	Tg ^{0}C	Mn	Mw	Mz	Mw/Mz
1	0.45M	4.3	117	1.67×10^{4}	4.16×10^{4}	8.28×10^{4}	2.49
2	0.51M	4.9	126	1.99×10^{4}	5.27×10^{4}	1.12×10^{4}	2.65
3	0.31M	2.9	122	1.85×10^{4}	5.56×10^{4}	1.41×10^{4}	3.01
4	0.14M	1.4	121	1.39×10^{4}	5.07×10^{4}	1.81×10^{4}	3.65
5	0.60M	0.6	125	2.11×10^{4}	8.04×10^{4}	4.45×10^{5}	3.81
6	0.22M	2.2	114	1.23×10^{4}	4.74×10^{4}	1.31×10^{5}	3.85
7	0.13M	1.3	123	1.76×10^{4}	6.07×10^{4}	2.16×10^{5}	3.45

EXPERIMENTAL RESULTS

1 PHOSPHORESCENCE LIFETIMES OF VINYL CARBAZOLE/METHYL METHACRYLATE COPOLYMERS

The decay of the carbazole-unit triplet state was measured at 410nm and the lifetime of the emission calculated, (Table 4.2), discarding any initial non-exponential decay as before. Several interesting observations were made:

(a) It was not possible to obtain a decay above 225/250K for most of the higher concentration samples since the intensity of the decay had fallen to such a low value.

(b) There was a high degree of initial non-exponentiality in each copolymer decay. Using a combination of a 337nm filter and neutral density optical filters (Barr & Stroud) to reduce the excitation intensity of the laser, this initial process was removed and the decay became exponential (Figure 4.1).

(c) A three variable fitting routine for T-T annihilation, based on the method of differential coefficients (see Appendix), was used to analyse the experimental data. Only every tenth calculated value was plotted for simplicity. If a large enough reduction of laser intensity was achieved by filters, there was a large deviation to the T-T annihilation fit (Figure 4.1). This clearly suggests that by cutting down the excitation intensity and hence $[T^*]$, triplet-triplet annihilation plays a less significant role (Figure 4.2).

(d) The triplet state lifetimes of the copolymer samples were found to follow the same trends as the carbazole-doped homopolymers, i.e. as the number of carbazole units increased, the phosphorescence lifetime decreased.

TABLE 4.2

LIFETIME RESULTS

VINYL CARBAZOLE/METHYL METHACRYLATE COPOLYMER FILMS

Mole% VC [carbazole]/mol l^{-1}	4.9% 0.51M	4.3% 0.45M	2.9% 0.31M	1.4% 0.14M	0.06% 0.06M
80K	6.3	6.2	6.7	7.1	7.6
100K	6.3	5.9	6.6	6.9	7.4
125K	6.3	5.8	6.4	7.1	7.1
150K	6.1	5.7	6.4	7.0	7.1
175K	6.0	5.7	6.4	6.7	6.9
200K	5.7	5.8	6.1	6.1	6.6
225K	4.6	/	4.8	4.8	5.6
250K	/	/	/	/	4.2

FIGURE 4.1

EFFECT OF REDUCING LASER INTENSITY ON INITIAL NON-EXPONENTIALITY

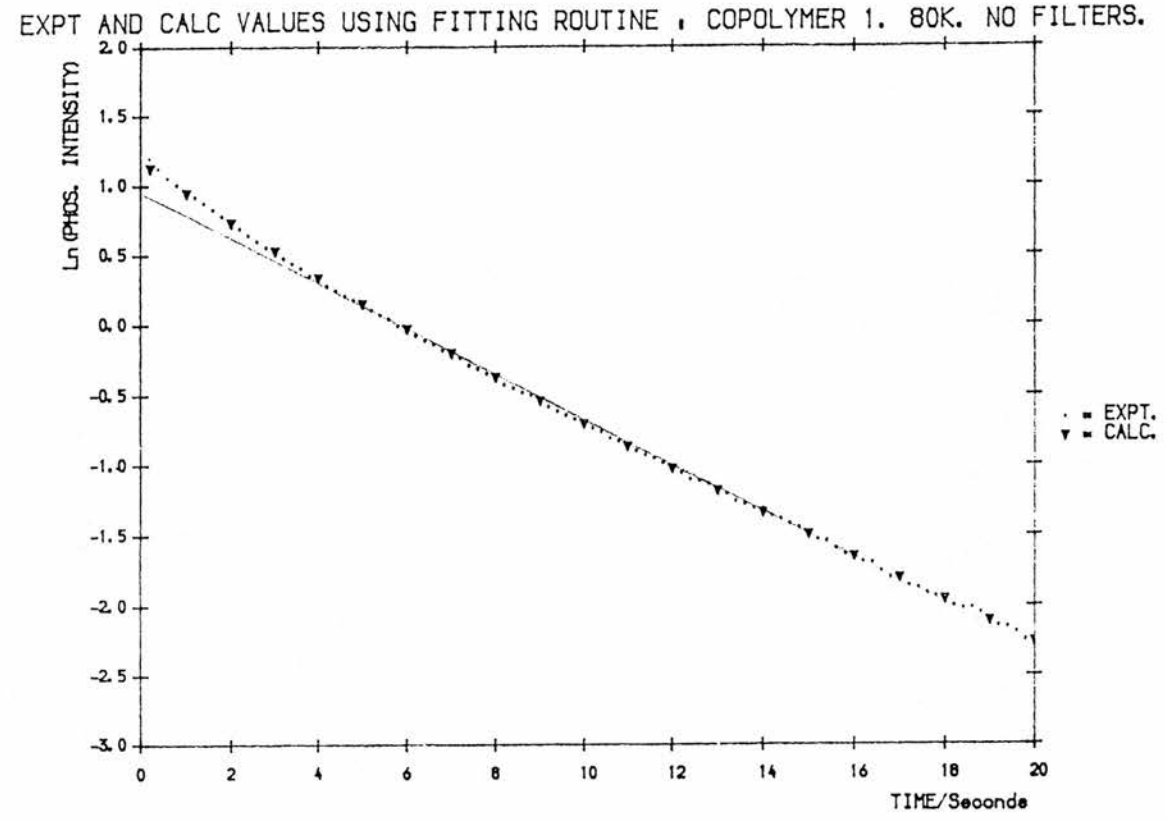

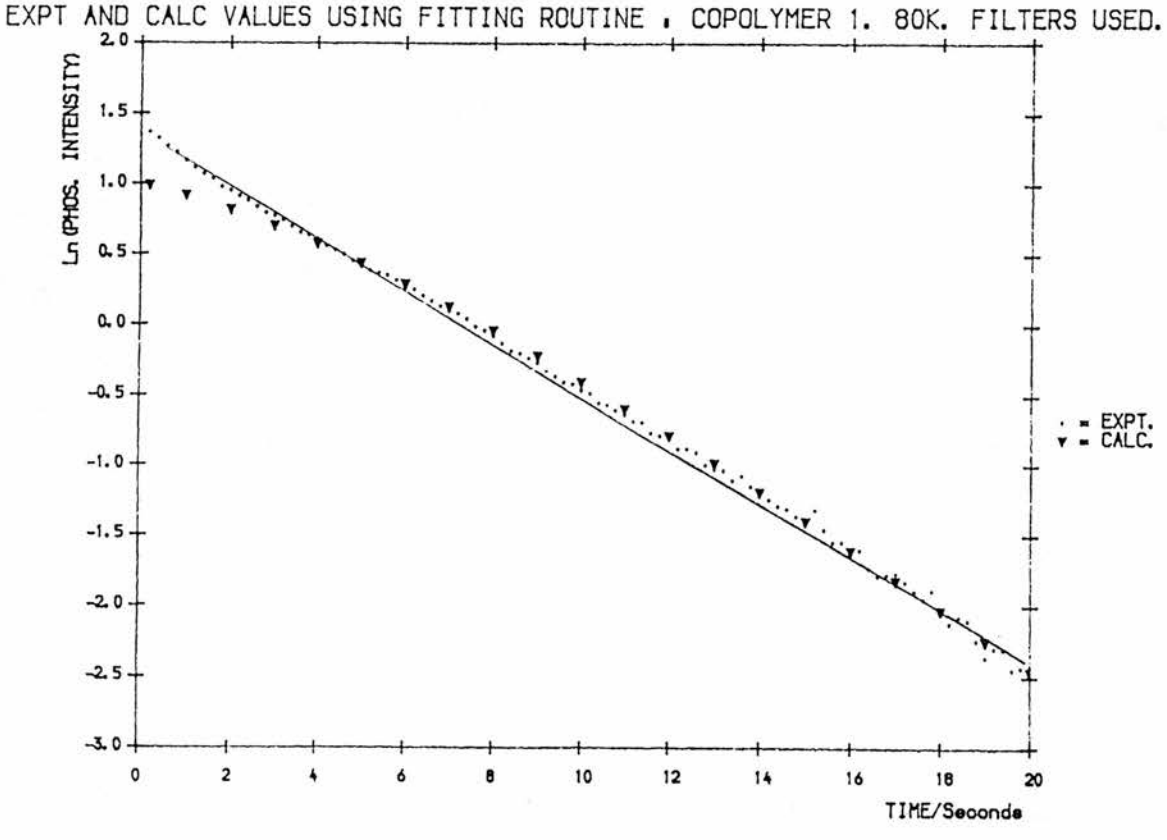

—— single exponential fit

FIGURE 4.2(a)

CURVE FIT WITH T-T FITTING ROUTINE

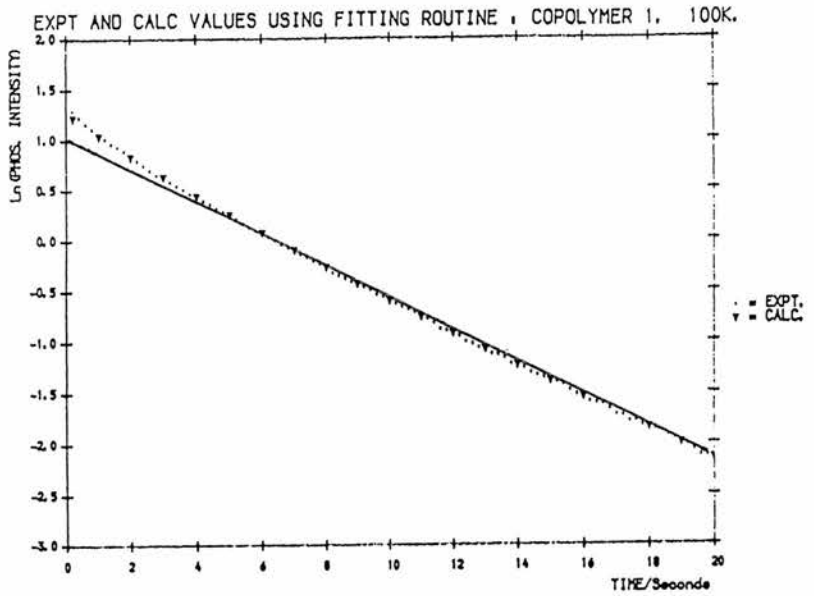

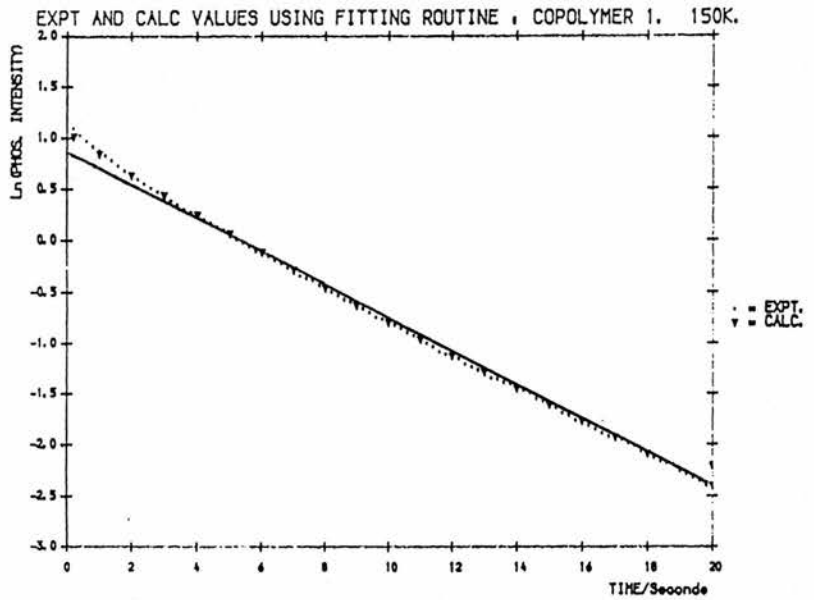

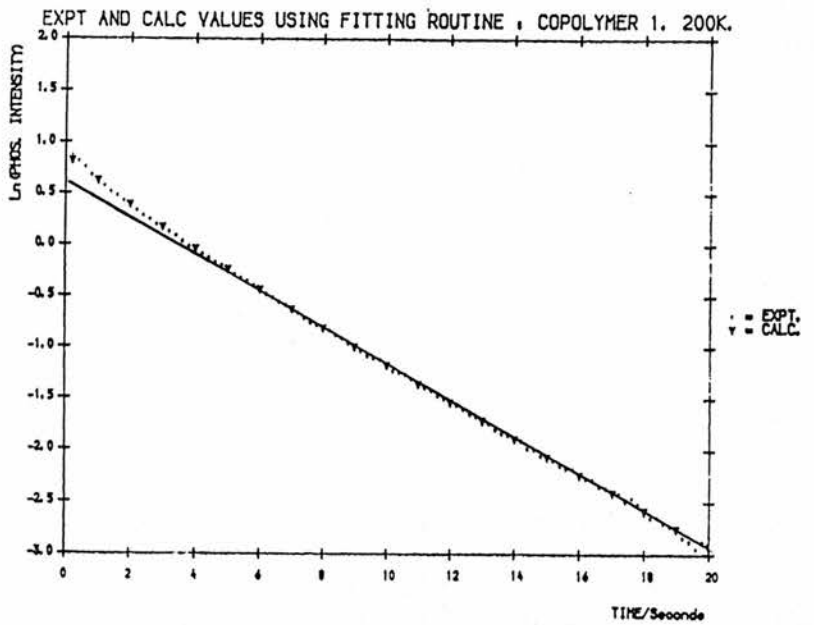

FIGURE 4.2(b)

CURVE FIT WITH T-T FITTING ROUTINE

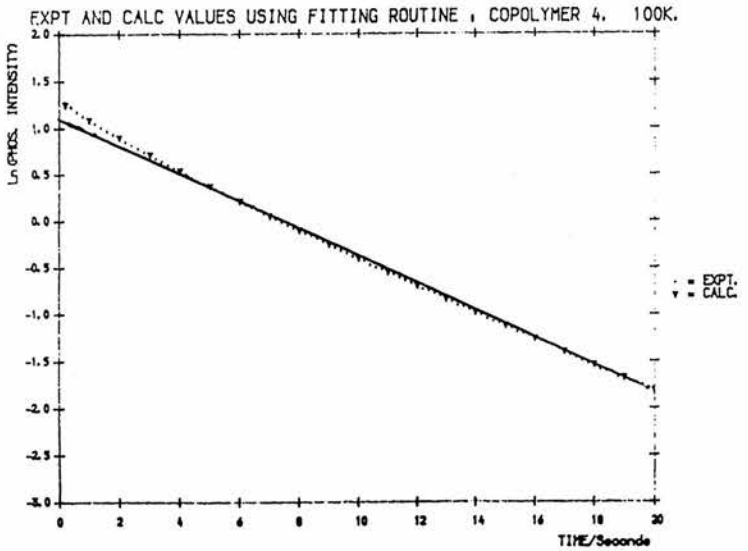

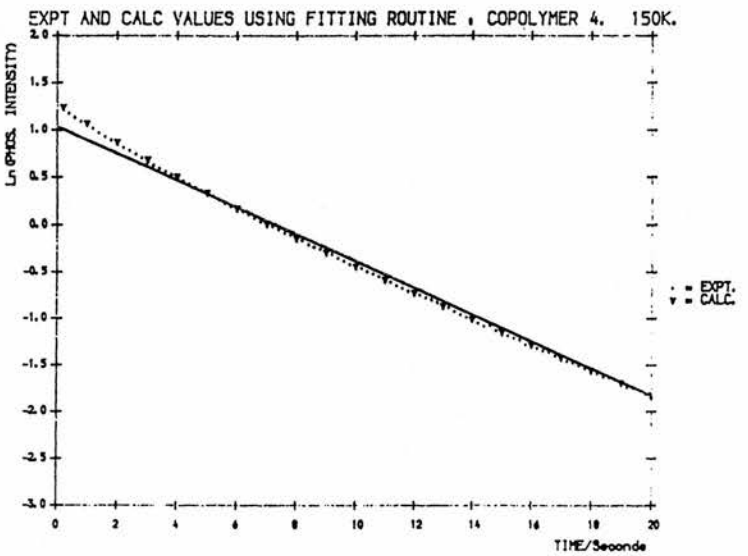

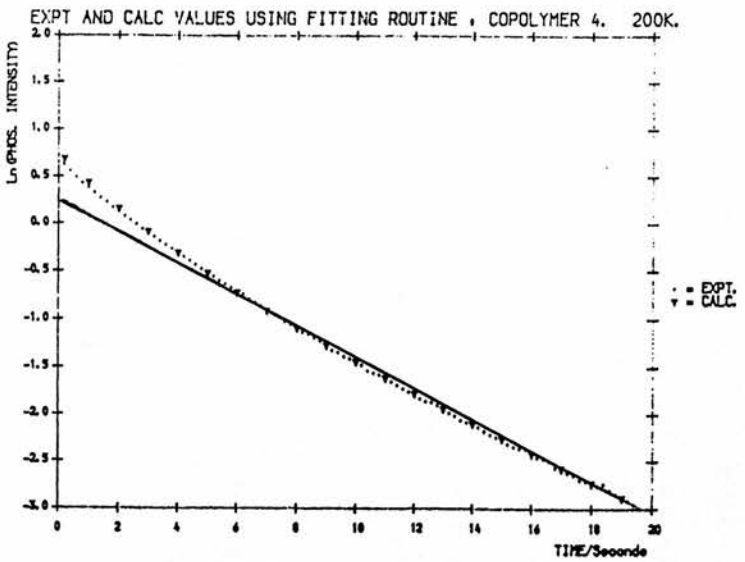

2 PHOSPHORESCENCE DECAY OF A VINYL CARBAZOLE/METHYL METHACRYLATE COPOLYMER IN THE PRESENCE OF 3-BROMOCARBAZOLE QUENCHER

Copolymer 5 (0.06M in vinyl carbazole) was doped with varying quantities of 3-bromocarbazole to determine whether or not intermolecular quenching would occur in the copolymer matrix. The lifetime of the sample was determined by calculating the regression of the best straight line using Minitab. The initial fast decay due to the bromocarbazole emission was ignored.

The results are shown in Table 4.3. There is definite quenching of the copolymer phosphorescence lifetime by the bromocarbazole. The triplet lifetime falls from 7.6 seconds at 0M bromocarbazole concentration (80K) to 2.8 seconds at 0.025M Br-carbazole concentration. It must be noted that the values at 0.025M Br-carbazole were measured over a small number of points. No attempt was made to use these values in an energy transfer fitting routine since they do not obey the condition that the quencher should not absorb the excitation wavelength. 3-Bromocarbazole does absorbed at 337nm.

TABLE 4.3

LIFETIME RESULTS

VARIOUS CONCENTRATIONS OF 3-BROMOCARBAZOLE IN COPOLYMER 5

Copolymer 5 : 0.06M in carbazole units

%Br-Cz/Cz Br-Cz]	0% 0M	4% 0.0025M	8% 0.005M	17% 0.01M	25% 0.015M	42% 0.025M
80K	7.6	6.8	6.4	6.0	5.1	2.8
100K	7.4	6.8	6.2	5.9	5.3	2.4
125K	7.1	6.6	6.4	5.8	5.2	2.3
150K	7.1	6.7	6.3	5.8	5.4	2.5
175K	6.9	6.5	6.4	5.9	5.4	2.7
200K	6.6	6.6	6.4	5.3	5.4	2.6
225K	5.6	6.0	5.8	3.6	4.6	2.4
250K	4.2	4.9	3.6	/	2.8	/
275K	/	3.8	/	/	/	/

3 PHOSPHORESCENCE DECAY OF A VINYL CARBAZOLE/METHYL METHACRYLATE COPOLYMER IN THE PRESENCE OF $Pr[18\text{-CROWN-6}](NO_3)_3$

The results are shown in Table 4.4. As the concentration of the crown complex increases, there is a small decrease in the phosphorescence lifetime of the copolymer.

TABLE 4.4

LIFETIME RESULTS

$Pr[18\text{-CROWN-6}](NO_3)_3$ IN COPOLYMER 6

	$Pr[18\text{-CROWN-6}](NO_3)_3$ CONCENTRATION			
TEMP	OM	$8.55X10^{-3}M$	0.043M	0.085M
80K	7.9	6.7	6.5	6.5
100K	7.8	6.7	6.5	6.4
125K	7.7	6.7	6.5	6.5
150K	7.6	6.7	6.5	6.4
175K	7.5	6.6	6.5	6.3
200K	7.4	6.5	6.4	6.2
225K	7.0	6.4	6.3	6.1
250K	6.2	5.7	5.8	5.7
275K	5.0	4.6	4.1	3.9

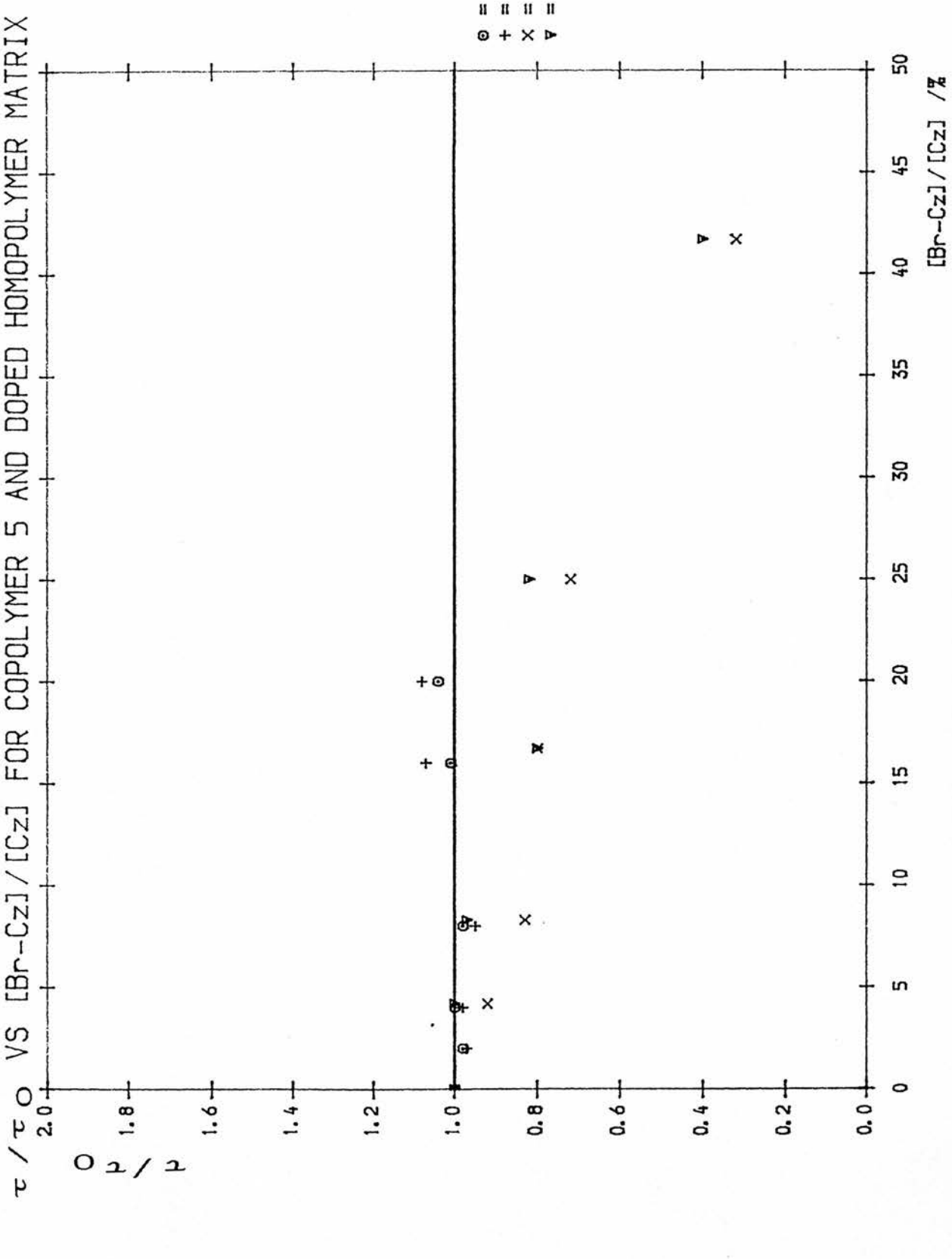

τ/τ_0 Vs [BrCz]/[Cz] FOR COPOLYMER 5 AND DOPED HOMOPOLYMER

DISCUSSION

A plot of τ/τ_0 vs [Br-carbazole]/[carbazole] % at 100K and 200K for both the copolymer and the homopolymer matrices (Figure 4.3) clearly shows certain fundamental differences between the doped homopolymer matrices and the VC-MMA copolymers. τ_0 in this case is the value of τ with no quencher present. In the homopolymer matrices, addition of 3-bromocarbazole was found to have no significant effect on the carbazole triplet state lifetime, as shown by the scattering of points about $\tau/\tau_0 = 1$. However, when the carbazole unit was incorporated into the backbone of the polymer chain, bromocarbazole reduced the phosphorescence lifetime of the carbazole chromophore quite considerably. Similar results were observed with the Pr-crown complex as additive.

In Chapter 3, an energy transfer process from the triplet state of the additive, T_1^*, to the triplet state of the polymer host, P_T^*, was proposed. There were several routes for P_T^* deactivation, namely

P_T^*	----> P_0	radiative/nonradiative
$P_T^* + P_0$	----> $P_0 + P_T^*$	energy migration
$P_T^* + T_1^*$	----> $P_0 + S_0$	
	----> $P_0 + S_1^*$	T-T annihilation
S_1^*	----> $S_0 + h\nu_{DF}$	

If energy migration was an important step in the deactivation of P_T^* in homopolymer matrices, then the added quenching impurities would be more efficient in reducing the triplet state lifetime. However, this was not observed for PMMA, Psty and PVA, and the fast radiative/non-radiative return to ground state was concluded to be the preferred

route. Triplet energy migration was not ruled out for poly(d^8-styrene), where P_T^* would have an extended lifetime.

In the copolymer films, T-T annihilation again appears to be an important process, as shown by the dependence of non-exponentiality on laser intensity, the observation of delayed fluorescence at 380nm at high photomultiplier intensity, and the excellent fit obtained for the experimental data by the T-T fitting routine. The process of energy migration does appear to be a more efficient mechanism in the VC/MMA copolymers compared with the doped PMMA and Psty matrices since the added quenchers have had a significant effect on the phosphorescence lifetime.

Intramolecular triplet energy migration in polymers has been reported by many authors. Studies by Lashkov and Ermolaev [55] of the impurity quenching of the phosphorescence of poly(N-vinylphthalimide) showed the occurrence of triplet energy migration along a polymer chain. Cozzens and Fox, in a series of papers [56-61], demonstrated such intramolecular triplet migration by observations of delayed emission in homopolymers of 1- and 2-vinyl naphthalene (P1VN and P2VN respectively), and copolymers with MMA and styrene. In P1VN in a rigid glass at 77K, they observed delayed fluorescence due to triplet-triplet annihilation, while no delayed emission was observed from 1-ethyl naphthalene at equivalent concentrations. Delayed emission from the polymer but not from 1-ethyl naphthalene was quenched by piperylene. They concluded that intermolecular energy transfer was taking place along the homopolymer chain by way of the naphthalene rings, until two triplets could come close enough to undergo T-T annihilation. Cozzens and Fox also reported [57] that sequences of a few MMA units in (vinyl naphthalene/MMA) copolymers are sufficient to inhibit triplet migration through the chain. This observation is entirely consistent with the

mechanism proposed in Chapter 3, where the efficiency of energy transfer is based on the donor-acceptor energy level separation, E_{D-A}. McGlynn et al [62] have proposed that a thermally activated transfer step is limited to $E_{D-A} < 35$ kJ mol^{-1}. In the polymers studied by Cozzens and Fox, the donor and acceptor levels are 254 kJ mol^{-1} and 297 kJ mol^{-1} respectively, and $E_{D-A} = 43$ kJ mol^{-1}. Hence, energy transfer between the naphthalene and MMA groups would not be expected to take place, and energy migration along the polymer chain would be considerably reduced by the presence of sequences of MMA units. In the present work, E_{D-A} is very small and therefore the carbazole and PMMA units can occur quite readily.

Other examples of triplet energy migration and delayed fluorescence in polymers have been well documented. David et al [63-65] used measurement of the phosphorescence quenching of poly(vinyl benzophenone) and poly(phenyl ketone) to show that energy exchange distances were larger than the usual molecular collision diameters. Intramolecular tripet energy migration was invoked to explain the high critical energy transfer values, R_0, for the aromatic ketone polymers. Somersall and Guillet [66] reported delayed emission of poly(naphthyl methacrylate) and, by studying the effect of triplet quenching by piperylene and 1,3-cyclo octadiene, proposed that triplet energy migration was taking place. Webber and Avots-Avotins [67] studied quenching of the triplet excitons in poly(2-vinyl naphthalene) and poly(acenaphthylene) by biacetyl. The phosphorescence of a polymer-biacetyl mixture showed a strong component of biacetyl at times very long (1-2 seconds) compared with the biacetyl lifetime (milliseconds), demonstrating that the polymer triplet continues to sensitise the biacetyl. The authors concluded that migration distances were longer in P2VN than in poly(acenaphthylene). Burkhart et al [68-71] and Klopffer

et al [72-74] have reported many studies of triplet energy migration in poly(N-vinyl carbazole).

THE MECHANISMS OF ENERGY TRANSFER

Energy transfer has been reported by Guillet to occur by various pathways [75,76]:

(a) Energy hopping from group to group along a polymer chain.
(b) Movement of excitation energy along the carbon-carbon backbone of the chain.
(c) Energy migration along a chain and hopping across loops in the chain.

Each of these processes is illustrated in Figure 4.4.

As discussed in Chapter 3, energy transfer probably occurs in these polymer systems by the exchange mechanism. Three types of energy transfer steps which contribute to energy migration in a polymer chain have been proposed by Guillet: these will now briefly be discussed.

(1) 'Nearest neighbour' transfer (Figure 4.5, step 1). This is defined as transfer between chromophores where n, the number of monomer units between those bearing the transfer sites, is equal to zero. This energy transfer process is important in polymers containing small chromophores attached to flexible chains which permit the proximity of nearest neighbour groups, such as in Psty.

(2) 'Non-nearest neighbour' transfer (Figure 4.5, step 2). where n = 1,2,3. This will occur with chromophores which are prohibited by steric or structural effects from approaching an adjacent chromophore by facile

bond rotation. The most stable conformation of flexible polymer chains usually places large substituent groups as far apart as possible, and thus nearest neighbour interactions may not be feasible. Energy transfer in which there are 1,2 or 3 monomer units has been shown to occur.

(3) 'Loop transfer' (Figure 4.5, step 3), where n > 3 can occur resulting in the transfer of excitation across many units along the length of the polymer chain.

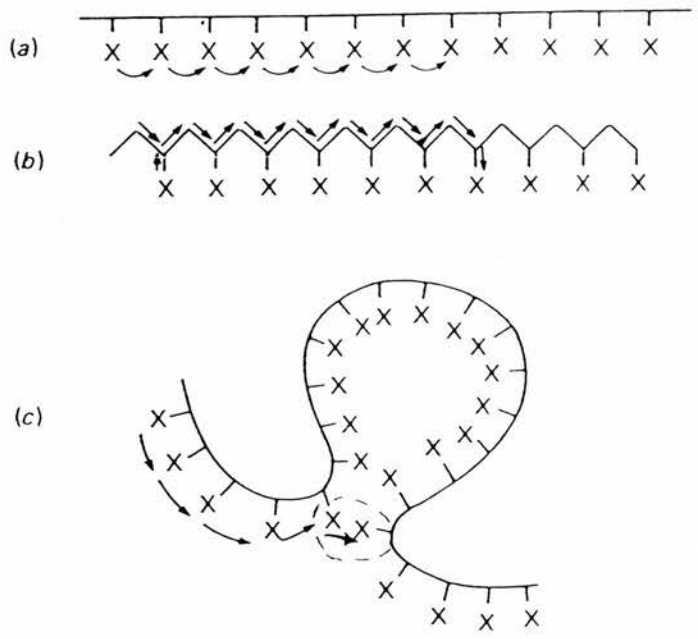

FIGURE 4.4

Intramolecular Energy Exchange In Polymers

(Taken from Guillet, Pure & Appl. Chem., 1977 [75])

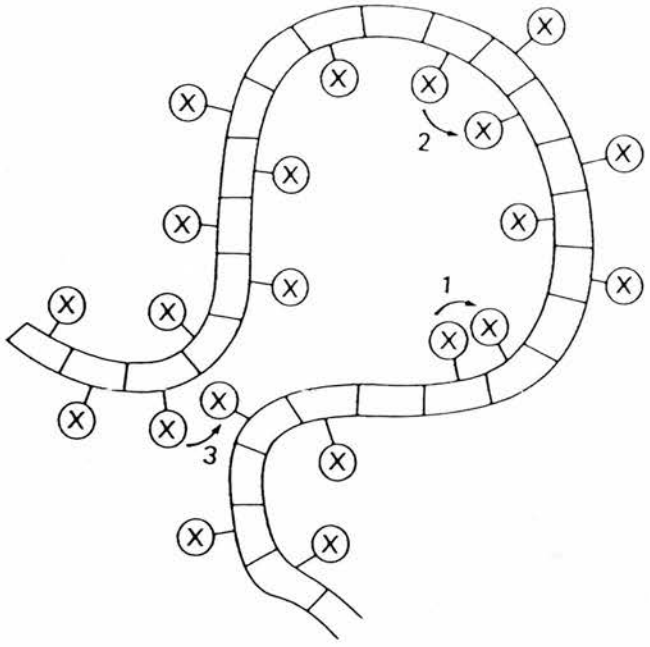

FIGURE 4.5

Possible Energy Transfer Steps in Intramolecular Migration

(Taken from Guillet, Polymer Photophysics and Photochemistry, Chapter 9 [76]

THE PROPOSED MECHANISM

The mechanistic scheme proposed in Chapter 3 for carbazole-doped homopolymer matrices also appears to be consistent with the results for VC/MMA copolymers. However, energy migration is a much more efficient process in the copolymers; this may be due to steric or conformational effects which provide better overlap of chromophores in the copolymer. This increased intramolecular energy migration when the chromophore is incorporated into the backbone of the polymer chain has applications in the field of photodegradation and photostabilisation of polymers e.g. an energy sink attached to the polymer allows internal conversion to the ground state more efficiently than the equivalent sink dissolved in the polymer. Photodegradation would therefore be inhibited.

CHAPTER 5

CHAPTER 5

MAGNETIC FIELD EFFECTS ON TRIPLET STATE PROCESSES

In this chapter, the effect of a magnetic field on the phosphorescence lifetime was looked at, using the magnetic field apparatus described in Chapter 2. Attempts were also made to look at the magnetic field effect on delayed fluorescence, but this was found difficult due to limitations of the apparatus. This will be detailed later.

LITERATURE SURVEY OF MAGNETIC FIELD EFFECTS ON TRIPLET STATE PROCESSES

The influence of a static magnetic field on triplet state processes was first reported by Johnson et al [77] in 1967. In experiments on anthracene crystals at room temperature, they found that the rate of triplet-triplet annihilation was markedly influenced by the strength of the magnetic field. Two regions of magnetic field effect were reported:

(a) The low field effect (0-350 Oe) gave an increase in the delayed fluorescence intensity up to a maximum increase of 5% for a field strength of 350 Oe.

(b) The high field effect (>350 Oe) resulted in a decrease of delayed fluorescence intensity. At approximately 3000 Oe the intensity had decreased to about 85% of the zero-field value. Very little change occurred for fields up to 20,000 Oe.

The authors demonstrated that the magnetic field was influencing the bimolecular annihilation rate constant, k_{TT}, and not the absorption coefficient for the excitation source, Σ, or the triplet lifetime, τ, by employing pulsed field techniques. In these experiments the field was turned on in a short time compared to the lifetime of the triplet, and it was found that the delayed luminescence intensity followed the time dependence of the field effectively instantaneously. If either Σ or τ were affected by the magnetic field, the change in triplet population would take place in a manner characteristic of the triplet lifetime, and hence the change in delayed fluorescence would have a slow build-up and decay compared with the rapid risetime (2 ms) and falltime (<2 ms) of the field pulse. This was not observed and the T-T annihilation constant was deduced to be the only magnetic field-dependent step. These results were explained in terms of quantum theory calculations by Merrifield [78], and later extended by Johnson and Merrifield [79] and by Suna [80].

Magnetic field effects in crystals have been extensively reviewed by Steiner and Ulrich [82], Swenberg and Geacintov [82], Avakian and Merrifield [83] and Avakian [84].

The magnetic field effect on the efficiency of the T-T annihilation in fluid solution at room temperature was first reported by Faulkner and Bard [85]. A 5% reduction in the delayed fluorescence of anthracene with increasing field was observed. Wrysch and Labhart [86] observed the opposite field effect in the study of P-type delayed fluorescence of 1,2-benzanthracene in solution.

Faulkner and Bard [87] found that the quenching of anthracene triplets by a radical cation was inhibited by the presence of a magnetic field. The shape of the intensity-magnetic field curve was also found to be solvent dependent.

The quenching reaction of the triplet state by triplet oxygen

$$^3M^* + {}^3O_2 \text{ -----> } {}^1M + {}^1O_2$$

is analogous to the T-T annihilation process with respect to spin, and would therefore be expected to be field-dependent. This was indeed found to be the case by Faulkner and Bard [88] studying delayed fluorescence intensity. A decrease in the rate of oxygen quenching of anthracene and pyrene was observed. However, an investigation by Geacintov and Swenberg [89] into the oxygen quenching of the phosphorescence intensity of several aromatic hydrocarbons adsorbed on a polystyrene matrix showed no effect for magnetic fields as large as 145kG.

Magnetic field effects on phosphorescence intensity and lifetime have been reported in a few cases. Sixl and Schwoerer [90] found an increase in the phosphorescence intensity and a decrease in τ_p for fields up to 2kG for isolated naphthalene molecules in a mixed crystal at 1.6K. In 1,4-dibromonaphthalene crystals at 2K, Vanken and Veeman [91] reported an increase in phosphorescence emission intensity. Similarly, Kaneto et al [92], in a study of a Pt-phthalocyanine crystal at 4.2K, found an enhanced phosphorescence intensity and decreasing decay time as the magnetic field was increased up to 100kG. It is interesting to note that all these reports of phosphorescence-dependence of magnetic field are at very low temperatures. Wrysch and Labhart [86] and Johnston [1], in studies at room temperature of benzanthracene in fluid solution and anthracene crystals respectively, could find no dependence of phosphorescence on magnetic field.

Magnetic field effects have also been shown to affect the rate of T-T annihilation processes in polymers [93]. The intensity of delayed

fluorescence increased to 6% above the zero field value at a field strength of 600 Oe; the intensity passed through the zero field value at 17 kOe and reached a saturation value ca 12% below the zero field value for fields in excess of 10 kOe.

EXPERIMENTAL RESULTS

1 THE DELAYED FLUORESCENCE OF CARBAZOLE IN HOMOPOLYMER MATRICES - EFFECT OF A MAGNETIC FIELD

It was reported in Chapter 3 that, when using phosphorescence lifetime apparatus, a delayed fluorescence emission could be observed at 380nm for the higher additive concentration samples. This occurred at a considerably lower intensity than that of the corresponding phosphorescence decay obtained at 410nm. However, when the delayed and prompt emissions were looked for in the magnetic field apparatus, no delayed emission was observed, even in the high concentration samples. The emission intensity reaching the photomultiplier tube in the magnetic field apparatus is very much reduced compared to the phosphorescence lifetime apparatus. There are many more parts in the magnetic field apparatus where light intensity can be lost through internal reflections and refraction, e.g. the surfaces of the quartz sample holder and quartz window dewar, and in the liquid nitrogen surrounding the sample holder. Despite moving the sample as near as possible to the photomultiplier, no delayed emission was observed, even at relatively high photomultiplier sensitivities.

For the same reasons, no comment can be made on the magnetic field effect on the bimolecular rate constant in VC/MMA copolymers.

2 MAGNETIC FIELD EFFECTS ON PHOSPHORESCENCE LIFETIME

The results obtained for the effect of a magnetic field on τ_p were not consistent and were often conflicting.

RESULTS

CARBAZOLE IN HOMOPOLYMER MATRICES - EFFECT OF AN APPLIED MAGNETIC FIELD ON τ_p

Initially, the strength of the magnetic field was found to have a significant effect on the carbazole phosphorescence lifetime, τ_p.

TABLE 5.1

0.023M carbazole in PMMA

Field/kG	Regression	k_τ/sec^{-1}	τ_p/sec	R-sq	
0	y=1.41-0.136x	0.136	7.4	99.2%	
0.26	y=1.23-0.145x	0.145	6.9	99.2%	Drop
0.32	y=1.15-0.153x	0.153	6.5	99.2%	in τ_p
0.78	y=0.949-0.161x	0.161	6.2	99.4%	
1.10	y=0.863-0.170x	0.170	5.9	99.3%	
1.25	y=0.888-0.167x	0.167	6.0	99.2%	

However, the middle part of the decay (4-10 seconds) was non-exponential (Figure 5.1), and this was found to be due to the very high photomultiplier sensitivity. The wooden sample box was altered to move the sample nearer to the photomultiplier tube, thereby allowing each run to be studied with the photomultiplier at a lower voltage. The decays were found to be much more exponential in this middle region, but the magnetic field effect on the phosphorescence lifetime was considerably reduced (Table 5.2).

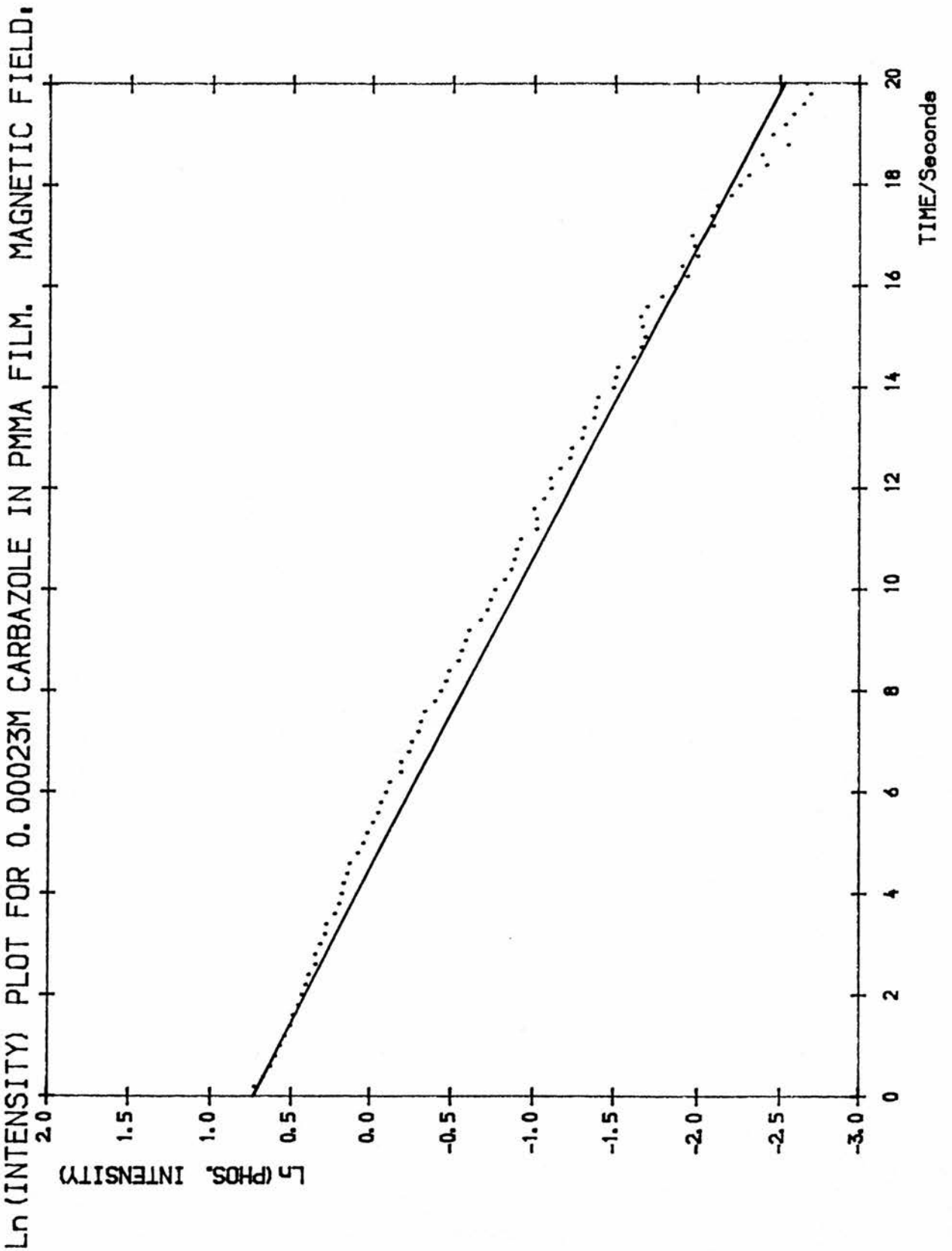
Ln (INTENSITY) PLOT FOR 0.00023M CARBAZOLE IN PMMA FILM. MAGNETIC FIELD:
Ln (PHOS. INTENSITY)
2.0
1.5
1.0
0.5
0.0
-0.5
-1.0
-1.5
-2.0
-2.5
-3.0
0
2
4
6
8
10
12
14
16
18
20
TIME/Seconds

FIGURE 5.1

TABLE 5.2

0.023M carbazole in PMMA

Field/kG	Regression	k_τ/sec^{-1}	τ_p/sec	R-sq
0	y=1.28-0.140x	0.140	7.1	99.8%
0.65	y=1.24-0.140x	0.140	7.1	99.8%
1.25	y=1.18-0.144x	0.144	6.9	99.8%

No major effect on τ_p

Similar results were obtained for 0.019M carbazole in PMMA i.e. no significant drop in phosphorescence lifetime was observed when the magnetic field was increased.

TABLE 5.3

0.019M carbazole in PMMA

Field/kG	Regression	k_τ/sec^{-1}	τ_p/sec	R-sq
0	y=1.35-0.142x	0.142	7.0	99.9%
0.26	y=1.30-0.142x	0.142	7.0	99.9%
0.52	y=1.29-0.143x	0.143	7.0	99.9%
0.78	y=1.27-0.143x	0.143	7.0	99.9%
1.10	y=1.23-0.146x	0.146	6.8	99.9%
1.25	y=1.20-0.147x	0.147	6.8	99.9%

No major effect on τ_p

In 0.0147M carbazole in PMMA, there was some decrease in the phosphorescence lifetime as the strength of the applied field was increased (Table 5.4).

TABLE 5.4

0.0147M carbazole in PMMA

Field/kG	Regression	k_τ/sec^{-1}	τ_p/sec	R-sq	
0	y=1.48-0.154x	0.154	6.5	99.8%	Drop
0.26	y=1.37-0.158x	0.158	6.3	99.8%	in τ_p
0.52	y=1.32-0.163x	0.163	6.1	99.8%	
0.78	y=1.26-0.170x	0.170	5.9	99.7%	
1.10	y=1.20-0.169x	0.169	5.9	99.6%	
1.25	y=1.28-0.171x	0.171	5.8	99.8%	

Similar decreases in τ_p were obtained for 0.0735M carbazole in PMMA. The results, run at two different photomultiplier sensitivities, are shown in Tables 5.5 and 5.6.

There are some interesting observations associated with these results:

At photomultiplier sensitivity of 1.3kV, the phosphorescence lifetime decreased as the magnetic field increased. However, this steady decrease in lifetime continued even when the field was switched off and the photomultiplier sensitivity decreased to 1.2kV. Clearly, if the magnetic field <u>is</u> affecting the sample lifetime, it is not the only effect. There appears to be a time-dependent process affecting the phosphorescence lifetime, as shown by the two consecutive runs at 0.26kG in Table 5.6. The lifetime decreased from 5.4 s to 5.0 s. Several runs later, a lifetime of 5.0 s at 0.26 kG was obtained. Similarly, the lifetimes when no field was present dropped from 6.3 s to 5.3 s to 4.5 s. The exponentiality of the decay also decreased considerably over the course of these runs, as did the initial decay intensity.

There are several possible explanations for these observed results:

TABLE 5.5

0.0735M carbazole in PMMA

Photomultiplier voltage = 1.3kV

Field/kG	Regression	k_τ/sec^{-1}	τ_p/sec	R-sq
0	y=1.51-0.159x	0.159	6.3	99.6%
0.26	y=1.48-0.167x	0.167	6.0	99.6%
0.32	y=1.44-0.168x	0.168	6.0	99.6%
0.78	y=1.42-0.174x	0.174	5.7	99.5%
1.10	y=1.39-0.183x	0.183	5.5	99.2%
1.25	y=1.37-0.190x	0.190	5.3	99.3%

TABLE 5.6

0.0735M carbazole in PMMA

Photomultiplier voltage = 1.2kV

Field/kG	Regression	k_τ/sec^{-1}	τ_p/sec	R-sq
0	y=0.764-0.189x	0.189	5.3	99.5%
0.26	y=0.788-0.186x	0.186	5.4	99.6%
0.26	y=0.761-0.199x	0.199	5.0	99.2%
0.32	y=0.762-0.198x	0.198	5.1	99.1%
0.78	y=0.815-0.221x	0.221	4.5	99.3%
1.10	y=0.759-0.226x	0.226	4.4	99.3%
1.25	y=0.714-0.244x	0.244	4.1	95.2%
0	y=0.634-0.222x	0.222	4.5	96.4%
0.26	y=0.177-0.202x	0.202	5.0	99.0%

(a) Ice forming on the sample holder and dewar as the experiment progressed would account for the decrease in emission intensity.

(b) Oxygen may be gradually leaking into the system and quenching the emission. This would account for both the drop in intensity and triplet state lifetime over the duration of the experiment.

(c) The phosphorescence lifetime is in some way dependent on the history of the magnetic field on the sample.

(d) The voltage of the photomultiplier may be affecting the measurement of the triplet lifetime. This would account for the differences in lifetime values between Tables 5.5 and 5.6. Although the photomultiplier is shielded from the magnetic field to prevent interference, some interaction cannot be dismissed.

The 0.0735M carbazole in PMMA sample was left standing for four hours, the dewar refilled with liquid nitrogen and the effect of an applied field on the phosphorescence lifetime re-run at 1.3kV. Since the position of the sample and the conditions were not altered in any way, it would be expected that if the decrease in τ_p was due solely to the effects of photomultiplier sensitivity, the results should be the same as before (i.e. Table 5.5). This was not found.

TABLE 5.7

0.0735M carbazole in PMMA

Photomultiplier voltage = 1.3kV

Field/kG	Regression	k_τ/sec^{-1}	τ_p/sec	R-sq	
0	y=1.37-0.184x	0.184	5.4	99.0%	
0.26	y=1.42-0.181x	0.181	5.5	99.1%	No
0.32	y=1.41-0.186x	0.186	5.4	99.3%	major
0.78	y=1.46-0.183x	0.183	5.5	99.2%	effect
1.10	y=1.33-0.193x	0.193	5.2	99.3%	on τ_p
1.25	y=1.39-0.189x	0.189	5.3	99.2%	
0	y=1.37-0.191x	0.191	5.2	99.2%	

There is now no significant decrease in the phosphorescence lifetime over the duration of the experiment. However, it must be noted that, comparing Tables 5.5 and 5.7, the lifetime has decreased from 6.3 to 5.4 seconds, suggesting that there may be some leakage of oxygen into the system. This was found in a later experiment not to be the case since over a period of three hours the lifetime remained constant when no field was applied.

In Table 5.4, a film of 0.0147M carbazole in PMMA was found to show a decrease in τ_p as the magnetic field was increased. However, results to the contrary were found in an experiment designed to examine the consistency of the lifetime results on varying the field strength.

TABLE 5.8

0.0147M carbazole in PMMA

Photomultiplier voltage = 1.280kV

Field/kG	Regression	k_τ/sec^{-1}	τ_p/sec	R-sq	
0	y=1.52-0.158x	0.158	6.3	99.8%	No
1.25	y=1.51-0.159x	0.159	6.3	99.8%	major
0	y=1.44-0.158x	0.158	6.3	99.8%	effect
1.25	y=1.42-0.160x	0.160	6.3	99.8%	on τ_p
0	y=1.39-0.161x	0.161	6.2	99.8%	

It can be seen from Table 5.8 that the magnetic field had no effect on the phosphorescence lifetime of the carbazole in PMMA. Again, the intensity of the emission dropped as the experiment progressed and this was found to be caused by a build-up of ice on the surfaces of the sample holder and dewar, thereby reducing the intensity of the light reaching the photomultiplier.

A change in the photomultiplier sensitivity was found to have no effect on the observed lifetime (Table 5.9).

TABLE 5.9

0.0147M carbazole in PMMA

Photomultiplier voltage = 1.280kV

Field/kG	Regression	k_τ/sec^{-1}	τ_p/sec	R-sq	
0	y=0.798-0.160x	0.160	6.3	99.5%	No
1.25	y=0.813-0.160x	0.160	6.3	99.4%	major
0	y=0.791-0.160x	0.160	6.3	99.3%	effect
					on τ_p

VINYL CARBAZOLE/METHYL METHACRYLATE COPOLYMERS - EFFECT OF AN APPLIED MAGNETIC FIELD ON τ_p

Similar inconsistencies were found in the copolymer results:

TABLE 5.10

VC/MMA copolymer (2.9% VC = 0.31M VC)

Field/kG	Regression	k_τ/sec^{-1}	τ_p/sec	R-sq	
0	y=1.34-0.147x	0.147	6.8	99.8%	Drop
0.26	y=1.30-0.151x	0.151	6.6	99.8%	in
0.32	y=1.19-0.154x	0.154	6.5	99.8%	τ_p
0.78	y=1.13-0.155x	0.155	6.5	99.8%	
1.10	y=1.04-0.157x	0.157	6.4	99.8%	
1.25	y=1.02-0.160x	0.160	6.3	99.8%	
0	y=1.02-0.161x	0.160	6.2	99.8%	

There was a definite decrease in τ_p as the experiment progressed. Again the lifetime with no applied field at the end of the run was different from the corresponding lifetime at the start of the run. Oxygen leaking into the system was found not to be a factor. The decrease in the decay intensity was again found to be due to ice formation on the dewar and sample holder.

Another copolymer film (copolymer 0.6% VC) was run in the magnetic field apparatus. Initially, a decrease in τ_p was observed (Table 5.11), but when running the sample 2 days later under the same conditions there was no magnetic field effect (Table 5.12).

TABLE 5.11

VC/MMA copolymer (0.6% VC = 0.06M VC)

Field/kG	Regression	k_τ/sec^{-1}	τ_p/sec	R-sq	
0	y=1.43-0.132x	0.132	7.6	99.9%	
0	y=1.39-0.134x	0.134	7.5	99.9%	Drop
0.26	y=1.39-0.135x	0.135	7.4	99.9%	in
0.78	y=1.36-0.137x	0.137	7.3	99.9%	τ_p
1.10	y=1.25-0.138x	0.138	7.2	99.9%	
0	y=1.15-0.137x	0.137	7.1	99.9%	

TABLE 5.12

VC/MMA copolymer (0.6% VC = 0.06M VC)

Field/kG	Regression	k_τ/sec^{-1}	τ_p/sec	R-sq	
0	y=1.30-0.136x	0.136	7.3	99.8%	No
0	y=1.22-0.138x	0.138	7.2	99.9%	major
0.78	y=1.11-0.138x	0.138	7.2	99.9%	effect
1.10	y=1.07-0.138x	0.138	7.2	99.9%	on τ_p
0	y=1.01-0.138x	0.138	7.2	99.9%	
0	y=0.935-0.138x	0.138	7.2	99.9%	

CONCLUSIONS

The results obtained in this study on the effect of a magnetic field on the phosphorescence lifetime are very inconsistent. In some cases, it appeared that τ_p was dependent on the history of the magnetic field on the sample, and in other cases, (perhaps even on the same sample), there was no field effect whatsoever. It is likely that the effects observed in this work are due to some spurious instrumental effect (possibly caused by the applied magnetic field), rather than a magnetic field effect on τ_p.

CHAPTER 6

CHAPTER 6

POLYMER PHOTODEGRADATION

INTRODUCTION

The breakdown of polymers under UV and visible light in the presence of atmospheric oxygen is a serious problem in the polymer industry. It is usually the absorption of high energy near-wavelength UV light which leads to cleavage of the polymer chain. This photodegradation eventually results in a deterioration of the mechanical properties of the bulk polymer; for example, drastic loss of elasticity or conversion of a film to a fine powder. Discolouration can also occur.

Knowledge of the energy transfer processes discussed previously has direct applications in the field of photostabilisation and photodegradation of these polymers [1,2]. In this present chapter, the effect on the extent of photodegradation of PMMA in toluene solution containing N-ethyl carbazole was examined, and compared with the degradation of the corresponding VC/MMA copolymer. All studies were made in the presence of atmospheric oxygen and the molecular weights of the polymers before and after irradiation were determined by viscometry measurements. From these results, information may be gained on the energy transfer processes taking place in each polymer system.

Firstly, it is necessary to outline some of the general mechanisms which lead to photodegradation, and the methods used to inhibit, or accelerate, this process.

PHOTODEGRADATION MECHANISMS

Polymers such as polyethylene, polypropylene and poly(vinyl chloride) might be expected to have a high stability to photodegradation because of the low density of chromophores capable of light absorption above 290nm, the lowest wavelength to reach the surface of the earth [1,2]. The observed instability to UV light above 290nm originates in the photoprocesses initiated by UV absorbing impurities or substituents introduced during synthesis, processing or storage. The commonest such impurities are hydroperoxides (R-O-O-H) and peroxides (R-O-O-R) or aldehydes and ketones. In the absence of oxygen, high purity polyethylene is a relatively stable material when exposed to UV light. It is the presence of oxygen that leads to a build-up of hydroperoxide and carbonyl impurities in the material. The stages of this auto-oxidation reaction, which converts a hydrocarbon, RH, into a hydroperoxide, ROOH, [94]

$$RH + O_2 \longrightarrow ROOH \qquad \text{auto-oxidation}$$

is shown in Scheme 1.

Initiation	initiator $\longrightarrow X\cdot$
	$X\cdot + RH \longrightarrow R\cdot + HX$
Propagation	$R\cdot + O_2 \longrightarrow ROO\cdot$
	$ROO\cdot + RH \longrightarrow ROOH + R\cdot$
Termination	$ROO\cdot + ROO\cdot \longrightarrow$ non-radical products
	$ROO\cdot + R\cdot \longrightarrow$ non-radical products
	$R\cdot + R\cdot \longrightarrow$ non-radical products

SCHEME 1 :-The mechanism of auto-oxidation

Possible radical initiators of this oxidation reaction are radicals from hydroperoxide decomposition (HO·, H·, R· and RO·) or from carbonyl compound decomposition. Carbonyl compounds can undergo two types of reaction on exposure to UV light:

Norrish type I reaction

In acyclic ketones, α-cleavage is usually designated the Norrish type I reaction [95].

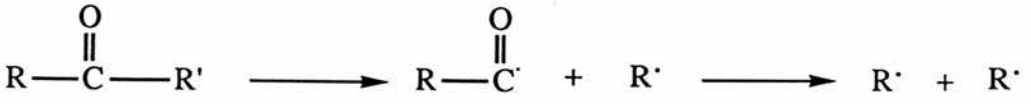

This results in the formation of radicals which can induce further photodegradation.

Norrish type II reaction [95]

If the ketone has at least one hydrogen atom in the ϒ position relative to the carbonyl group then a Norrish type II reaction may occur. This proceeds by intramolecular hydrogen transfer, yielding one olefin and one enol, ultimately rearranging to the more stable ketone.

e.g.

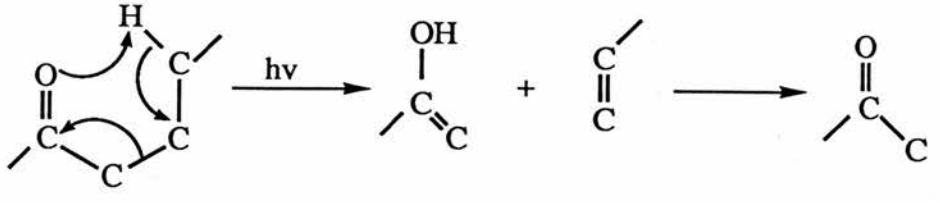

The Norrish type II reaction is not as important as type I since it involves cleavage to form non-radical fragments.

The mechanistic scheme for the photodegradation of polypropylene is shown in Figure 6.1 to demonstrate how the steps of auto-oxidation and Norrish-type I reactions contribute to the degradation of the polymer [96]. It can be seen that there is a build-up of impurities which can absorb more strongly than the bulk polymer and initiate further oxidative processes. Such processes lead to a reduction in the relative molecular mass of the polymer.

Similarly, high purity polystyrene is photochemically stable in the absence of oxygen. In the presence of oxygen, however, commercial samples are readily photodegraded (Figure 6.2) [97]. The formation of hydroperoxide groups and carbonyl groups, which then break down to form free radicals, are again key elements in the photodegradation process.

PHOTODEGRADATION OF POLYPROPYLENE

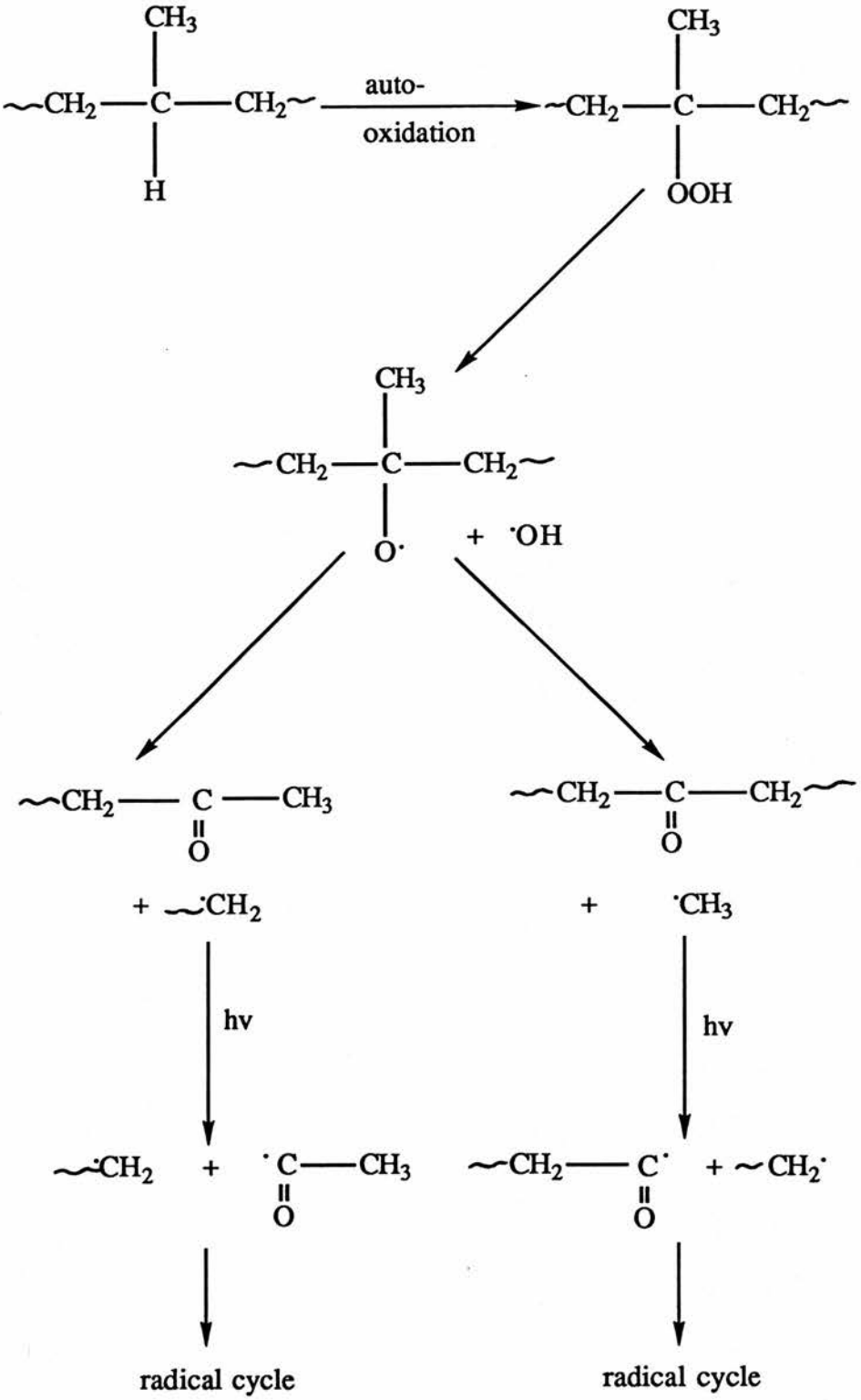

FIGURE 6.1

PHOTODEGRADATION OF POLYSTYRENE

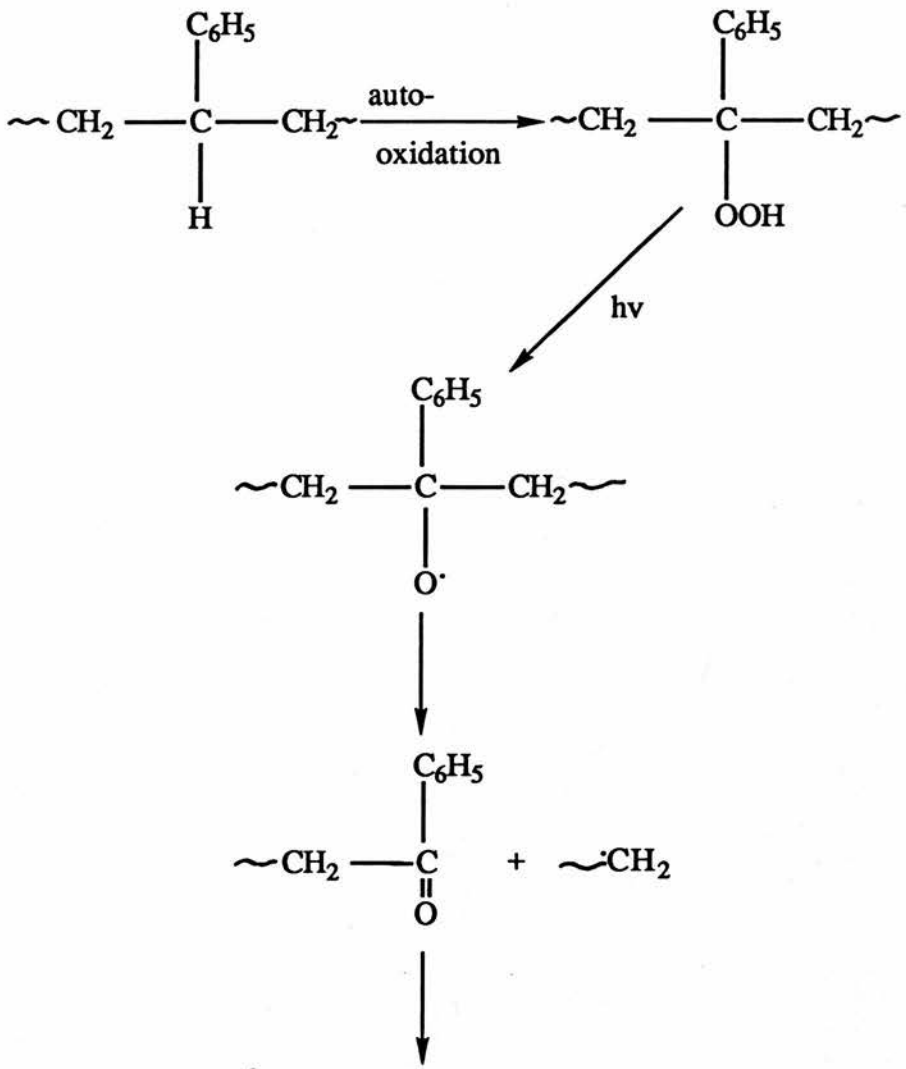

Initiation via chain scission and hydrogen abstraction

FIGURE 6.2

GENERAL METHODS OF POLYMER STABILISATION

Since photodegradation generally follows chain reaction kinetics, the photostationary concentration of radical intermediates in the chain critically determines the overall rate of photodegradation. There are three different types of stabiliser which can be added to the polymer to protect against photodegradation [96,98,99]:-

1 Addition of screens or absorbents which prevent light absorption by potential sensitisers

Light screens function either by absorbing damaging radiation before it reaches the polymer surface or by limiting its penetration into the polymer sample. A typical example is the coating of polyethylene with aluminium powder. Pigments dispersed in a polymer matrix are usually classified as light screens since particles concentrated at the surface do filter out radiation. ZnO and TiO_2 reflect efficiently in the region of 240 - 380nm and hence the addition of these pigments to polymers is a very effective method for increasing resistance to photodegradation. Carbon black is an excellent photostabiliser. The problem with the use of these additives is that they often introduce undesirable colouring and loss of mechanical properties. Also, both inorganic and organic pigments can initiate unwanted photoprocesses.

2 Addition of antioxidants which, by reaction with radical intermediates, reduce the concentration of these species in the photodegradation chain

Hydroperoxide groups are a key processes in the photodegradation of polymers, and any compound which can react chemically with these hydroperoxides will act as a photostabiliser. Several compounds have

been found, e.g. hydroxybenzophenones (I), metal dithiocarbamates (II), metal dithiophosphates (III) and cyclic phosphate esters (IV).

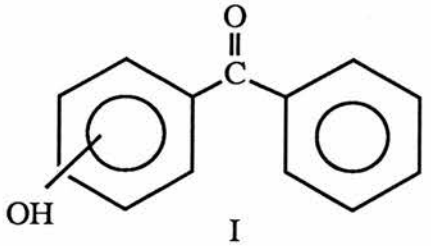

I

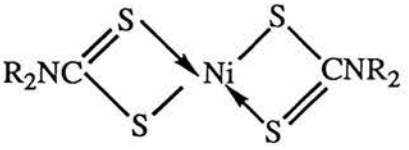

II

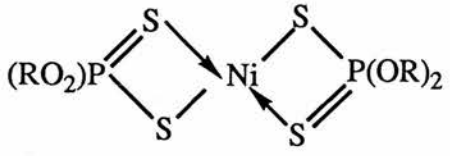

III

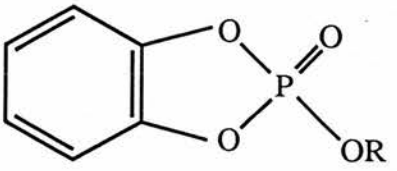

IV

Radical scavengers such as phenols, hydroquinones and thiols will also retard photodegradation.

3 Addition of quenchers which retard degradation by quenching the excited states responsible for the initiating and bond-breaking process

The use of quenchers is directed mainly at preventing relatively long-lived triplet states of ketones and aldehydes from initiating further photodegradation and at dissipation excited state energy from polymer molecules. If the energy absorbed by the polymer, either by the polymer itself or by energy transfer from some secondary impurity can be transferred effectively to a quenching molecule in the system before bond-breaking occurs, then photodegradation can be inhibited.

$$\text{polymer}^* + \text{quencher} \longrightarrow \text{polymer} + \text{quencher}^*$$

It is in this area of research that an understanding of the basic mechanisms of energy transfer in polymers is very important. It must be noted, however, that the most suitable quenchers to inhibit or increase photodegradation in commercial polymers can only be established by specific studies under different natural and artificial conditions of irradiation.

ACCELERATING POLYMER DEGRADATION

The deliberate acceleration of photodegradation by

(a) adding carbonyl groups - initiators of photooxidation - into the backbone of the polymer chain and/or
(b) adding a molecule which will transfer electronic energy to the polymer chain

produces a photodegradable plastic which forms a fine powder when exposed to light [2]. This has direct consequences in the reduction of environmental pollution caused by the large quantities of plastic waste, resulting from the use of plastics as packaging materials.

EXPERIMENTAL

VISCOMETRY

THEORY [100,101]

The coefficient of viscosity, η, is a measure of the resistance to flow of a fluid. It is measured by the determination of the time of flow of a given volume V through a capillary tube under the influence of gravity. This flow is governed by Poisseuille's law in the form of

$$\frac{dV}{dt} = \frac{\pi r^4 (P_1-P_2)}{8\eta L}$$

where dV/dt is the rate of liquid flow through a cylindrical tube of radius r and length L, and (P_1-P_2) is the difference in pressure between the two ends of the tube. However, since (P_1-P_2) is proportional to the density ρ, it can be shown that for a given total volume of liquid

$$\frac{\eta}{\rho} = Bt$$

where t is the time required for the upper meniscus to fall from the upper to lower fiducial mark, and B is an apparatus constant which must be determined through calibration with a liquid of known viscosity (e.g. water).

The addition of polymer molecules to a solution increase the viscosity over the pure solvent. In relating this increased viscosity to the properties of the solute, a number of functions of the measured viscosity coefficients η_0 of the pure solvent and η of the solution are used. These are listed below:-

NAME	DEFINITION
Relative viscosity, η_{REL}	η/η_0
Specific viscosity. η_{SP}	$\eta/\eta_0 - 1$
Reduced specific viscosity	$1/c\{\eta/\eta_0 - 1\} = \eta_{SP}/c$
Intrinsic viscosity, $[\eta]$	$\lim_{c\to 0} \{1/c(\eta/\eta_0 - 1)\}$ $= \lim_{c\to 0} \eta_{SP}/c$

The concentration, c, is usually defined as grams of polymer per 100 ml solution [101,102].

The intrinsic viscosity for a linear soluble high polymer has been shown to be a function of its molecular weight. There exists an empirical relationship of the form

$$[\eta] = KM^{\alpha} \qquad \text{Mark-Houwink equation}$$

where K and α are constants which depend on the solvent used and the temperature. The exponent α usually varies between 0.5 and 1.0 for different solvents, polymers and temperatures. For PMMA in toluene at 25^0C, the K and α values [103] are reported as

$K = 7.1 \times 10^{-5}$ 100ml/g

$\alpha = 0.73$.

DETERMINATION OF INTRINSIC VISCOSITY, $[\eta]$ [101,102]

Plots of η_{SP} vs c are generally linear at low solute concentrations, and the extrapolated value $[\eta]$ at zero concentration is easily determined. Another plot which can be used to determine $[\eta]$ is $1/c\ln(\eta/\eta_0)$ vs c. The two plots extrapolate to the same intercept, as

shown by expansion of the logarithm [102]

$$\ln(\eta/\eta_0) = \ln(1 + \eta_{SP}) = \eta_{SP} - \eta_{SP}^2/2 + \eta_{SP}^3/3 - \ldots$$

Second and higher order terms become negligible as compared with the first as the concentration approaches zero. The advantage of the double extrapolation is that the intercept may be determined more precisely than by using only one straight line.

THE SOLOMON AND CUITA EQUATION

The intrinsic viscosity can also be calculated from a single viscosity determination using the equation of Solomon and Cuita [104].

$$[\eta] = (\sqrt{2}/c)\ \sqrt{(\eta_{SP} - \ln \eta_{REL})}$$

This equation was verified for different polymer-solvent systems and was shown to be mathematically viable.

METHOD

The flow time in the viscometer was determined for 27ml water and the apparatus constant B calculated. η_0 was calculated from the flowtime of pure toluene. All flow time were calculated by taking the average time from 8 consecutive runs.

1.5g of polymer was dissolved in toluene and diluted quantitively to 100ml in a volumetric flask. 30ml of this solution was laid aside and irradiated with UV light for 14 days. The flow time for 27ml of the polymer solution was determined, the sample diluted and the flow time measured again. This procedure was repeated several times. Between each run the viscometer was thoroughly cleaned with toluene, then with

dichloromethane, and finally rinsed with acetone and dried. The samples were allowed to equilibriate to bath temperature for at least 1½ hours before any measurements were made.

For each of the polymer solutions studied, the viscosity η and concentration c in grams of polymer per 100ml of solution were calculated. The values for (η_{SP}/c) and $(1/c)\ln(\eta/\eta_0)$ vs c were plotted and extrapolated linearly to c=0 to obtain $[\eta]$ for the original and degraded polymers.

The average molecular weights were calculated using the Mark Houwink equation

$$[\eta] = 7.1\times10^{-5} M^{0.73}.$$

RESULTS

The apparatus constant was calculated as 2.42×10^{-5}

The flow time for pure toluene = 367.5 seconds

Density of toluene (25^0C) = 0.867

$\Rightarrow \eta_0 = 7.71\times10^{-3}$

The flowtimes and values of specific and limiting specific viscosity for various concentrations of irradiated and non-irradiated PMMA, PMMA + 0.31M NEC and VC/MMA copolymer (0.31M in VC) are shown in Tables 6.1 and 6.2. The intercepts on the η_{SP}/c and $1/c\ln(\eta/\eta_0)$ vs concentration plots for PMMA and the copolymer samples (Figure 6.3 and Figure 6.4) were shown to be in agreement with the values of $[\eta]$ calculated from the Solomon and Cuita equation, using the initial viscosity values (Table 6.3).

TABLE 6.1

VISCOMETRY RESULTS

PMMA -Before irradiation

Conc/ g/100ml	flowtime/ seconds	η_{SP}	η_{SP}/c	$1/c\ln(\eta_{REL})$
1.49	657.8	0.790	0.53	0.39
1.24	576.3	0.586	0.46	0.36
0.745	483.8	0.316	0.42	0.37
0.497	453.5	0.234	0.47	0.42
0.248	407.5	0.104	0.42	0.40

PMMA - After irradiation

Conc/ g/100ml	flowtime/ seconds	η_{SP}	η_{SP}/c	$1/c\ln(\eta_{REL})$
1.49	599.7	0.632	0.42	0.33
0.99	509.3	0.386	0.39	0.33
0.66	449.4	0.223	0.34	0.31
0.44	429.4	0.168	0.38	0.35
0.29	407.6	0.109	0.38	0.36

0.31M N-Ethyl carbazole in toluene solvent

flowtime = 378.2 seconds

PMMA + 0.31M N-Ethyl carbazole

conc/ g/100ml	flowtime/ seconds	$[\eta]_{Solomon\ equation}$
1.5	630.5	0.37

TABLE 6.2

VISCOMETRY RESULTS

0.31M VC/MMA COPOLYMER - Before irradiation

Conc/ g/100ml	flowtime/ seconds	η_{SP}	η_{SP}/c	$1/c\ln(\eta_{REL})$
1.51	562.0	0.529	0.35	0.28
1.26	516.8	0.406	0.32	0.27
0.755	459.7	0.251	0.33	0.30
0.503	427.3	0.163	0.32	0.30
0.252	396.4	0.079	0.31	0.31

0.31M VC/MMA COPOLYMER - After irradiation

Conc/ g/100ml	flowtime/ seconds	η_{SP}	η_{SP}/c	$1/c\ln(\eta_{REL})$
1.51	485.0	0.320	0.21	0.18
1.01	460.2	0.252	0.25	0.22
0.67	422.9	0.151	0.23	0.21
0.45	400.7	0.090	0.20	0.19
0.30	380.5	0.035	0.12	0.11

0.45M VC/MMA COPOLYMER - Before irradiation

conc/ g/100ml	flowtime/ seconds	$[\eta]_{Solomon\ equation}$
1.5	624	0.387

0.45M VC/MMA COPOLYMER - After irradiation

conc/ g/100ml	flowtime/ seconds	$[\eta]_{Solomon\ equation}$
1.5	480.4	0.187

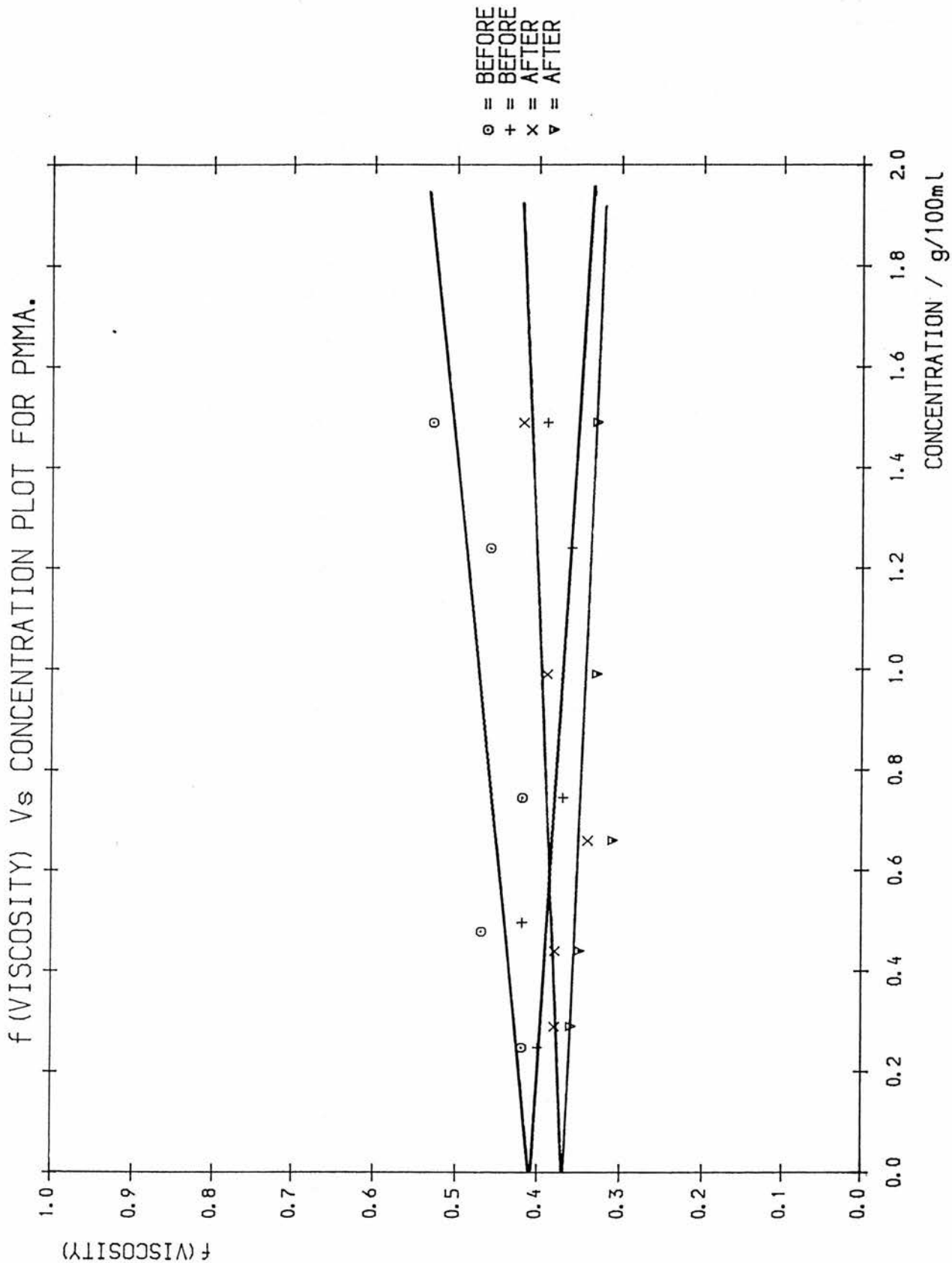
f (VISCOSITY) Vs CONCENTRATION PLOT FOR PMMA.
⊙ = BEFORE
+ = BEFORE
× = AFTER
▲ = AFTER
f (VISCOSITY)
CONCENTRATION / g/100ml
1.0
0.9
0.8
0.7
0.6
0.5
0.4
0.3
0.2
0.1
0.0
0.0
0.2
0.4
0.6
0.8
1.0
1.2
1.4
1.6
1.8
2.0

FIGURE 6.3

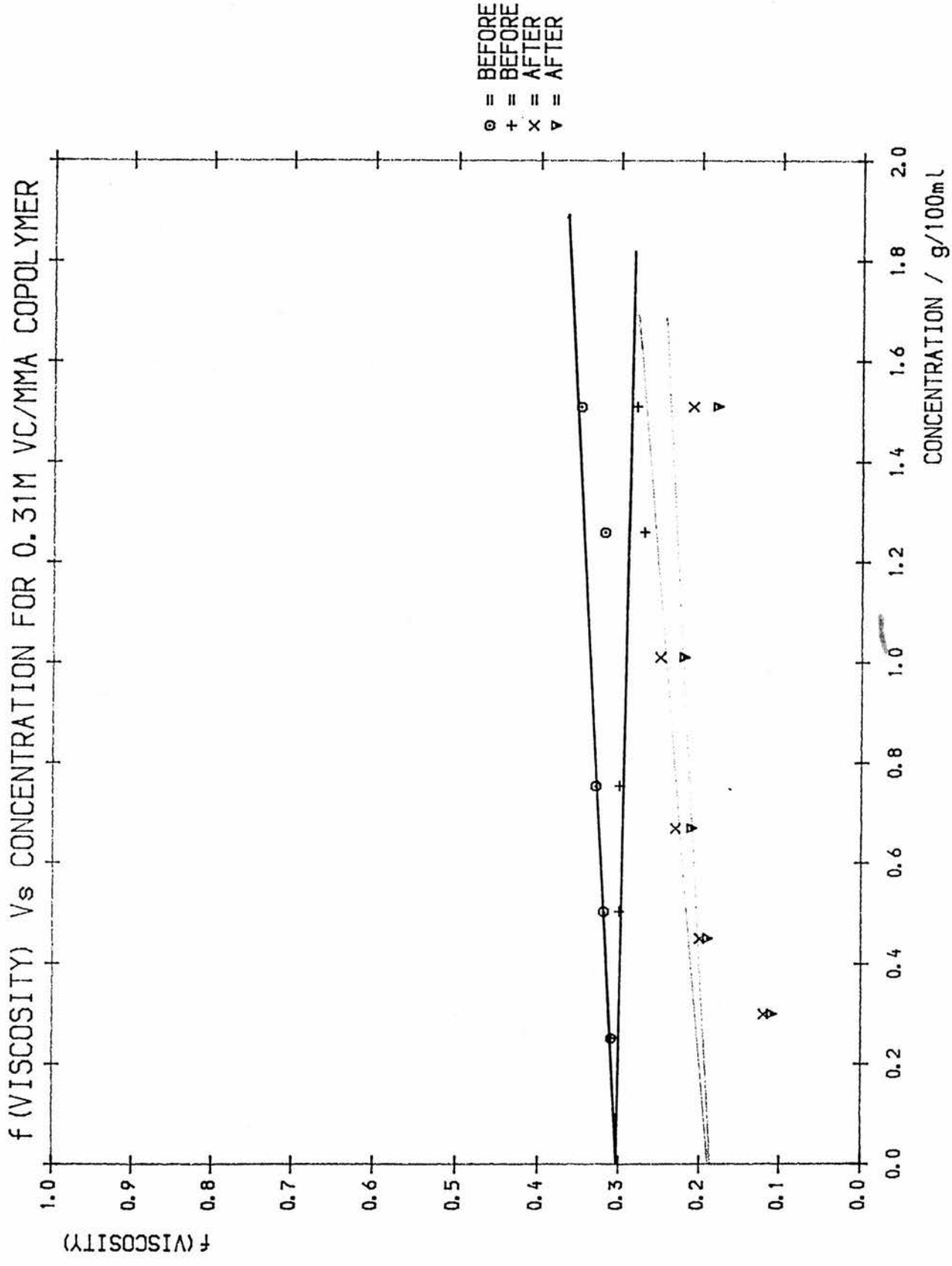
f (VISCOSITY) Vs CONCENTRATION FOR 0.31M VC/MMA COPOLYMER
⊙ = BEFORE
+ = BEFORE
× = AFTER
▲ = AFTER
f (VISCOSITY)
CONCENTRATION / g/100ml
1.0
0.9
0.8
0.7
0.6
0.5
0.4
0.3
0.2
0.1
0.0
0.0
0.2
0.4
0.6
0.8
1.0
1.2
1.4
1.6
1.8
2.0

FIGURE 6.4

TABLE 6.3

	PMMA		0.31M Copolymer	
	before	after	before	after
$[\eta]_{intercept}$	0.41	0.37	0.3	0.19
$[\eta]_{Solomon}$	0.43	0.36	0.3	0.19

Values of [η] for 0.31M NEC in PMMA and the 0.45M VC/MMA copolymer were calculated using the Solomon equation.

Yellowing occurred in the irradiated copolymer samples, and to a much lesser extent in the 0.31M NEC in PMMA solution.

MOLECULAR WEIGHTS OF NON-IRRADIATED AND IRRADIATED SAMPLES

The molecular weights were determined using the Mark-Houwink equation, and the % drop in molecular weight calculated as a percentage of the molecular weight of the non-irradiated sample.

POLYMER SOLUTION	mol. wt.	% drop in mwt.
pure PMMA - Before irradiation	$1.52x10^5$	/
pure PMMA - After	$1.19X10^5$	21.7%
0.31M NEC in PMMA - After	$1.24X10^5$	18.4%
0.31M VC/MMA copolymer - Before	$0.97X10^5$	/
0.31M VC/MMA copolymer - After	$0.50X10^5$	48.5%
0.45M VC/MMA copolymer - Before	$1.31x10^5$	/
0.45M VC/MMA copolymer - After	$0.48x10^5$	63.3%

DISCUSSION

Poly(methyl methacrylate) is normally extremely resistant to oxidative photodegradation, primarily because of the absence of any absorption in the 'pure' polymer down to 285nm. The degradation observed in this present study may have been initiated by

(a) UV light-absorbing impurities in the polymer itself and/or

(b) Photolysis of the toluene solvent. One plausible mechanism for this involves the auto-oxidation mechanism:

e.g.

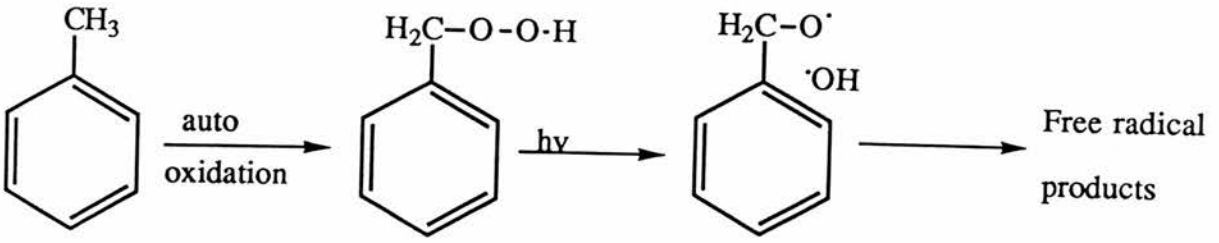

No evidence for step (a) was observed since the UV spectrum of pure PMMA gave no absorbance above 300nm. Degradation of the toluene is the more likely process. Toluene has a small UV absorption above 300nm, and thus the auto-oxidation is favoured. The free radical intermediates formed are stabilised by delocalisation over the aromatic ring.

In pure PMMA and in the NEC-doped homopolymer solution there is approximately 20% loss in the molecular weight on 14 days irradiation of each sample. This photodegradation is probably the result of solvent breakdown, forming free radicals which initiate the bond-breaking process. However, in the VC/MMA copolymers there is a further drop of up to 40% in molecular weight. An absorbance due to the carbazole unit of the copolymer was observed above 300nm. Attaching the carbazole unit to the backbone of the copolymer chain seems to have increased the rate

of photodegradation.

This result is consistent with the mechanism proposed in Chapters 3 and 4, where it was found that there is energy transfer from the triplet energy level of the carbazole unit to the triplet level of methyl methacrylate.

i.e. $$\text{carbazole} \text{ -----> } \text{carbazole}^*$$

$$\text{carbazole}^* + P_0 \text{ -----> carbazole} + P_T^*$$

In the doped homopolymer, the excited state polymer, P_T^*, rapidly loses its excess energy and returns to ground state, P_0. In terms of photodegradation, no significant increase in the rate of bond-breaking would be expected. In the copolymer however, a different situation arises. Triplet energy migration

$$P_T^* + P_0 \text{ -----> } P_0 + P_T^*$$

was shown in Chapter 4 to be a fairly efficient process in the VC/MMA copolymer, and when electronic energy is transferred from the excited state carbazole to the MMA unit, the polymer chain remains in an energy-rich state over a longer period of time. The probability of bond-breaking taking place is therefore increased, and the rate of photodegradation in the VC/MMA copolymer is enhanced.

CONCLUSIONS

CONCLUSIONS

It has been shown in this study that the phosphorescence lifetime of carbazole-type compounds embedded in polymer matrices was dependent on matrix, temperature, and additive concentration. An energy transfer mechanism between the triplet level of the carbazole and the polymer triplet level has been proposed. Since the energy levels of the additive and the polymer are very similar, this is a feasible process. At high dopant concentrations, an initial non-exponential decay and decrease in lifetime was observed, and this has been attributed to the onset of triplet-triplet annihilation.

The results indicate that care must be taken when choosing a polymer as a host medium for studies of the triplet state. There must be a prohibitively endothermic triplet energy level difference between the additive and the polymer, thereby preventing energy transfer to the matrix. When examining the triplet state using a doped polymer matrix, the concentration of the additive must be kept to a minimum to reduce the possibility of triplet-triplet annihilation occurring.

In the doped homopolymer matrices, energy migration along the chain is a very inefficient step. However, in the copolymer analogs, energy migration has been found to be a much more efficient process. This may have applications in the field of photodegradation and photostabilisation of polymers. In this present study, the rate of polymer decomposition in the presence of oxygen has been found to increase when the carbazole unit is attached to the backbone of the polymer chain. Energy transfer from the polymer to the carbazole triplet level, followed by energy migration along the chain ultimately leads to bond-breaking. No such mechanism takes place in the doped

homopolymer. Intermolecular energy transfer to the polymer is readily dissipated.

REFERENCES

REFERENCES

1 D.M. Wiles, Pure & Appl. Chem., 50, 29 (1978)

2 B. Baum and R.D. Deanin, Polymer - Plast. Technol. Eng., 2, 1 (1973)

3 C.H.J. Wells, Introduction To Molecular Photochemistry, Chapter 1-3, p1, Chapman and Hall, London (1972)

4 N.J. Turro, Molecular Photochemistry, Chapter 1-5, p1, W.A. Benjamin Inc, London (1965)

5 The Open University, S341, Photochemistry:Block 4. Physical Properties of Excited States

6 J.B. Birks, Photophysics of Aromatic Molecules, Chapter 2, p29, New York (1971)

7 M.D. Lumb, Organic Photoluminescence, Chapter 2, p93, Academic Press, London (1978)

8 C.N. Banwell, Fundamentals of Molecular Spectroscopy, Chapter 5, p157, McGraw-Hill, London (1972)

9 D. Phillips, Polymer Photophysics, p4, Chapman and Hall, London (1985)

10 Th. Forster, Z. Naturforsch, 4a, 321 (1949)

11 D.L. Dexter, J. Chem. Phys., 21, 836 (1953)

12 D.D. Perrin, W.L.F. Armarego and D.R. Perrin, Purification of Laboratory Chemicals, Permagon Press, Oxford (1971)

13 J-C.G. Bunzli and D. Wessner, Helvetica Chimica Acta, 61, 1454 (1978)

14 J-C.G. Bunzli, D. Wessner and H.T.T. Oanh, Inorganica Chimica Acta, 32,L33 (1979)

15 J. Pielichowski and J. Kyziol, Monatsch. Chem., 105,1306 (1974)

16 Adapted from program by D.A. Graham, Ph.D thesis, St Andrews (1974)

17 G. Oster, N. Geacintov and A.U. Khan, Nature, 196, 1089 (1962)

18 J.M.G. Cowie, Polymers: Chemistry and Physics of Modern Marterials, p7, Intertext Books, London (1973)

19 J.R. MacCallum, Eur. Polym. J., 9, 609 (1973)

20 I.B. Berlman, Handbook of Fluorescence Spectra of Molecules, Chapter 6, Academic Press, London (1971)

21 J.B. Birks, Photophysics of Aromatic Molecules, p228, p294, New York (1971)

22 R.B. Cundall and A. Gilbert, Photochemistry, p103, Nelson, London (1970)

23 D.S. McClure, J. Chem. Phys., 17, 905 (1949)

24 R.N. Griffin, Photochem. Photobiol., 7, 175 (1968)

25 N. Geacinov, G. Oster and T. Cassen, J. Opt. Soc. Amer., 58, 1217 (1968)

26 R.L. Clough, M.P. Dillon, K.-K. Iu and P.R. Ogilby, Macromolecules, 22, 3620 (1989)

27 P.F. Jones and S. Siegel, J. Chem. Phys, 50, 1134 (1969)

28 M.A. West, K.J. McCallum, R.J. Woods and S.J. Formoshino, Trans. Faraday Soc., 66, 2135 (1970)

29 F.E. El-Sayed, J.R. MacCallum, P.J. Pomery and T.M. Shepherd, J. Chem. Soc. Farad. Trans. II, 75, 79 (1979)

30 M.B. Ledger and G. Porter, J. Chem. Soc. Farad. Trans. I, 68, 539 (1972)

31 M. Berger, E. McAlpine and C. Steel, J. Am. Chem. Soc, 100(16), 5147 (1978)

32 J.L. Kropp and W.R. Dawson, J. Chem. Phys, 71, 4499 (1967)

33 W.E. Graves, R.H. Hofeldt and S.P. McGlynn, J. Chem. Phys., 56, 1309 (1972)

34 A.N. Jassim, J.R. MacCallum and T.M. Shepherd, Eur. Polym. J., 17, 125 (1981)

35 A.N. Jassim, J.R. MacCallum and K.T. Mor[illegible], Eur. Polym. J., 19, 909 (1983)

36 I.M. Fraser, J.R. MacCallum and K.T. Moran, Eur. Polym. J., 20, 425 (1984)

37 A. Charlesby and R.H. Partridge, Proc. R. Soc. London Ser. A, 283, 312 (1963)

38 A. Bousted, Eur. Polym. J., 6, 731 (1970)

39 A.C. Somersall, E. Dan and J.E. Guillet, Macromolecules, 7, 233 (1974)

40 K. Horie and I. Mita, Chem. Phys. Lett, 93, 61 (1982)

41 K. Horie, K. Morishita and I. Mita, Macromolecules, 17, 1746 (1984)

42 K. Horie and I. Mita, Eur. Polym. J., 20, 2037 (1984)

43 K. Horie, M. Tsukamoto, K. Morishita and I. Mita, Polymer J., 17, 517 (1985)

44 K. Horie, Polymer Preprints (Am. Chem. Soc., Div. Polym. Chem.), 27, 340 (1986)

45 R.N. Haward , The Physics of Glassy Polymers, Chapter 3, p201, Applied Science Publishers Ltd, London (1973)

46 H. Rutherford and I. Soutar, J. Polymer Sci., Polym. Phys. Ed., 15,2213 (1977)

47 H. Rutherford and I. Soutar, J. Polymer Sci., Polym. Phys. Ed., 18, 1021 (1980)

48 K.J. Smit, R. Sukurovs and K.P. Ghiggino, Eur. Polym. J., 19, 49 (1983)

49 N. Hirota, J. Chem. Phys., 43, 3354 (1965)

50 N. Hirota and C.A. Hutchison Jr., J. Chem. Phys., 42, 2869 (1965)

51 H. Sternlicht, G.C. Nieman and G.W. Robinson, J. Chem. Phys., 38, 1326 (1963)

52 K.R. Naqvi, Chem. Phys. Lett, 1, 497 (1969)

53 C.A. Parker, Trans. Faraday Soc, 60, 1998 (1964)

54 M.A. El-Sayed, J. Opt. Soc. Am., 53, 797 (1963)

55 G.I. Lashkov and V.L. Ermolaev, Opt. Spectrosc., 22, 462 (1967)

56 R.F. Cozzens and R.B. Fox, J. Chem. Phys., 50, 1532 (1969)

57 R.B. Fox and R.F. Cozzens, Macromolecules, 2, 181 (1969)

58 R.B. Fox, T.R. Price and R.F. Cozzens, J. Chem. Phys., 54, 79 (1971)

59 R.B. Fox, T.R. Price, R.F. Cozzens and J.R. MacDonald, J. Chem. Phys, 57, 2284 (1972)

60 R.B. Fox, T.R. Price, R.F. Cozzens and W.H. Echols, Macromolecules, 7, 937 (1974)

61 R.F. Cozzens and R.B. Fox, Polym. Preprints, 9, 363 (1968)

62 M. Kinoshita, K. Stolze and S.P. McGlynn, J. Chem. Phys., 48, 1191 (1968)

63 C. David, W. Demarteau and G. Geuskens, Eur. Polym. J., 6, 537 (1970)

64 C. David, W. Demarteau and G. Geuskens, Eur. Polym. J., 6, 1397 (1970)

65 C. David, N. Putman, M. Lempereur and G. Geuskens, Eur. Polym. J., 8, 409 (1972)

66 A.C. Somersall and J.E. Guillet, Macromolecules, 6, 218 (1973)

67 S.E. Webber and P.E. Avots-Avotins, Macromolecules, 12, 708 (1979)

68 R.D. Burkhart and R.G. Aviles, J. Phys. Chem., 83, 1897 (1979)

69 R.D. Burkhart and R.G. Aviles, Macromolecules, 12, 1073 (1979)

70 D.K. Chakraborty and R.D. Burkhart, J. Phys. Chem., 93, 4797 (1989)

71 D.K. Chakraborty and R.D. Burkhart, Macromolecules, 23, 121 (1990)

72 W. Klopffer, J. Chem. Phys., 50, 2337 (1967)

73 W. Klopffer and D. Fischer, J. Polym. Sci.; Symposium No. 40, 43 (1973)

74 W. Klopffer, Ann. N.Y. Acad. Sci., 336, 373 (1981)

75 J.E. Guillet, Pure & Appl. Chem, 49, 249 (1977)

76 J.E. Guillet, Polymer Photophysics and Photochemistry, An Introduction to the Study of Photoprocesses in Macromolecules, Chapter 9, p231, Cambridge University Press, London (1985)

77 R.C. Johnson, R.E. Merrifield, P. Avakian and R.B. Flippen, Phys. Rev. Lett., 19, 285 (1967)

78 R.E. Merrifield, J. Chem. Phys., 48, 4318 (1968)

79 R.C. Johnson and R.E. Merrifield, Phys. Rev. B, 1, 896 (1970)

80 A. Suna, Phys. Rev. B, 1, 1716 (1970)

81 U.E. Steiner and T. Ulrich, Chem. Rev., 89, 51 (1989)

82 J.B. Birks, Organic Molecular Photophysics vol 1, Chapter 10, p490, John Wiley and Sons, New York (1973)

83 P.Avakian and R.E. Merrifield, Mol. Crys., 5, 37 (1968)

84 P.Avakian, Pure Appl. Chem., 37, 1 (1974)

85 L.R. Faulkner and A.J. Bard, J. Am. Chem. Soc., 91, 6495 (1969)

86 D. Wyrsch and H. Labhart, Chem. Phys. Lett., 8, 217 (1971)

87 L.R. Faulkner and A.J. Bard, J. Am. Chem. Soc., 91, 6497 (1969)

88 L.R. Faulkner and A.J. Bard, J. Am. Chem. Soc., 95, 1672 (1973)

89 N.E. Geacintov and C.E. Swenberg, J. Chem. Phys., 57, 378 (1972)

90 H. Sixl and M. Schwoerer, Chem. Phys. Lett., 6, 21 (1970)

91 J.M.J. Vankan and W.S. Veeman, Chem. Phys. Lett., 94, 133 (1983)

92 K. Kaneto, K. Yoshino and Y. Inuishi, Chem. Phys. Lett., **40**, 505 (1976)

93 P. Avakian, R.P. Groff, A. Suna and H.N. Cripps, Chem. Phys. Lett., **32**, 466 (1975)

94 W.L. Hawkins, Polymer Stabilisation, p12,p18, Wiley and Interscience, London (1972)

95 J. Faure, Pure & Appl. Chem., **49**, 487 (1977)

96 W.L. Hawkins, Polymer Stabilisation, Chapter 4, p159, Wiley and Interscience, London (1972)

97 G. Geuskens and C. David, Pure & Appl. Chem, **49**, 479 (1977)

98 D. Phillips, Polym. News, **3**, 246 (1977)

99 D.J. Carlsson and D.M. Wiles, Am. Chem. Soc., Div. Org. Coat., Plast. Chem. Pap., **34**, 124 (1974)

100 F. Daniels, Experimental Physical Chemistry, Chapter 8, p 157, McGraw Hill, New York (1970)

101 P. Shoemaker and C.W. Garland, Experiments In Physical Chemistry, Chapter XI, p226, McGraw Hill, New York (1970)

102 F. Daniels, Experimental Physical Chemistry, Chapter 15, p329, McGraw Hill, New York (1970)

103 J. Brandrup and E.H. Immergut, Polymer Handbook, pIV-10, John Wiley and Sons, New York (1974)

104 O.F. Solomon and I.Z. Cuita, J. Appl. Polym. Sci., **6**, 683 (1962)

APPENDIX

APPENDIX

FITTING ROUTINES TRIP AND DEX

TRIPLET-TRIPLET ANNIHILATION (TRIP)

When triplet-triplet annihilation occurs the decay of the triplet is a combination of a first order decay

$$T_1^* \text{ -----> } S_0$$

and a second order decay

$$T_1^* + T_1^* \text{ -----> } S_0 + S_1^*$$

and/or

$$T_1^* + T_1^* \text{ -----> } 2S_0$$

If the repopulation of the triplet state from the newly formed S_1^* state is ignored, then the rate of decay is

$$-\frac{d[T]}{d[T]} = k_1[T] + k_2[T]^2$$

Integration of the above gives

$$\frac{1}{[T]} = \frac{1}{[T]_0} + \frac{k_2}{k_1}\exp(k_1 t) - \frac{k_2}{k_1}$$

where k_1 is the sum of the first order rate constants and k_2 is the second order rate constant. A three variable iterative fitting routine, based on the method of differential coefficients was used in the FORTRAN

computer program TRIP [16] to calculate the values for k_1 and k_2. The three variabbles were $[T_0]$, k_1 and k_2.

DOUBLE EXPONENTIAL (DEX)

If the emission observed is the combination of emissions from two types of excited molecules which have different lifetimes then the overall decay will be non-exponential and the sum of two exponential components. If the two processes are

$A^* \text{ -----> } A$ rate constant k_1

$B^* \text{ -----> } B$ rate constant k_2

the two rates of decay are

$$[A^*] = [A^*]_0 \, e^{-k_1 t}$$

$$[B^*] = [B^*]_0 \, e^{-k_2 t}$$

the observed intensity is $[A^*] + [B^*]$, hence

$$[I]_{obs} = [A^*]_0 \, e^{-k_1 t} + [B^*]_0 \, e^{-k_2 t}$$

A three variable fitting routine was used in a program DEX [16] to calculate the values of k_1 and k_2. The data was normalised so that $[B^*] = 1 - [A^*]$, the three variables were then $[A^*]$, k_1 and k_2.